Liberté • Égalité • Fraternité
RÉPUBLIQUE FRANÇAISE

MINISTÈRE
DE LA DÉFENSE

DGA Techniques aéronautiques

EXAMINATION REPORT

EXAMINATION REPORT

N° 16-DGATA-MTI-P1501516001002-DR-F-Â

This document is a courtesy translation of the original examination report issued by the French DGA/TA and, as requested by the French judicial authorities. As accurate as this translation may be, the original text in French is the work of reference

DGA

DIRECTION GÉNÉRALE DE L'ARMEMENT

RESTRICTED CIRCULATION

DIRECTION GÉNÉRALE
OF L'ARMEMENT
DGA Technical aéronautiques

TI

Liberté • Égalité • Fraternité
RÉPUBLIQUE FRANÇAISE

MINISTÈRE DE LA DÉFENSE

EXAMINATION REPORT

REPORT

N° 16-DGATA-MTI-P1501516001002-DR-F-Â

	N/A	Visa	Date	Post (Entity)
Author				Head of Department of « Investigations following incidents or accidents »
Technical Check				Head of the division « Materials and Technologies »
Approval				Head of the division « Materials and Technologies »

RESTRICTED CIRCULATION

Liberté • Égalité • Fraternité
RÉPUBLIQUE FRANÇAISE

MINISTÈRE DE LA DÉFENSE

DIRECTION GÉNÉRALE OF L'ARMEMENT

DGA Technical aéronautiques

REPORT	
Title or Subject	**EXAMINATION REPORTs**
Identification	**16-DGATA-MTI-P1501516001002-DR-F-Â**
Beneficiary	Ministère of the Justice – TGI Paris
N° of task sheet or contract	P1501516001
Date of issue of task sheet or contract	10/11/2015
Date report sent *(Réservé Service Courrier)*	

CLASSIFICATION	☒ **DIFFUSION RESTREINTE FOR CAUSE OF SECRET OF L'INSTRUCTION**

Durée d'archivage : the durée d'archivage standard of the reports est the durée of vie of the matériel or équipement in test

Déclassification		**Prestation**	
☒	Fiche signalétique	Lieu	DGA Technical aéronautiques
☐	A compter of the XXX	Début	01/08/2015
☐	On ordre of l'émetteur	Fin	30/06/2016

References of l'appendix of sécurité | OP N° XXX | AS N° XXX | of the XXX / XXX / XXX

Composition of the report	238 Pages dont	61 Plate(s)	13 Appendix(s)	XXX Fichier(s)	XXX Film(s)	XXX Photo(s)	XXX CD(s)
Auteur(s) :	N/A		Mot(s) clé(s) :	MH370, 777, Flaperon, Composite, Aluminium			

Métiers	**Pôles**
7 - Matériaux, Ateliers et Bureaux d'études	7 - Matériaux, composants, maîtrise risques environnementaux

Prestation étatique : Oui ☐ Non ☒ | Report joint in Indigo : Oui ☐ Non ☒

Summary :

Following the discovery on 29/07/2015 on a beach on the island of la Réunion of a part from the flight controls (a flaperon), the Tribunal of Grande Instance of Paris (TGI Paris) requested assistance from the DGA techniques aéronautiques (DGA TA) in order to perform examinations on this part.

The part arrived on site on 01/08/2015 and was placed in the Hall 42, which was secure. The seals were broken on 05/08/2015 in the presence of members of the judicial investigation and of the technical investigation.

In the light of the parts available, all of the examinations that could be undertaken on that day were performed. This report is thus intended to present the results from them.

- SUMMARY (continued) -

- SUMMARY -

Pages n°

PLATES

- SOMMAIRE - suite

Pages n°

- SOMMAIRE - suite

Pages n°

1. BACKGROUND

Following the discovery on 29/07/2015 on a beach on the island of La Réunion of a part from the flight controls (a flaperon), the Tribunal of Grande Instance of Paris (TGI Paris) requested assistance from the DGA techniques aéronautiques (DGA TA) in order to perform examinations on this part.

The part arrived on site on 01/08/2015 and was placed in Hall 42, which was secure. The seals were broken on 05/08/2015 in the presence of members of the judicial investigation and of the technical investigation.

In the light of the parts available, all of the examinations that could be undertaken on that day were performed. This report is thus intended to present the results from them.

2. HISTORY OF DOCUMENT

Version	Date	Type
A	26/07/2016	Initial Document

3. REFERENCE DOCUMENTS

1. Ordinance of expert commission (appendix 1),
2. Oath taken by expert not registered on a list of experts (appendix 2),
3. Technical proposal n°15-DGATA-MTI-P1501516001-A,
4. MMM 57-63-05 : COMPONENT MAINTENANCE MANUAL WITH ILLUSTRATED PARTS LIST - WING TRAILING EDGE FLAPERON ASSEMBLY,
5. Repairs to the flaperon seal retainers (joint mouldings), Malaysia Airliness Engineering note n° 77 IN- 57 - 20215 issue A (appendix 3).
6. Boeing responses (mail, word and powerpoint documents in appendix 13),

4. OBJECTIVES OF EXAMINATION

The objectives of the examination are detailed in the expert commission ordinance (reference 1) and in the technical proposal (reference 3) which details the requirement, which were to:

- determine if the part belonged to aircraft 9M-MRO which was performing flight MH370 on 8 March 2014,
- identify the damage and the fracture zones on the part,
- determine the buoyancy characteristics of the part,
- analyze the most significant zones in order to determine the fracture mode,
- make calculations on the broken parts, where possible (depending on the observations and of the data available).

5. PROGRESS OF THE EXAMINATION

It is useful to detail here the progress of the examination, whose various sections are then detailed item by item:

- Arrival of the part on 01/08/2015,
- Breaking of the seals on 05 August 2015, search for elements to identify various elements of the part (number, paint samples, repair), the decision was taken not to turn over the flaperon until the crustaceans expert had taken samples,
- On 06 August 2015, new search for numbers with boroscope, characterisation of defects with Boeing, 3D measurements of flaperon,
- On 09 August 2015, visit by Doctor Poupin who took the samples of the crustaceans,
- While waiting for confirmation that this flaperon belonged to aircraft 9M-MRO, work on the paints and on the repair continued through August and the buoyancy test was prepared (sample of the crustaceans, weighing, 3D measurements aimed at the construction of a model of the outside shape…),
- From 24 to 28 August 2015, performance of buoyancy tests with DGA TH,
- On 03 September 2015, confirmation by the Paris Public Prosecutor's office that the flaperon did in fact belong to aircraft 9M-MRO,
- On 16 September 2015, visit by M. Daniel of Météo France for calculations of retro-drift, M. Daniel joined up with DGA TH in order to check that the buoyancy tests had made it possible to adequately characterize the part for the purpose of these retro-drift calculations,
- On 05 Octobre 2015, validation of change to examination phase requiring dismantling and cutting for micrographic and fractographic examinations,
- From 14 to 18 December 2015, meeting in Malaysia in the context of the request for international criminal assistance, presentation of the results to the Malaysian safety investigation and to the judicial investigation drawing attention to the absence data from Boeing,
- At the start of 2016, organisation of a visit to chez Air France Industries in order to observe a flaperon in the airplane aboutment (visit on 2 March 2016). In parallel, request for information via Boeing's lawyers (partial answer only supplied on 18 March 2016),
- Organisation of a visit by the victims' families on 23 June 2016.

6. SECTION 1: IDENTIFICATION OF THE PART

The objective of section 1 was to get information that made it possible to identify the part and to check that it did in fact belong to aircraft 9M-MRO that undertook flight MH370 on 8 March 2014.

When the crate was opened, it was noted that the identification plate was missing (see plate n°1). It was then decided to :

- sample a piece of the paint that seemed to be a touch-up for analysis (see plate 2),
- check the presence of a temporary repair which had not been replaced, according to Malaysia Airliness (see plate n°3 and appendix 3 for the plan),
- undertake an boroscope search for the numbers identifying the various parts that make up the flaperon.

The boroscope inspection initially made it possible to find numbers on the panels in the area of the leading edge:

- 557 CB,
- 657 BB,
- 657 AT,
- 657 DB,
- 657 CT.

These numbers, photos of which are shown in plate n°4, correspond to those used to identify the Boeing 777 flaperon leading edge panels, these being the same as on any Boeing 777.

Passing through a hole made by corrosion, an boroscope inspection inside the box section was made. This made it possible to read off several serial and part numbers (see plate n°5). These references were provided to the Judge and to the Judicial Expert in order to determine, with the manufacturer CASA, if the part belonged to aircraft 9M-MRO from flight MH370.

According to information supplied by Boeing during the day on 06/08/2015, the correspondence between the basic parts (numbers found) and the assembled part (flaperon number) is only kept for 7 years, in theory. Thus, while waiting for the confirmation of identification by CASA the parts likely to belong to this part such as the repairs or paint touch-ups were subjected to physico-chemicals analyses in order to characterize them and to compare them to the parts supplied by the airline. The following examinations were thus performed by DGA-TA:

- paint samples from lower and upper surfaces were taken, analyzed and compared to the sample from the zone that seemed to have been touched-up (results in appendix 4),
- work to inspect the presence of a repair and specifically the characterisation of the zone that was supposed to have been repaired was continued (see plate n°3 and appendix 5 for the material and paint results).

On 03 September 2015, the Paris Public Prosecutor's office confirmed that the flaperon did in fact come from 9M-MRO, the above-mentioned no longer being useful for identification of the part and were thus not continued.

7. SECTION 2: OBSERVATION OF THE PART

The objective of section 2 was to characterize the part and the defects (fractures, damage…) that it had.

7.1. OVERVIEW

This paragraph will list different types of damage noted. In order not to dissociate the overview from the detailed examination, all of the parts with significant damage, i.e. which could explain the separation of the flaperon, is covered in section 4.

The flaperon had the following damage (those examined in section 4 are in **bold** type):

- **the inboard and outboard hinge fittings were fractured in two places** :
    - at the level of the leading edge,
    - on the lower surface of the flaperon.
- the fracture surfaces on the hinge fittings were highly corroded,
- the ribs at the edge of the flaperon show, in their metallic area, holes due to corrosion,
- **the leading edge showed dents and cracks**,
- **the trailing edge was generally broken**,
- **the lower and upper surface panels showed localised dents and the upper surface had a large crack**,
- the mounting attachment zones on each side of the flaperon were damaged or broken off.

In addition the flaperon was covered with a colony of crustaceans.

7.2. METROLOGICAL CONTROL OF THE FLAPERON

A metrological and morphological control of the flaperon was undertaken in order to determine the position and the extent of the damage noted. This included taking photos and making measurements (3D for example).

All of the metrological characteristics of the part as well as the damage and fracture zones were noted.

The first measurement on 06 August 2015, presented in appendix 6, only related to the upper surface and the ribs to prevent any manipulation of the part that could be damaging for the biological examination. It showed the absence of any significant distortion of the flaperon as can be seen in the illustration below.

RESTRICTED CIRCULATION

The 3D measurement shows that the three lines measured remained aligned on the upper surface and appear to be together seen from the side, indicating the absence significant distortion on the part

ron -

Other 3D measurements of the part were undertaken to prepare for the buoyancy test .

7.3. CRUSTACEANS

On its arrival, the flaperon was covered with a colony of crustaceans. On 5 August 2015, it was decided by the Judicial Expert not to perform any examination before these crustaceans were seen by an expert in marine biology.

This expert, Doctor Poupin, came to the DGA TA on 9 August 2015 to examine the crustaceans and take some samples for analysis. The objective was to deduce, based on the size of the crustaceans, their age and origin. In addition, siting of the crustaceans could make it possible to determine the position of the flaperon while it drifted across the sea.

To be able to continue the examinations, the upper surface and the inboard and outboard sides of the flaperon were mapped in order to determine the zones where the crustaceans were found. Each of these zones is represented on plates 8 to 13. It should be noted that there was only one crustacean present inside flaperon. The crustaceans were mainly positioned on the upper surface of the part, which led us to believe that the flaperon drifted with the upper surface immersed, on the surface of the water a priori considering their positing, as indicated by Dr. Poupin.

Then the crustaceans were sampled by zones, weighed and put into a freezer while waiting to be placed under seal and taken to the CNRS at Gif on Yvette on 24 November 2015. The total weight of the crustaceans sampled at that time was 468.3 grams. This weight did not represent that the total weight of the crustaceans since some had been taken by Dr Poupin for his analyses.

A table summarizing the samples and the weights of the crustaceans by zone can be found in plate n°14.

7.4. X-RAY FLAPERON

X-rays of the flaperon were made in order to check the presence or absence of metallic elements inside the box section formed by the two spars and the ribs.

Plate n°15 shows the local x-ray and the zones referenced 1 to 12 on the flaperon for the x-rays. The surface of the flaperon was about 2.42m^2. Plate 16 contains the relevant photos.

The lightest zones on the x-rays corresponded to salt deposits following the penetration by sea salt into the cracks in the composite panel (see §9.1 for the detail of the flaperon's structure).

The total of the surfaces bleached by the salt (slat water penetration) in the composite was approximately 0.153m^2 (see plate n°17). The thickness of the honeycomb was about 0.02m. The maximum volume of water contained would thus have been 0.00306m^3, that's to say 3.1 kg taking into account volume weight of ocean water of 1025 kg/m^3.

An boroscope inspection was made in a suspect zone (shining mark on the x-ray), the examination showed the presence of a crustacean inside the flaperon.

No traces of metallic shards was found during the examinations.

7.5. WEIGHT, DIMENSIONS OF FLAPERON AND 3D MEASUREMENTS

The flaperon was weighed, its weight being 40 kg (see plate n°18).

The dimensions and the approximate position of the centre of gravity in line with the lower surface (position not referenced in the thickness) of the flaperon are in plate n°19.

Measurements of the flaperon were undertaken for the buoyancy tests in order to supply the DGA TH with a model of the outer envelope. The dimensions of this model shown in plate 20 differ slightly from those measured in plate 19 since it did not include the joints and only slight approximations were made. The important thing being the outer volume of the part, this was not prejudicial.

8. SECTION 3: BUOYANCY TEST

The objective of this section was to determine the part's buoyancy characteristics. In order to avoid any chemical reactions that could prejudice the examinations to follow, as well as to be representative of the Indian Ocean, the test had to be performed in salt water. The fracture surfaces were protected with a varnish so as to avoid worsening the corrosion.

The test was performed by DGA TH with the support of DGA TA in salt water pool situated on the DGA TA's premises. The measurements made by DGA TH made it possible to determine the buoyancy characteristics of the par, that's to say:

- the surface attitude at rest and thus the corresponding air draft,
- the linear and angular stiffness for this attitude.

The test was performed in both possible floating positions for the part (see plates n°21 to 23). The holes made by the corrosion on the hinge fittings were blocked in order to check their possible influence on the buoyancy. It was shown that with or without these, the balance position was identical.

The tests performed showed that in that, the buoyancy was quite high. The position with the upper surface immersed seemed more stable, which is consistent with a significant presence of crustaceans on the upper surface. However, the waterline noted did not correspond to that suggested by the zones where the crustaceans were located, that's to say on the water, while the trailing edge was significantly out of the water.

In order to evaluate the conditions in which the buoyancy in this position would have been possible, the flaperon was weighted to make the waterline coincide with that defined by the presence of the crustaceans. The effective weight (real weight of 40kg minus the buoyant upthrust) to completely immerse the flaperon was 37 kg distributed across the lower surface.

By adding weights only at the level of the trailing edge, the following results were obtained:

- lower surface upwards, it was necessary to add 13.5 kg along the trailing edge,
- when the upper surface was placed upwards, only 5 kg was required.

Taking into account the x-rays made (see §7.4), absorption of about 3.1 kg of water in the honeycomb structure of the panels is not sufficient to explain this gap. Equally, the small amount of residual trailing edge structure did not make it possible to absorb sufficient water to cause the flaperon to tip over towards the rear.

The detailed results of this test are in the reports n°E611374 parts 1 and 2 written by DGA-TH. (see appendices 7 and 8).

In addition, DGA TH also made calculations of drift coefficients that were used by Météo France for the retro-drift calculations for the flaperon. The report on this work, numbered E611374 part 3, is in appendix 9.

9. FLAPERON COMPOSITION AND ENVIRONMENT

This chapter details the composition of the flaperon and its environment. These data are useful in understanding the various examinations as well as the conclusions.

9.1. FLAPERON COMPOSITION

Although we had not received the exact plans of the flaperon, the various parts at our disposal as well as the observations performed made it possible to detail the composition of this flight control surface.

The structure of the flaperon is hybrid as it contains metallic parts, in particular the hinge fittings, assembled with the parts in organic matrix composite materials, which will subsequently be referred to as composite materials.

In order to avoid any confusion there follows a short definition of what a composite structure can be, with examples linked to the flaperon :

A composite structure is made up of two basic parts: fibres and resin. When the fibres are pre-assembled in folds, they are laid out according to a draping plan with some resin. Cooking then takes place and the part is then formed. Unlike a metallic part, the material really only exists once it is assembled according to the plan for the part and then cooked. Thus, it is inseparable from the part that it constitutes as it does not pre-exist and its mechanical characteristics depend on its plan.

There are two main types of composite structure on fixed-wing aircraft:

- *monolithic structures containing only fibres and resin (the leading edge of the flaperon is made this way),*
- *sandwich structures which include two monolithic skins in the middle of which is glued a third component such as in the case of the flaperon skins where a honeycomb is found.*

The following diagram details the parts at our disposal and those that we observed.

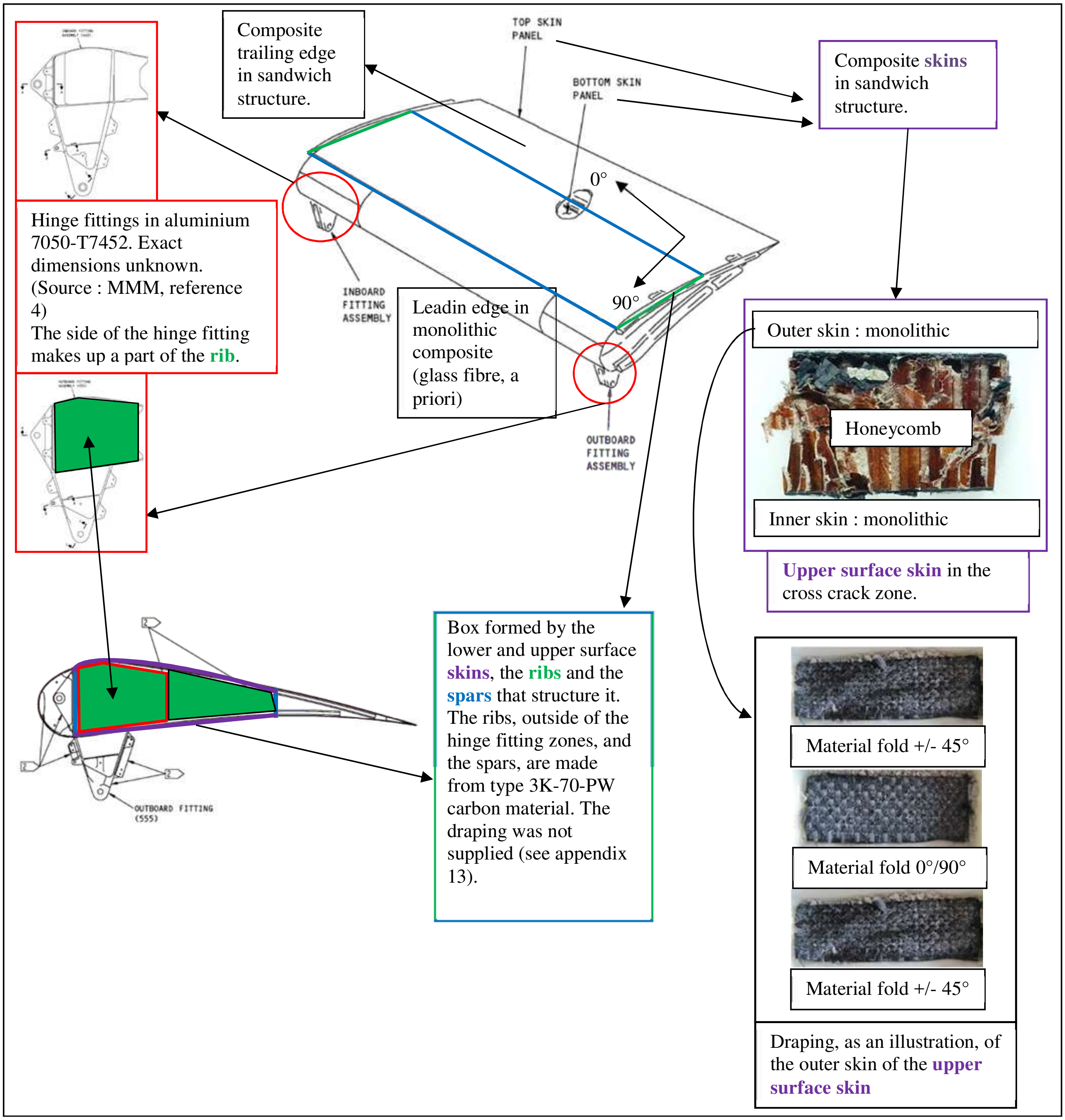

- Composition of the flaperon -

The two hinge fittings connect with the structure of the wing. The flaperon's resistance is in itself ensured by the box formed by the 2 spars, the two ribs and the skin. The leading edge and the trailing edge are subject to lower stress and mainly have an aerodynamic role.

9.2. CONNECTIONS WITH THE WING

The hinge fittings located on the aeroplane and on the flaperon are those parts that ensure attachment of the latter to the aeroplane. The other attachment parts visible on the diagrams constitute secondary load paths.

The two hinge fittings on the flaperon side have two lugs:

- The one at the level of the leading edge that picks up loads from the actuator,
- The one located in the lower part is directly linked to the wing by an hinge point that serves as the hinges around which it pivots. The lower part of the hinge fitting seems to be designed to pick up forward-aft axial loads (logical given the function of the flaperon) and its bearing of lateral loads, i.e. in the direction of the flaperon span, seems limited.

On the aeroplane side, the same number of lugs is found, one attached to the other end of the activator and the other directly opposite the lower flaperon lug. The image below shows this attachment system for the inboard hinge fitting.

All of the links, which should allow rotational movement, are ensured by of the hinge points passing through the lugs.

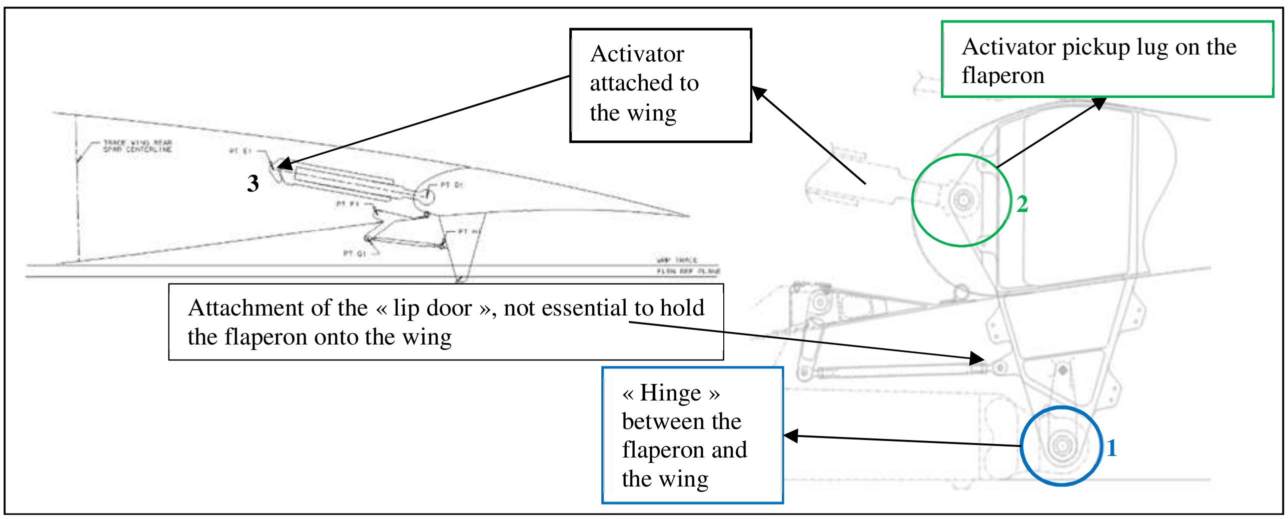

- Flaperon attachments -

The number of critical flaperon attachment points can thus be reduced to three on each side (see diagram above) since the lower wing lugs and flaperon constitute a hinge by being attached to a single hinge point. The loss of one of these attachment points is likely to lead to the separation of the flaperon by causing a possible chain-reaction fracture of the other attachment points.

It should be noted that, according to Boeing (meeting on 06 August 2015), the loss of a flaperon does not prevent the flight being continues and that some of its parts are even « fuses ». These “fuse” zones on the flaperon were not provided by Boeing (see appendix 12).

9.3. FLAPERON ENVIRONMENT

The parts supplied by Boeing, in addition to the visit to a Boeing 777, made it possible to define the flaperon's environment which might explain some of the damage noted. The image below shows the flaperon in the retracted position as well as the parts of structure facing it.

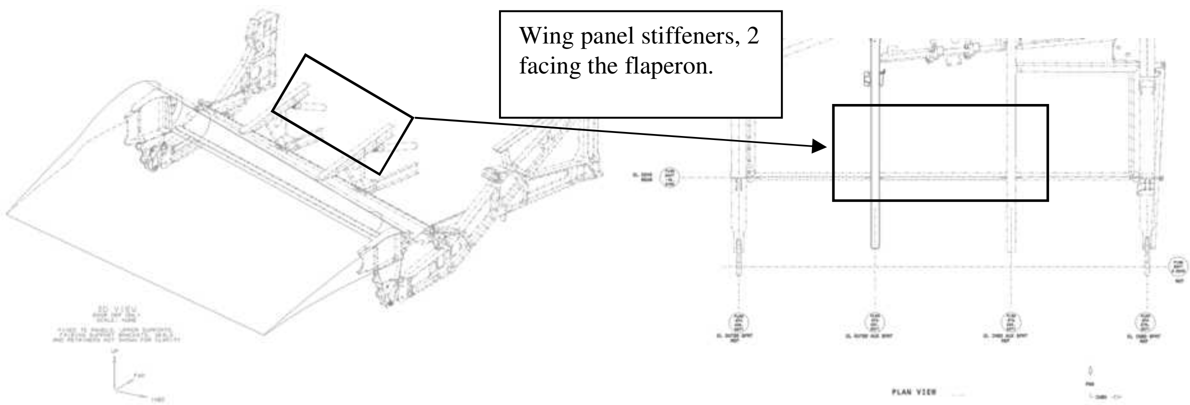

- Flaperon in retracted position, wing parts nearby -

The flaperon is surrounded by other flight control surfaces. Profile continuity between these parts and the flaperon explains why the latter is thicker outboard than inboard. Finally, it should be noted that the flaperon that we received is completely hidden by the engine when seen from the front of the aeroplane. The following images show the flaperon in the aeroplane environment.

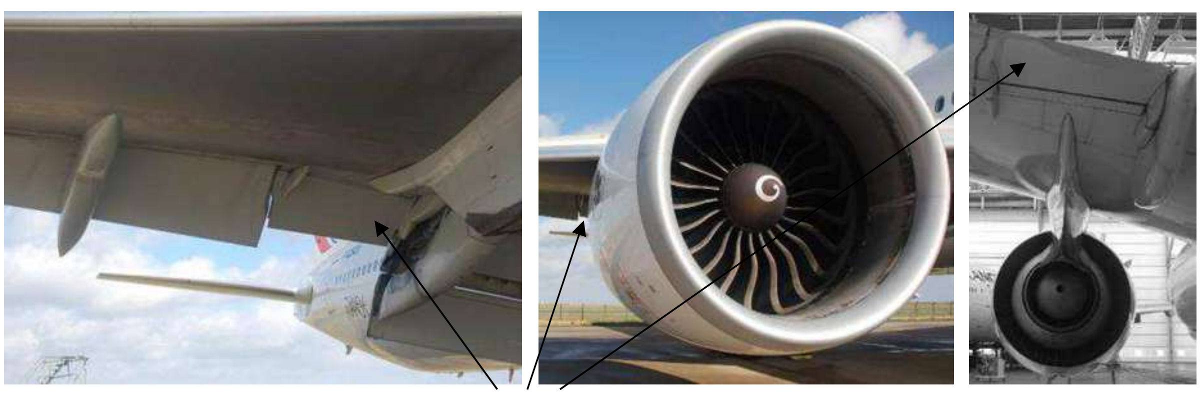

- Flaperon fitted on aeroplane -

10. SECTION 4: TECHNICAL LABORATORY ANALYSES

The fracture zones and the damage identified in section 2, judged to be interesting in determining the phenomenon that caused the separation of the flaperon from the aircraft, were analyzed so as to determine the cause of the damage, the type of fracture and possibly the direction of loads, given the work planned in section 5.

The analyses are presented in two sub-sections, one relating to the metallic parts which, with the exception of the ribs, means the links with the wing, the other on the parts made of composite materials, thus the structure of the flaperon itself.

When it was possible, a materials compliance analysis was also undertaken.

10.1. METALLIC PARTS – LINKS WITH THE WING

Initially, it should be stated here that the level of corrosion of the various fracture surfaces of the metallic parts ma de it impossible to undertake a Scanning Electron Microscope (SEM) examination. In fact, this initial condition made it impossible to reach the level of preparation required to undertake the appropriate observations. It was thus not possible to confirm the observations made by the macrographic examinations with the micro-fractographic examinations.

10.1.1. OUTBOARD HINGE FITTING AND NEARBY ELEMENTS

Plate n°24 shows the two fractures on the outboard flaperon hinge fitting (lower surface and leading edge sides after disassembly of the panel).

Plate n°25 shows the direction of the distortions and the tears at the level of the ribs near to the fracture on the leading edge side and plate n°26 shows the direction of the distortions on the parts located behind the hinge fitting.

Visual examinations showed that the loads causing the distortions were oriented from inboard towards outboard, which is particularly notable at the level of the leading edge ribs.

In order to perform a metrological inspection on the hinge fitting, the latter was dismantled (see plate n°27). The fracture surfaces on the leading edge side and lower surface are shown in plates n°28 to 30. All of the fractures were of static-type morphology and were highly oxidized.

The hinge fitting side had numerous oxidized holes due to exposure to sea water.

10.1.2. INBOARD HINGE FITTING AND NEARBY ELEMENTS

Plate n°31 showed the inboard hinge fitting after removal of the leading edge panel, and shows, after disassembly of the seal retainer, that a repair had been made. This repair could not be identified. A priori it was not in the in the Malysia Airlines aeroplane log as it was not mentioned as a means of identifying the part and Boeing did not indicate that the flaperon had any variance (see appendix 10). It thus seems possible that this repair, which can be considered as minor, was not recorded.

Plate n°32 shows general view of the fractures on the lower surface side and leading edge of the inboard hinge fitting.

Plate n°33 shows the fracture on the leading edge side, the distortions of the rib next to the lug, as well as those on the upper surface panel. The examinations showed that the loads were oriented inboard towards outboard.

Plates n°34 and 35 had fractures on the lower surface side of the hinge fitting and at the level of cover attachment. The latter had no particular distortion that could be examined and its fracture surface was highly oxidized.

The inboard hinge fitting was disassembled for a metrological inspection (see plate n°36). Plates n°37 to 39 show the inboard hinge fitting fractures after disassembly. All of the fractures were of static-type morphology and were highly oxidized.

10.1.3. METROLOGY OF THE OUTBOARD AND INBOARD HINGE FITTINGS

In the absence of any plans of the hinge fittings and for the purpose of measuring possible overall distortion of the latter, references were made by the metrology department based on non-distorted parts, as illustrated below, on the inboard hinge fitting. The distortions were thus measured against these references and not against the plans of the part. The complete metrology report is in appendix n°10.

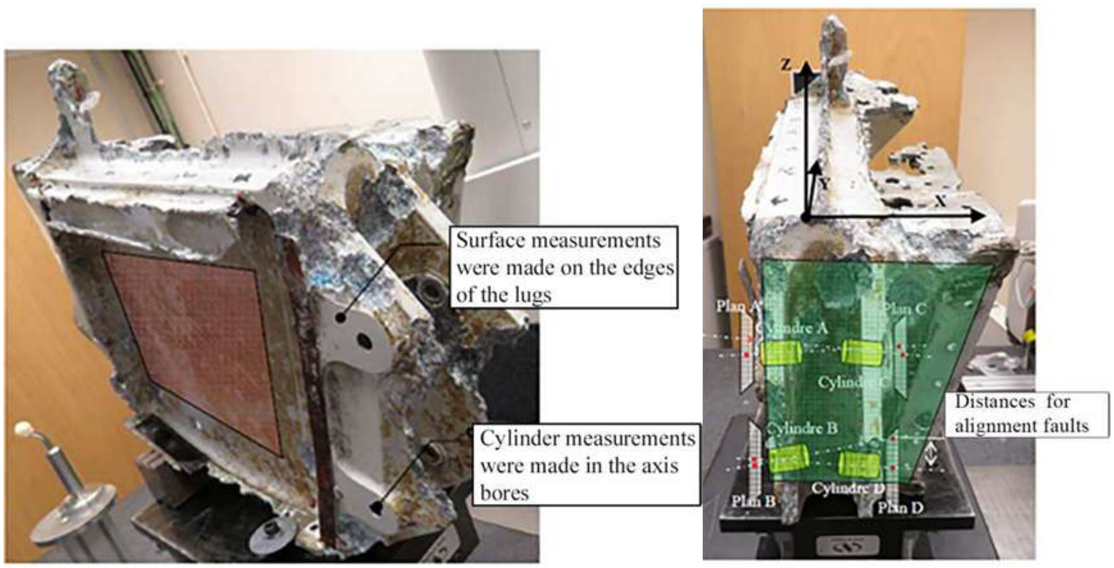

- Creation of references for the measurements and measurements on the inboard hinge fitting -

Plate n°40 shows a slight distortion of the outboard hinge fitting towards the outside of the aeroplane.

The inboard hinge fitting also shows minor distortion towards the outboard hinge fitting (outside of the aeroplane, see plate n°41).

10.1.4. MATERIAL COMPLIANCE OF THE HINGE FITTINGS

A metallurgical inspection (chemical analysis, measurement of conductivity and hardness tests) was performed on one of the hinge fittings without damaging it in order to check its compliance against the MMM specifications (reference 4). The metallurgical analyses required slight polishing of the surface of the hinge fitting.

The MMM indicates hinge fittings with type 7050 aluminium of T7451 grade. The chemical composition of the hinge fitting analyzed (see appendix n°11) as well as the other examinations performed produced of results in accordance with this specification: XXX

- The grade of aluminium corresponds to that of a type 7050 alloy,
- The values for conductivity (**23.25** MS/m on average) and Brinell hardness (**162** HB2.5/62.5 on average) corresponded to 7050 alloy of T73651 grade according to IGC 04.02.110B. The T73651 metallurgical grade (European standard) is equivalent to metallurgical grade T7451 (American standard).

10.1.5. DAMAGE NOTED ON THE LEADING EDGE RIBS

In addition to the hinge fittings, it was useful to contrast the supposed distortion direction with what was observed on the nearby parts, in particular at the level of the leading edge.

Plate n°42 summarizes the direction of the distortions of the hinge fittings with those noted on the ribs close to the hinge fittings. All of these distortions were correlated and were going in the inboard – outboard direction. The image below shows an example of these observations for the outboard side.

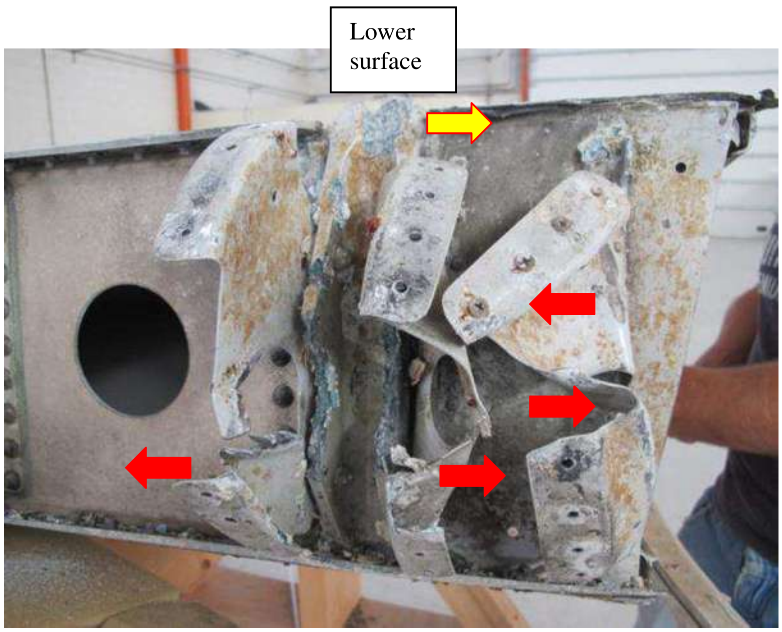

Direction of the hinge fitting against the reference plan

Direction of distortion of the ribs

- Distortions of the outboard hinge fitting and of the leading-edge ribs

The leading edge ribs were bent and in places seemed to have been torn by another part. After the visit made to an aircraft, it appeared that the hinge point that allowed the return of the activator at the level of the hinge fitting could be the cause of the tears of the while the ribs could have pressed on the shaft or the body of the activator, which would explain the form of the folds (see plate 43).

10.1.6. CONCLUSION ON METALLIC PARTS

The examinations performed showed that :

- the separation of the flaperon from the aeroplane occurred on the flaperon side with :
  - the activator return lugs being broken,
  - the lower parts of each hinge fitting at the level of the lower surface being broken,
- all of the fracture surfaces were a one hundred percent static morphological type, but it was not possible to confirm that using the SEM due to the high level of oxidization,
- the damage noted on the ribs seemed to be linked to the hinge point attachments to the activators as well as to the shaft or body of these activators,
- the slight distortions measured on the hinge fittings and the distortions of the ribs were all oriented in the direction, inboard towards outboard,
- the materials inspected on the hinge fittings was in compliance with the information in the MMM (reference 4).

10.2. COMPOSITE MATERIAL PARTS – STRUCTURE OF THE FLAPERON

Before any other considerations, it should be noted here the most significant oservation the on the parts made of composite materials was that performed macroscopically In fact, the make-up of the material, with fibre folds oriented in different directions according to a draping plan, meant that analysis of the fracture surfaces at the microscopic level could sometimes be complicated or even made contradictory since each fold, due to its orientation, was not loaded in the same manner as another. In addition, the observations performed here were sometimes only able to be performed on small thicknesses because of the pollution, thus in some cases only representing one fold, thus only one orientation. Nevertheless, the microfractographic observations confirmed in the vast majority of cases those of the macroscopic observations.

10.2.1. OVERVIEW

Comparison with an undamaged flaperon showed that the part behind the rear spar was missing (see plate 44). The missing part represented about 1/3 of its original surface.

10.2.2. LEADING EDGE

The leading edge had several areas of damage :

- dents and tears at the level of the removable access doors, in particular on the outboard side,
- four vertical impacts in the central zone.

A small part of the access door on the inboard side was missing. On the outboard side, the access door made of several parts was broken and had a tear indicating indicating being hit by another part. (see plate 45).

The leading edge had four vertical impacts that suggested interaction with a part directly next to the flaperon (see plate 46). The fact that the leading edge was not destroyed equally suggests a secondary impact, i.e. after that which caused the separation of the flaperon.

In the absence of any precise data being supplied by Boeing, it was decided to check on a Boeing 777 if the nearby structure could explain these marks. This was not the case. The data supplied by Boeing a posteriori confirmed the absence of a part directly next to the flaperon that may have caused an impact that would leave these four marks with spacing observed (see plate 47).

10.2.3. LOWER SURFACE

10.2.3.1. VISUAL OBSERVATION

The observations made on the lower surface with it oriented upwards.

The lower surface of the flaperon had several dents (see plate 48).

The fracture on the trailing edge consisted of two distinct parts. The first two-thirds were straight and the fracture followed the rear spar (coming from the outside of the aeroplane towards the inside). The last third was not straight and had a more uneven surface (see plate 49).

10.2.3.1. OBSERVATION OF THE IRREGULAR TRAILING EDGE FRACTURE

Observation of the irregular part showed a smooth fracture, without protruding fibres, characteristic of a compression fracture (see plate 49).

A piece of composite was sampled (see plate 50) at the level of the irregular trailing edge fracture, then observed with the FEG-SEM. This piece consisted of an inner skin, honeycomb and an outer skin. Both skins were examined.

The inner skin fracture consisted of both the parts characteristic compression (fibres in the same fracture plane; steps) and of the parts characteristic traction (radiating fibres on the fracture surfaces, various fibre fracture planes). However, observation of all of the fracture surfaces showed that the compression zones seemed to be in the majority.

The fracture of the outer skin also exhibited compression and traction. But, in this case, observation of all of the fracture surfaces showed that the traction zones seemed to be in the majority.

Taking into account the macroscopic and microscopic observations, the irregular trailing edge fracture seemed to have occurred in bending, from the lower surface towards upper surface.

10.2.3.2. STRAIGHT TRAILING EDGE FRACTURE

Observation of the straight fracture (see plate 51) brought to light the irregularity of the fracture in the upper layers of composite and the regularity of the fracture of the lower layers of composite, with no protruding fibres. The upper layers thus seemed to have failed in traction around of the attachments (peeling) and the lower layers in compression. Observation of this straight fracture also showed the material to be oriented towards the bottom (lower surface oriented upwards).

A piece of composite was sampled (see plate 52) at the level of the straight trailing edge fracture, then observed under the FEG-SEM.

Observation of the fracture on the intermediate folds indicated that the compression zones seemed to be in a majority, even if there were some zones of traction present.

It was the same for the fracture on the inner folds: there were some zones of traction present, however compression zones seemed to be in a majority.

Taking into account the macroscopic and microscopic observations, the straight trailing edge fracture seemed to have occurred in bending, from the lower surface towards upper surface.

10.2.4. UPPER SURFACE

10.2.4.1. VISUAL OBSERVATION

The observations were made with the upper surface oriented upwards.

The top of the upper surface of the flaperon had several dents (see plate 53), several impact marks and a crack several centimetres long.

The trailing edge was broken. The fracture was regular, with no protruding fibres (see plate 54).

The impact at the end of the crack as well as a part of the crack were extruding (see plate 56). The damage observed indicated the presence of a « high energy » event.

10.2.4.2. TRAILING EDGE FRACTURE

Taking into account the regular appearance of the fracture with no protruding fibres, there was likely some compression present (see plate 54). Further, observation of the fracture also showed the material to be oriented towards the bottom (lower surface oriented upwards).

A piece of composite was sampled (see plate 55), then observed with the FEG-SEM. This piece consisted of an inner skin, honeycomb and an outer skin. Both skins were examined.

Observation of the fracture of the inner skin showed the presence of traction. However, many of the zones were not observable, as they were highly polluted: it was thus impossible to state categorically that there was no compression.

Observation of the fracture of the outer skin indicated that the traction seemed to be in a majority, even if there were some zones of compression present.

The macroscopic observations indicated at first sight compression loading on this zone, even some bending towards the outside, i.e. lower surface towards upper surface, due to various folds of enshrouding matter observed. This was not confirmed by SEM observations. In fact, under pure bending load from the lower surface towards the upper surface, it was expected to find mainly traction on the inner skin and compression on the outer skin. The following sections may explain this inconsistency:

- the loading was not oriented in a uniform manner which, on a composite part with various fold orientations, made correlations even more complex,
- the zones observables with the SEM were small due to the pollution and made it impossible to confirm compression as the principal mode in the outer skin with any certainty,
- this fracture could be the consequence of the preliminary trailing edge fracture on the lower surface.

10.2.4.3. UNPIERCED CRACK

A piece of composite was sampled at the level of the crack, in a part where the latter was not pierced (see plate 57): only the outer skin was broken and was thus observed.

Macroscopically, the outer skin seemed to have broken in bending. Microscopically, it seemed that the closer the observations were made to the paint, the more traction seemed to be in the majority. And, the closer the observations were performed to the honeycomb, the more compression seemed to be in the majority.

The fracture at the level of the unpierced crack was thus in bending, probably due to skin bowing.

In this zone, a calcination test was performed so as to establish the orientation of the folds of the outer skin of the box. The results are presented in plate 58.

10.2.4.4. PIERCED CRACK

A piece of composite was sampled at the level of the crack, in a part where the latter was pierced (see plate 59). This piece consisted of an outer skin, of honeycomb and an inner skin. At the level of the outer skin, material orientation towards the bottom was observed. It thus seems that a part from outside the flaperon pierced or dented this zone (part of the aeroplane, water penetration?).

Observation on the FEG-SEM (see plate 60) of the fractures on the outer skin and on the inner skin showed that on the usable zones (very polluted fracture surfaces), traction seemed to be in the majority, even if there was some compression present.

The low usable thickness made it impossible to conclude that there was a simple traction fracture, though a fracture resembling traction could be a consequence of a shearing load given the draping observed in this zone.

10.2.5. SUMMARY OF THE EXAMINATIONS

It appears that the flaperon lost nearly one third of its surface behind the rear spar. The observations were performed with the upper surface upwards (see plate 61).

- Leading edge

The access door on the inboard side was partially broken off. On the outboard side, note dents and tear were noted, suggesting contact with one or more nearby parts.

In its central part, the leading edge had inexplicable dents and vertical cracks.

- Lower surface(trailing edge)

At the level of the fracture of the trailing edge, the material was oriented upwards. The straight trailing edge fracture was linked to bending loads. The irregular trailing edge fracture was from bending: mainly traction on the outside and compression on the inside.

- Upper surface(crack and trailing edge)

The upper surface had some dents, impacts, of which one was salient and a crack with one salientpart.

The trailing edge fracture was uneven but was locally clean with no protruding fibres which, combined with material orientation upwards, suggested bending. However, microscopic examinations indicated mainly fractures in traction in this zone. This fracture of the trailing edge side upper surface could have occurred after that on the lower surface, which would explain its uneven character.

In its non-salient part, the fracture at the level of the crack occurred in bending: traction mainly on the paint side and compression mainly on the honeycomb. This leads to the assumption of bowing.

In its salient part, the fracture at the level of the crack seemed to have occurred in traction. The material was oriented downwards in this zone, which suggests possible penetration by a part from outside the flaperon, which then fell out, or damage linked to water ingestion.

10.3. CONCLUSION – SEPARATION AND DAMAGE SCENARIO

Concerning the dents, it is likely that some ‘objects’ struck the the flaperon forcibly.

The perforations observed were likely due to the presence of salient parts on these ‘objects’.

On the base of the observations and examinations performed, it is possible to **hypothesize** a scenario that could have led to the separation and to the damage noted on the flaperon.

First of all, it appears possible to exclude in-flight loss of the flaperon since its weight is concentrated forwards, which would a priori lead to a fall with the leading edge forwards and the probable destruction of the latter. The damage to the trailing edge would also likely be different. A simulation of a flaperon fall with an initial speed corresponding to that of an aeroplane in flight would enable this to be definitively eliminated.

The hypothesis for a separation and damage scenario would be as follows:

1. Considering an impact with water as likely, and considering the damage observed, it seems that the flaperon must have been deflected at the time of the impact,

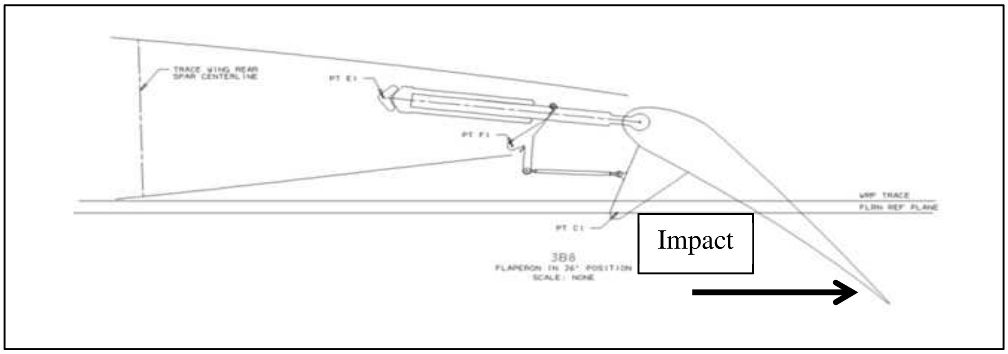

- Presumed position of the flaperon on impact -

2. The damage being greater on the trailing edge on the inboard side, notably on the lower surface side, it appears that the contact occurred first in this zone. The loads generated, pushing from the lower surface towards the upper surface locally (unlike uniform aerodynamic loading), resulted in a bending load from the rear towards the front as well as of inboard towards outboard. This caused torsion on the flaperon.

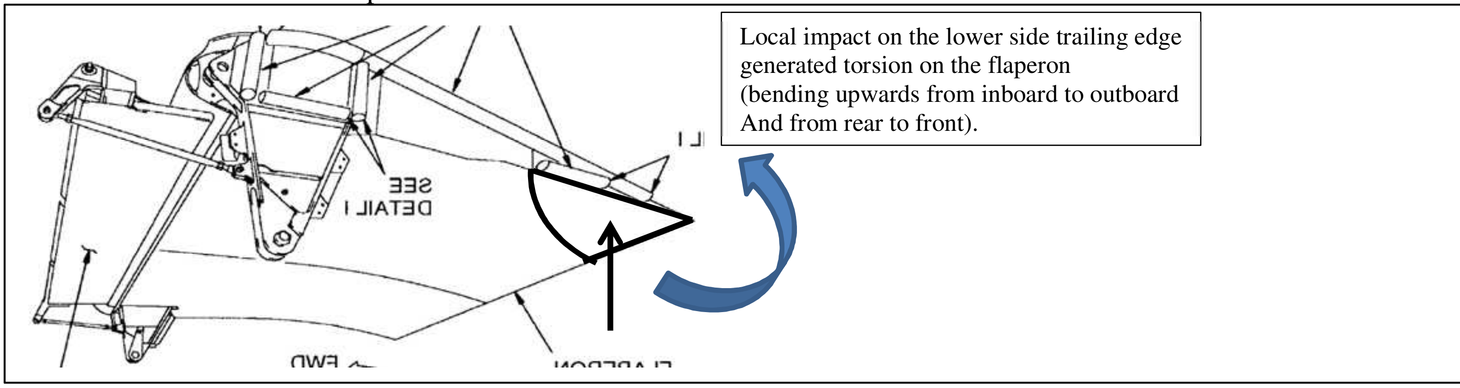

- Impact point and torsion loading on the flaperon -

3. This contact led to the dispappearance of a large part of the trailing edge, behind the rear spar (trailing edge bending upwards). The crack observed on the upper surface could be a consequence of the loads linked with the torsion that would

have generated bowing near the forward spar and a shearing fracture in more in the centre of the flaperon.

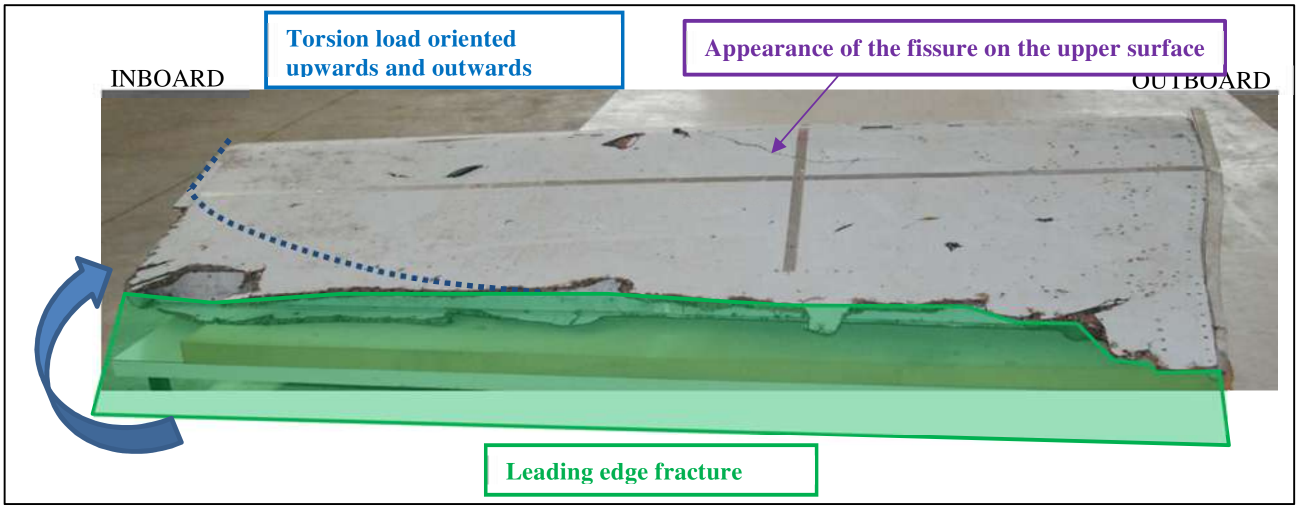

- Fracture of the trailing edge and appearance of the crack on the upper surface-

4. Almost simultaneously, this torsion from inboard towards outboard and from the rear to the front broke off the lower part of the inboard hinge fitting, not designed for this type of load.

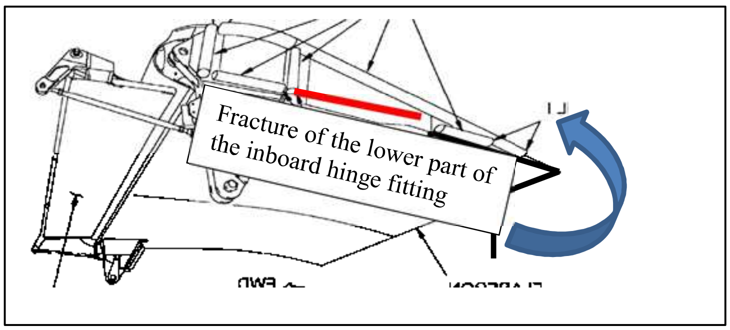

- Fracture of the lower part of the inboard hinge fitting -

5. The flaperon pivoted from the inside towards the outside around the outboard hinge fitting (anticlockwise direction). This caused the fracture of the lower part of the outboard hinge fitting as well crushing the fairing of leading edge and pushing the of leading edge ribs onto the actuating cylinders, which would explain their being crushed. The inboard then the outboard lugs, which the activators are attached to, broke off and the flaperon detached. The moment when the fracture of the lugs occurred during this sequence is not clearly definable, in particular the fracture of the inboard lug before that of the lower part of the outboard hinge fitting.

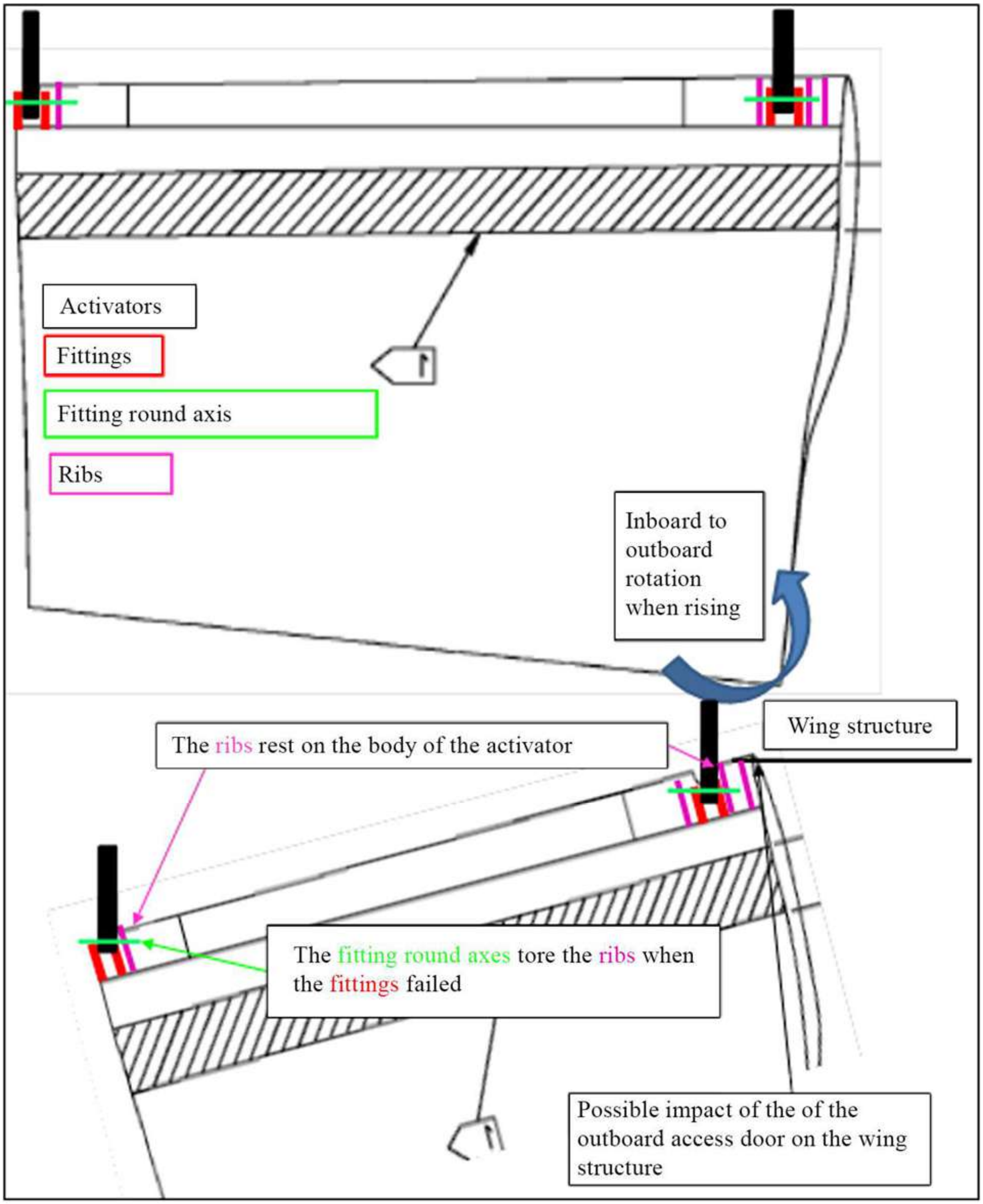

- Ribs and lugs fracture damage sequence: separation of the flaperon -

Beyond the possible in-flight loss, which is not entirely excluded, this scenario can only be considered as a hypothesis since:

- no available parts allowed us to perform the work in section 5 that could corroborate this,
- the flaperon is aft of the engine which leaves some doubt as to its loading during aeroplane impact with the water,
- the phenomena at issue are highly dynamic and thus difficult to exploit.

11. SECTION 5: CALCULATIONS AND SIMULATIONS

As stated above, the parts available to us did not make it possible to perform work planned for this section (see appendix 12 for the missing parts).

12. CONCLUSIONS

The identification numbers of the flaperon components found thanks to the boroscope inspection allowed the manufacturer of the part to confirm to the Judge and to the Judicial Expert that the part did indeed belong to the Malaysia Airliness aeroplane registered 9M-MRO of (communication by the prosecutor's office on 3 September 2015).

Before any destructive tests, the part was examined in its entirety. Its characteristics were recorded. Damage to it, as well as the colony of crustaceans on it, was mapped.

A buoyancy test was performed by DGA TH in the premises of the DGA TA and allowed flaperon bouyancy to be characterized.

The significant damage was appraised for the purpose of determining a scenario for separation of the part from the aeroplane. In the absence of data from Boeing, and despite the deterioration of some fracture surfaces, a hypothesis was nevertheless formulated: taking into account the results of the examinations, it appears that the flaperon impacted the water while still attached to the aeroplane and that at the time of the impact it was deflected. A fall simulation for the flaperon with an initial speed corresponding to that of an aeroplane in flight could definitively exclude the loss of the latter in flight.

The little data supplied by Boeing did not enable the examination to be progressed by making calculations that would have made it possible to confirm or reject the proposed hypothesis.

- PLATES -

PAGE SANS TEXTE

Planche 1 : **Photos of presentation of the flaperon received for examination**

Leading edge

Trailing edge

Missing identification plate

Inboard side

Outboard side

Planche 2 : **Paint sample in a zone that appeared to have been touched up**

Cut

Paint sample

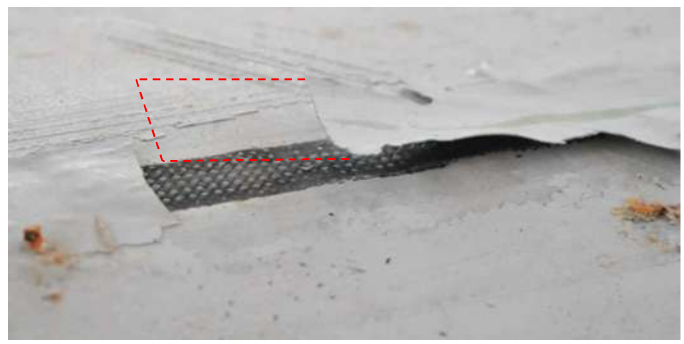

Piece of paint sampled

Sampling to search for explosive residues

Planche 3 : **Check on the presumed repair made by Malaysia Airlines**

Addition of a riveted piece on the back of the joint

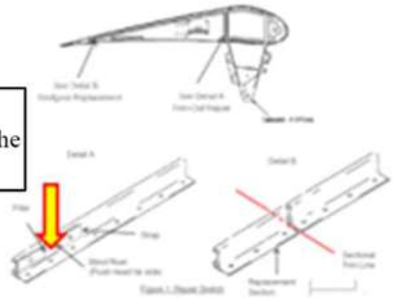

Repair on the joint moulding

Repair on the joint moulding

Removal of joint

Cutting off joint moulding to check repair

No repair on joint moulding

Joint moulding (see from behind)

View of area after cutoff

This repair is a minor and temporary repair and that should be replaced by a modification (according to ref. 6 in appendix 11). It thus seems probable that application of the modification was not recorded.

Planche 4 : **Boroscope inspection – leading edge**

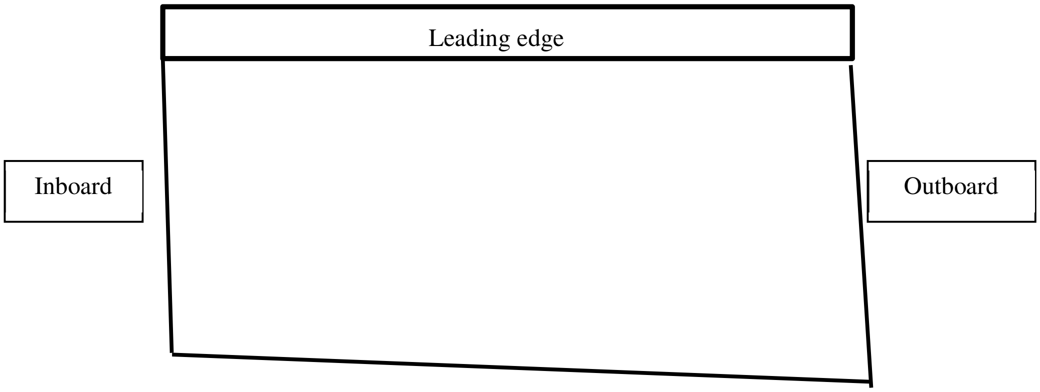

Numbers on the leading edge access panels

557 CB

657 BB

657 AT

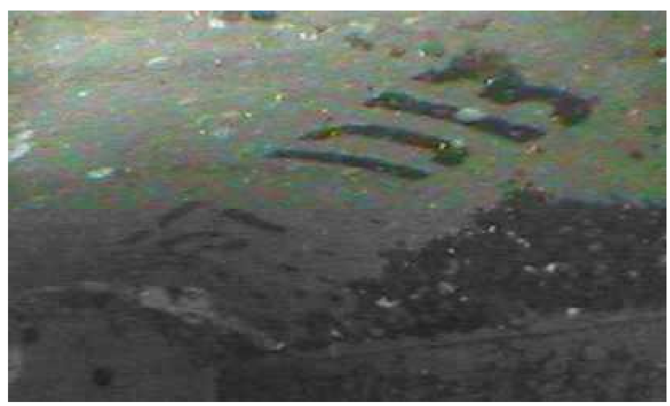

657 DB

657 CT

Planche 5 : **Boroscope inspection - box**

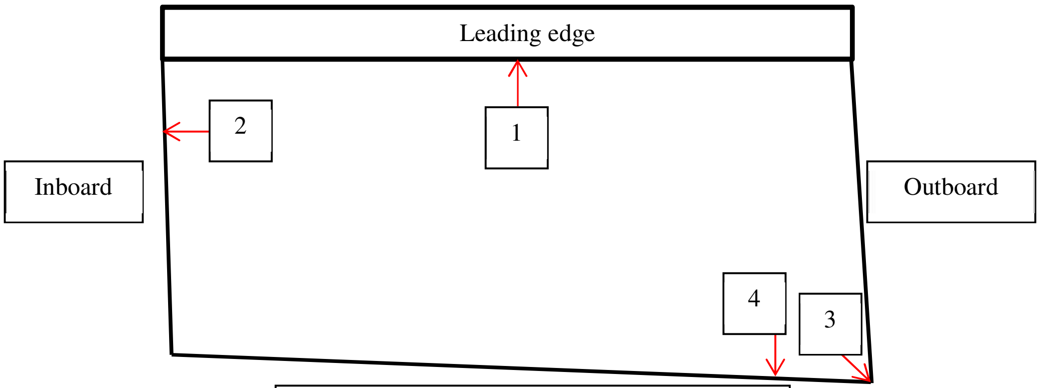

Position of references noted

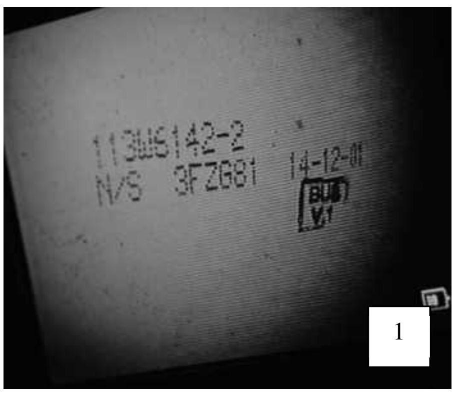

Reference n°1 on forward spar

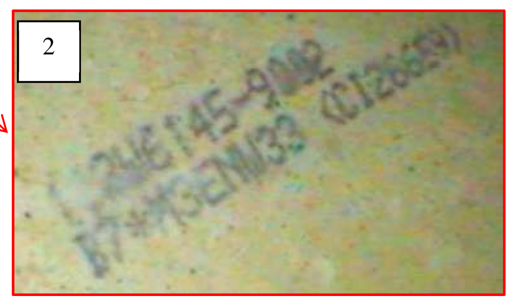

Reference n°2 on inboard side

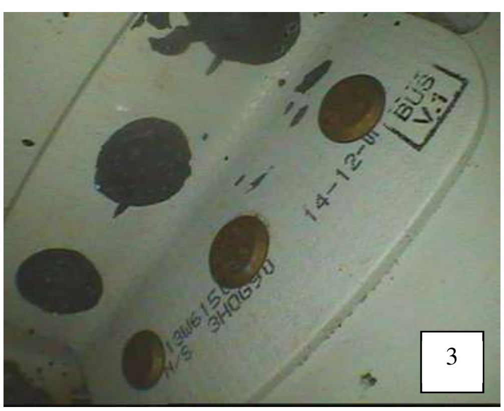

Reference n°3 on the bracket between the outboard side and the aft spar

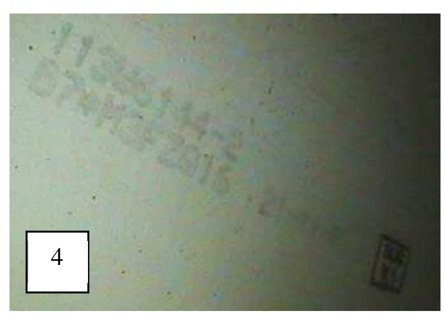

Reference n°4 on the aft spar

LOCALISATION OF THE CRUSTACEANS AND SAMPLES

Planche 6 : **References of the zones on the flaperon**

Leading edge

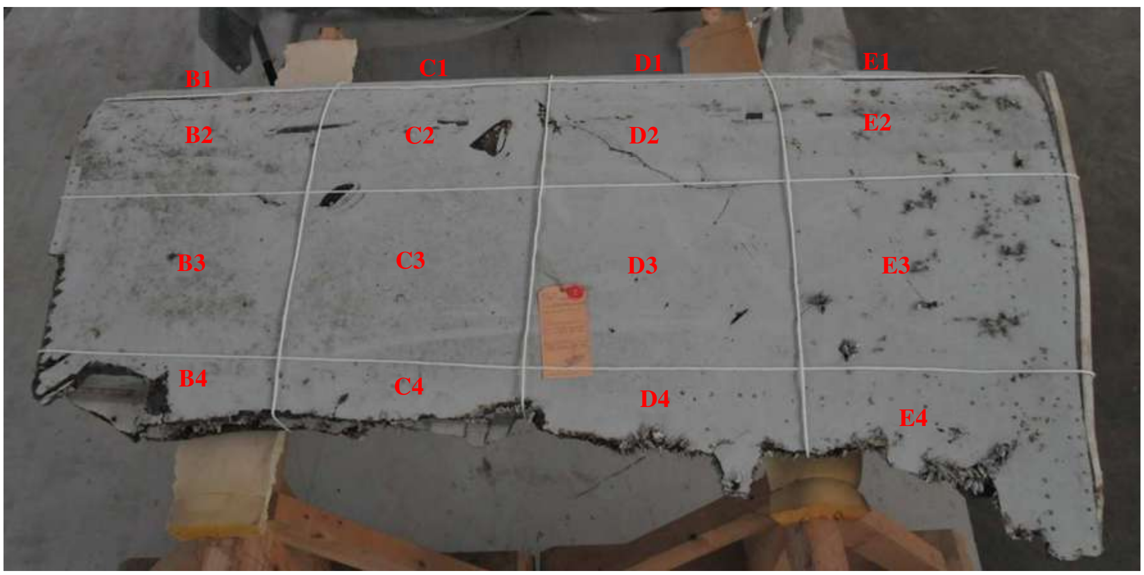

Upper surface side

Trailing edge

Planche 7 : **Rferences of the zones on the flaperon**

Side A

Côté A

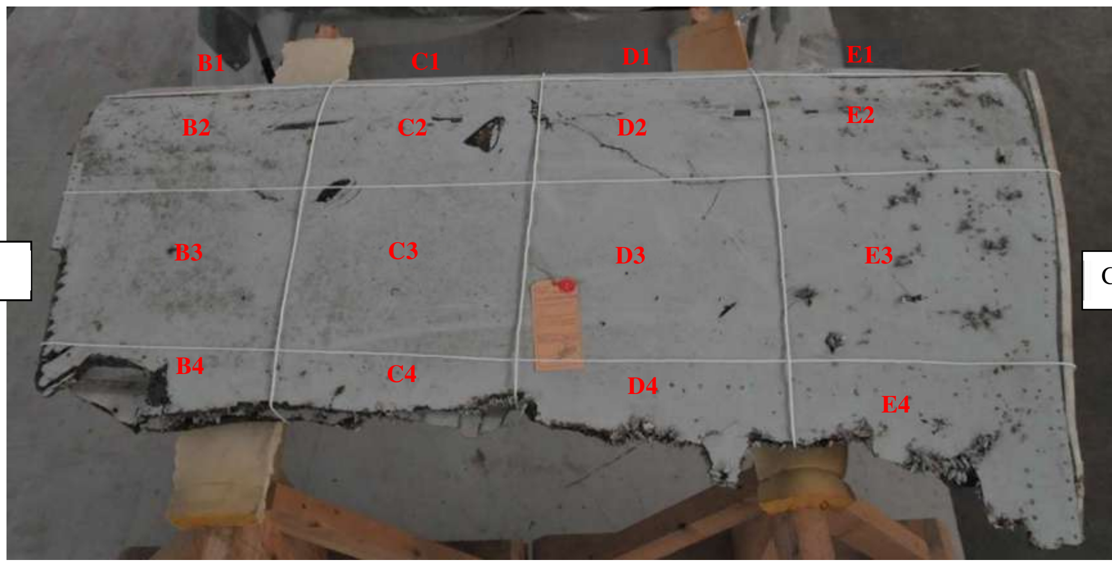

Côté F

Upper surface

Side F

Planche 8 : **Detail of zones A on the flaperon**

Side A

Zone A1

Zone A2

Zone A3

Zone A4

Planche 9 : **Detail of the zones B on the flaperon**

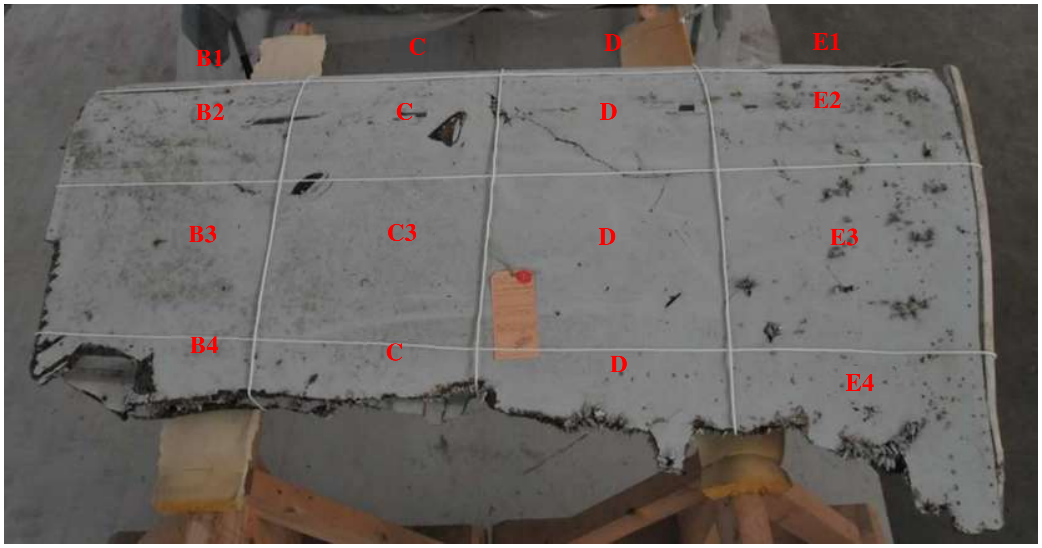

Zone B1

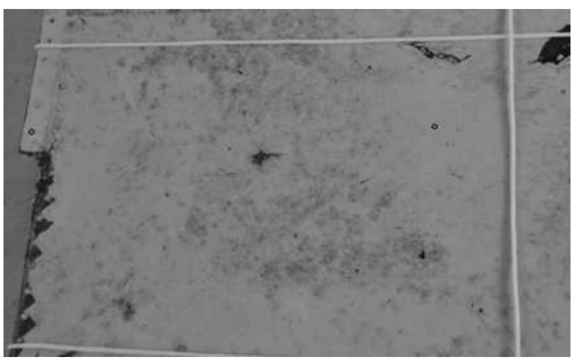

Zone B3

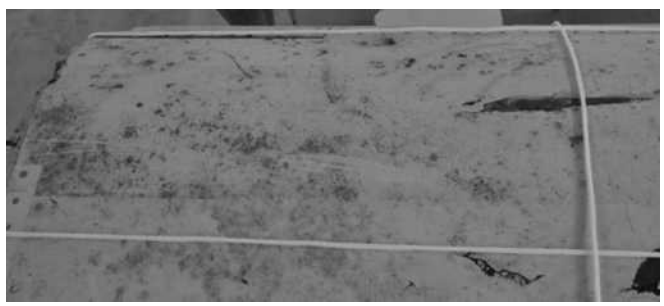

Zone B2

Zone B4

Planche 10 : **Detail of the zones C on the flaperon**

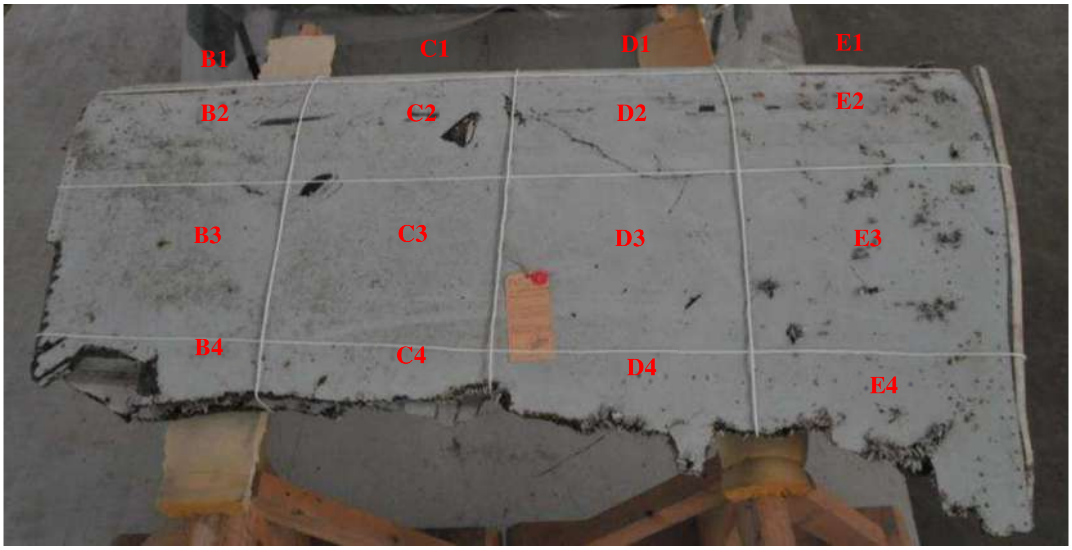

Zone C1

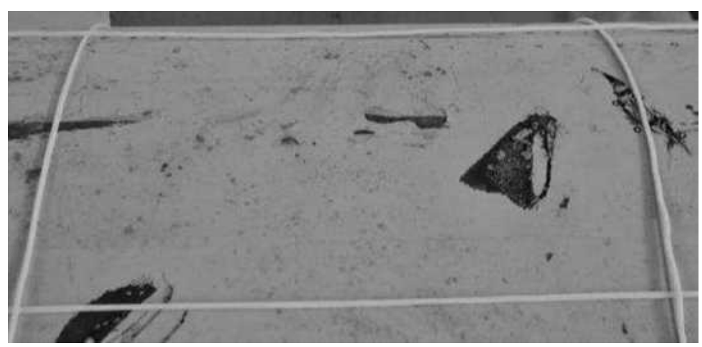

Zone C2

Zone C3

Zone C4

Planche 11 : **Detail of the zones D on the flaperon**

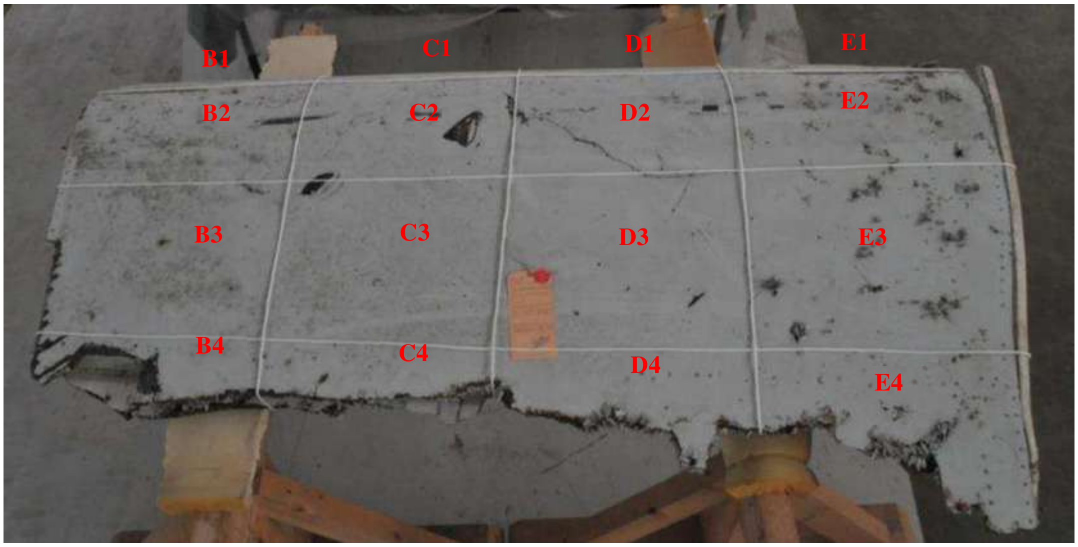

Zone D1

Zone D3

Zone D2

Zone D4

Plate 12: Detail of zones E on the flaperon

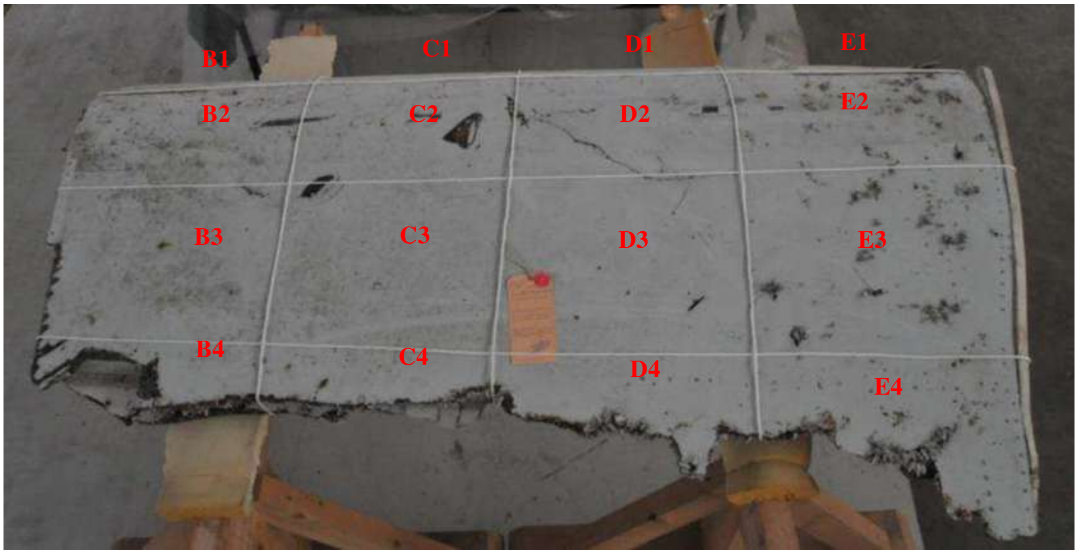

Zone E1

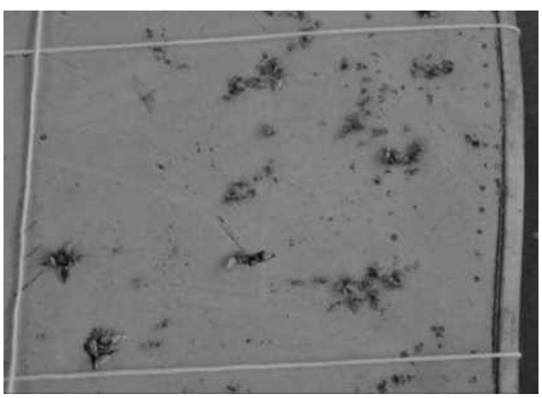

Zone E3

Zone E2

Zone E4

Planche 12 : **Detail of zones F on the flaperon**

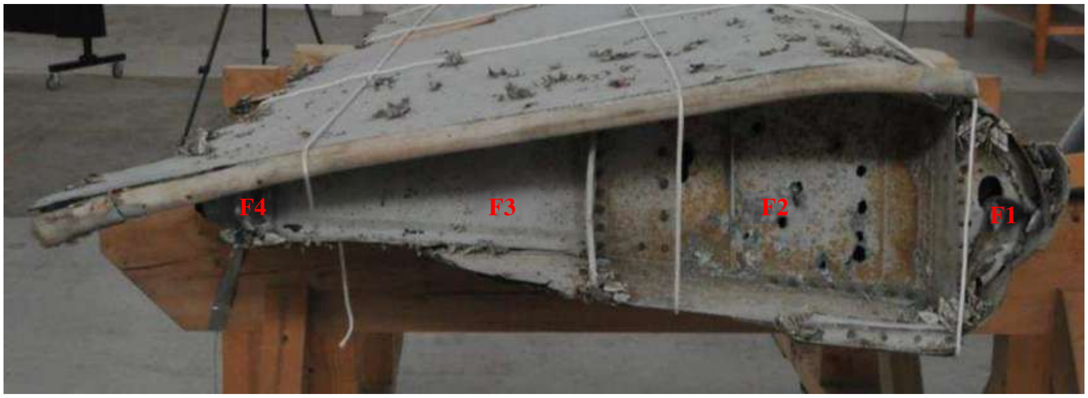

Zone F2

Zone F1

Zone F4

Zone F3

Planche 13 : **Weights of the crustaceans sampled by zone**

Zone identified	Weight of crustacean sampled in gr	observations
A1	16	Sampled by DGA TA
A2	36	Sampled by DGA TA
A3	12,6	Sampled by DGA TA
A4	0	
B1	?	Sampled by expert crustacean
B2	?	Sampled by the SR
B3	0	
B4 upper surface B4 lower surface	9.6 14,9	Sampled by DGA TA
C1	0	
C2	5	Sampled by DGA TA
C3	0	
C4 upper surface C4 lower surface	17,1 18,3	Sampled by DGA TA
D1	0	
D2	0	
D3	0	
D4 upper surface D4 lower surface	39,9+ ? 28,2+ ?	Sampled by DGA TA and expert crustacean
E1	35,4	Sampled by DGA TA
E2	13,2	Sampled by DGA TA
E3	20,5+ ?.	Sampled by DGA TA and expert crustacean
E4 upper surface E4 lower surface	47,9+ ? 29,4+ ?	Sampled by DGA TA and expert crustacean
F1	43,7	Sampled by DGA TA
F2	45,2	Sampled by DGA TA
F3	32,3	Sampled by DGA TA
F4	12,7	Sampled by DGA TA

Total weight sampled by DGA TA and sent to Gif sur Yvette : 468.3 grams.

X-RAYS OF THE FLAPERON

Planche 14 : **X-raysof the flaperon – localisation of the zones x-rayed**

RX x-ray area

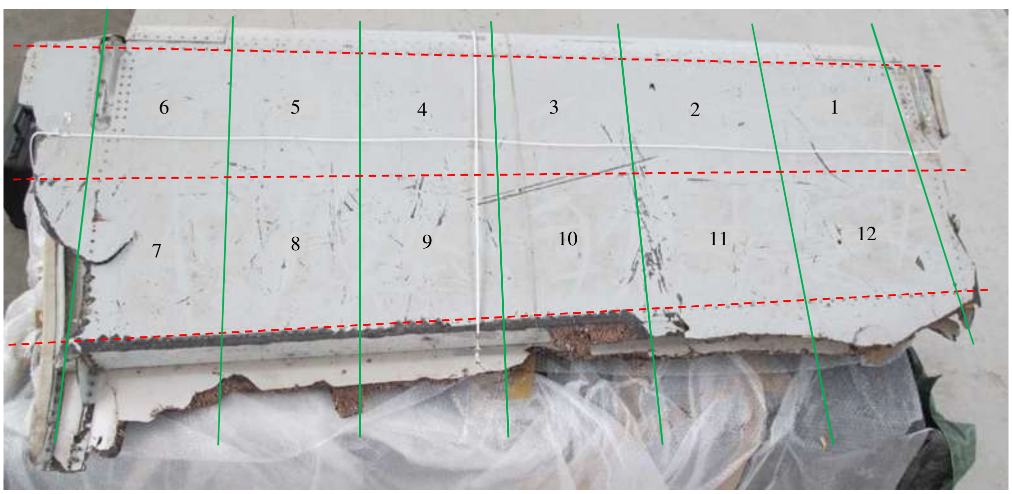

X-ray zones

Planche 15 : **X-rays of the flaperon**

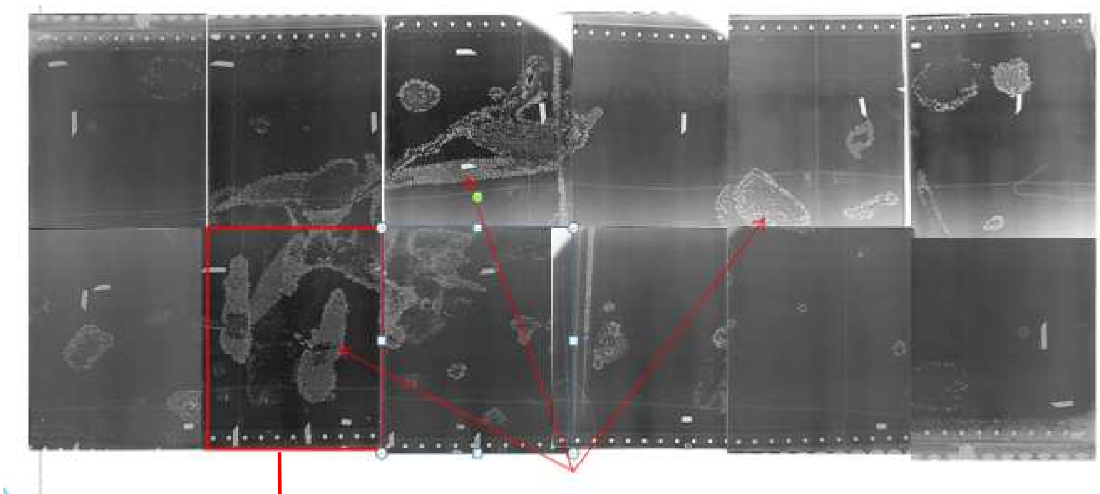

The lightest zones correspond to salt deposits following sea water penetration in the cracked composite

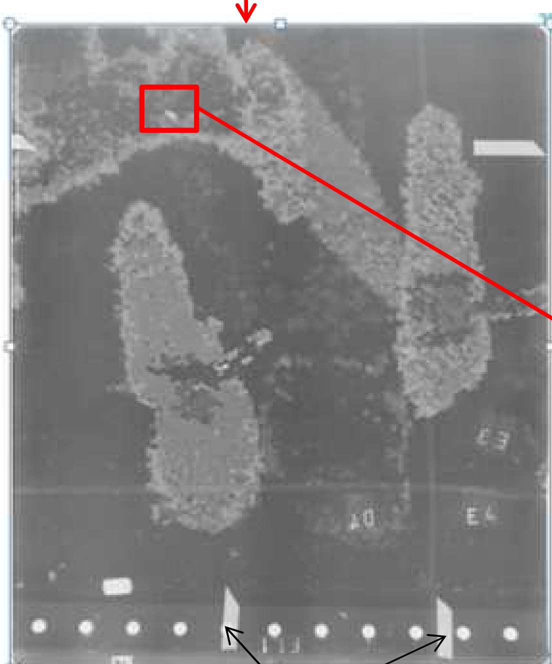

Boroscope of the zone: presence of a crustacean inside the flaperon

Adhesive strip for reference

Planche 16 : **Area of the zones covered in salt**

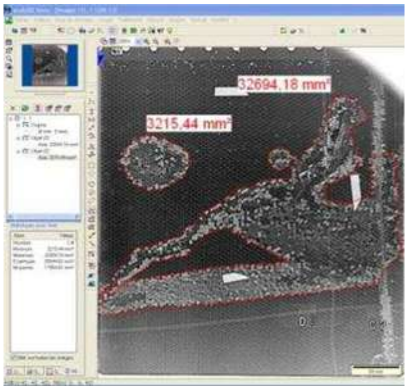

35909,62 mm^2

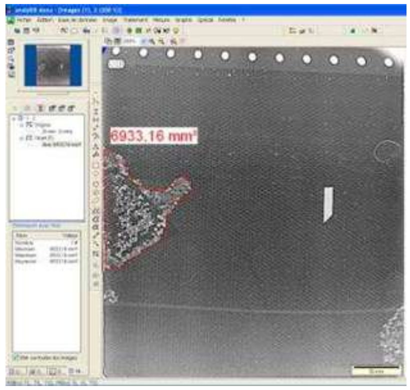

6933,16 mm^2

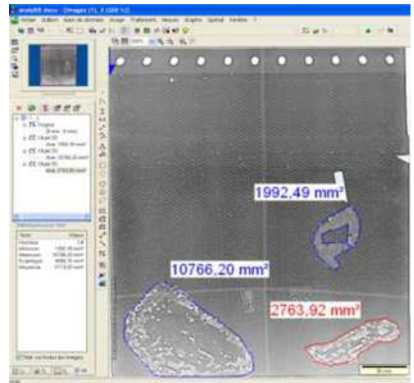

15522,61 mm^2

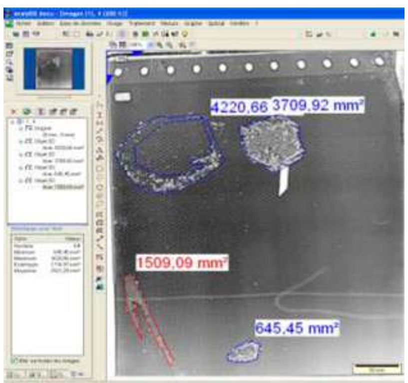

10085,12 mm^2

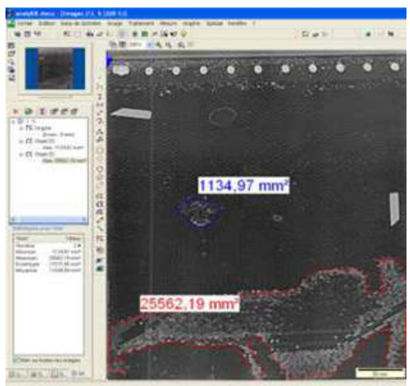

26697,16 mm^2

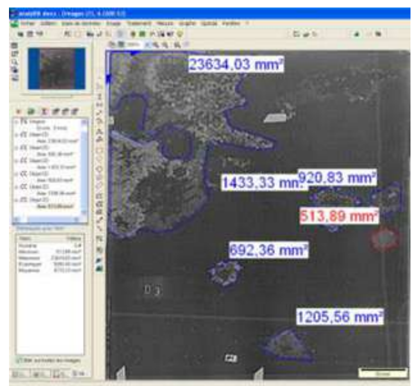

28400 mm^2

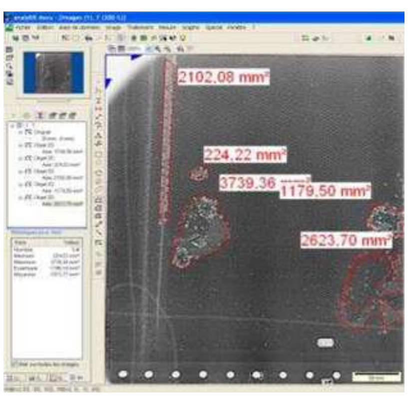

9868,86 mm^2

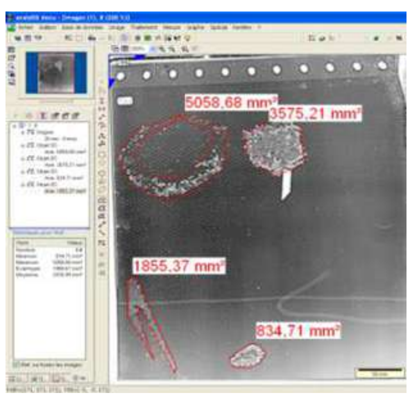

11323,97 mm^2

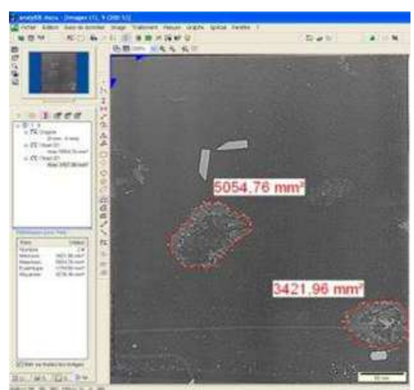

8476,72 mm^2

Total area = 153217 mm^{2,} (0.153 m$^{2)}$

PHYSICAL CHARACTERISTICS OF THE FLAPERON

Planche 17 : **Weight of the flaperon**

Planche 18 : **Dimensions and position of the centre of gravity lower surface side**

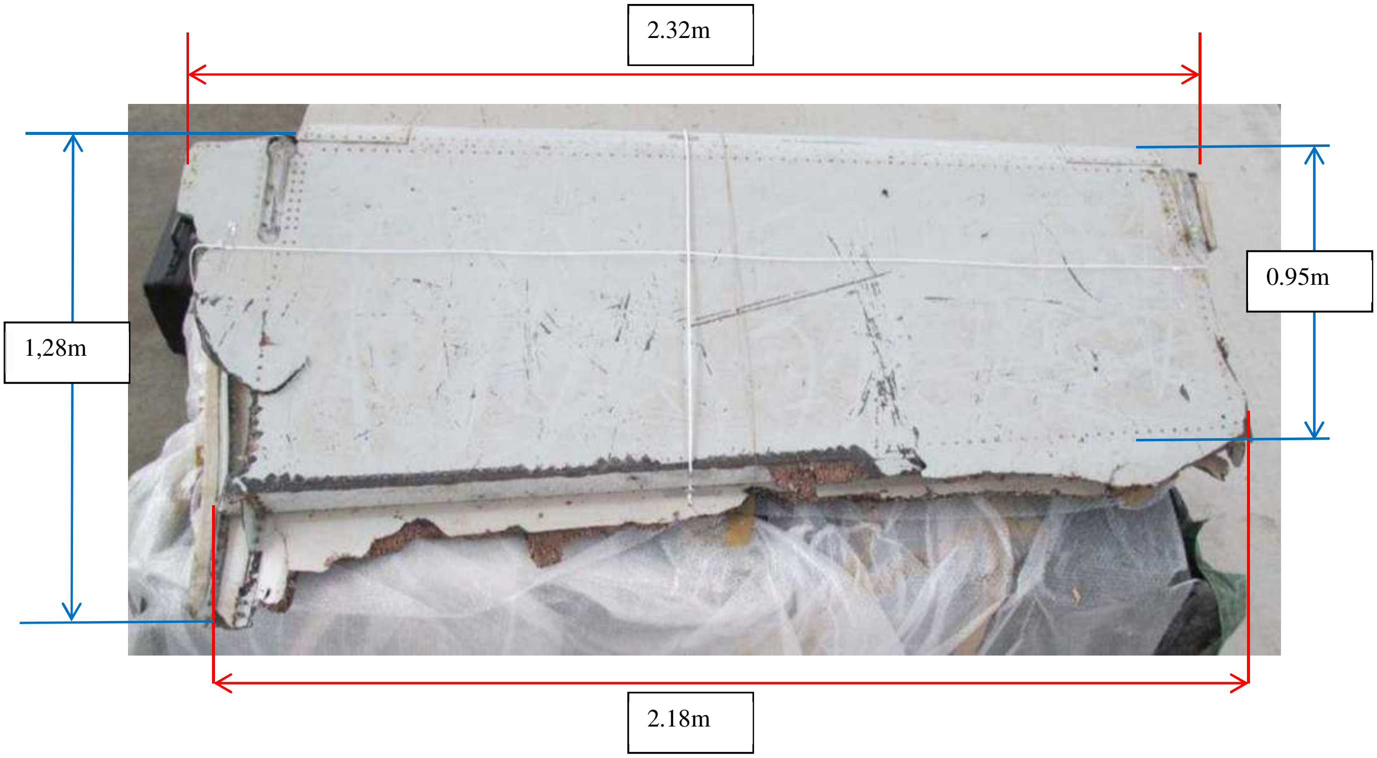

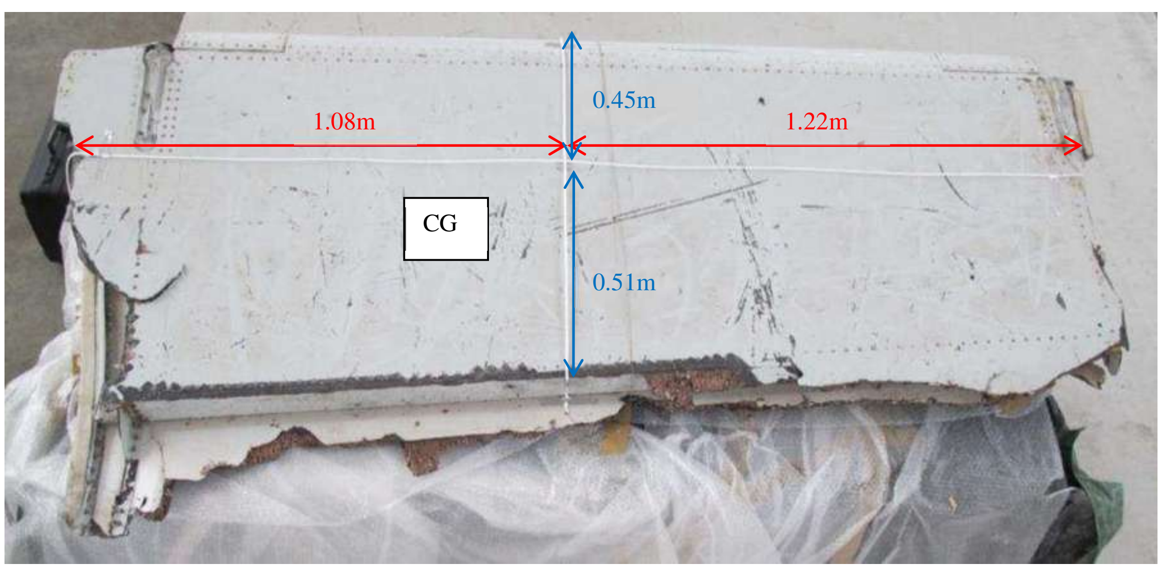

Position of centre de gravity on the lower surface side

Planche 19 : **3D model of the flaperon**

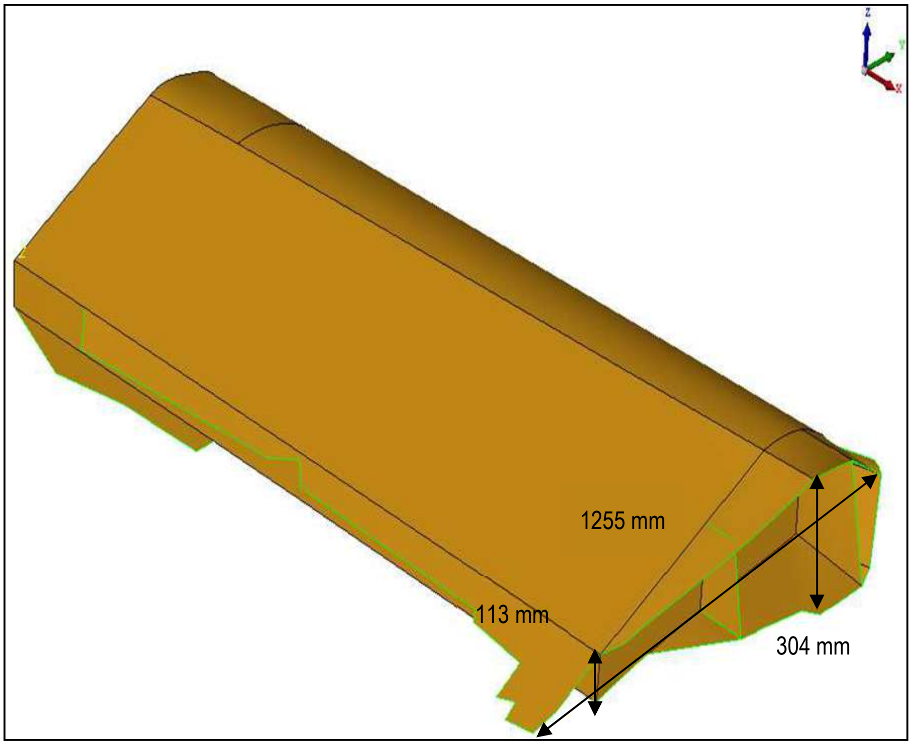

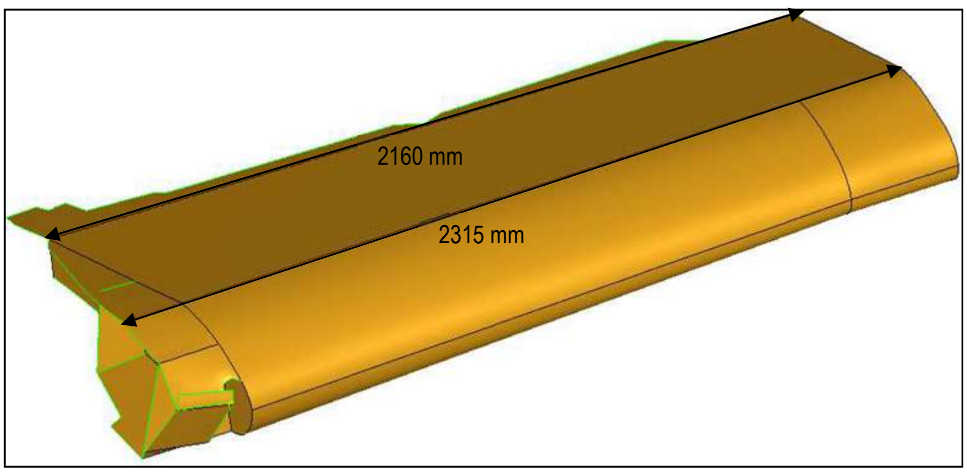

BUOYANCY TEST

Planche 20 : **Buoyancy test**

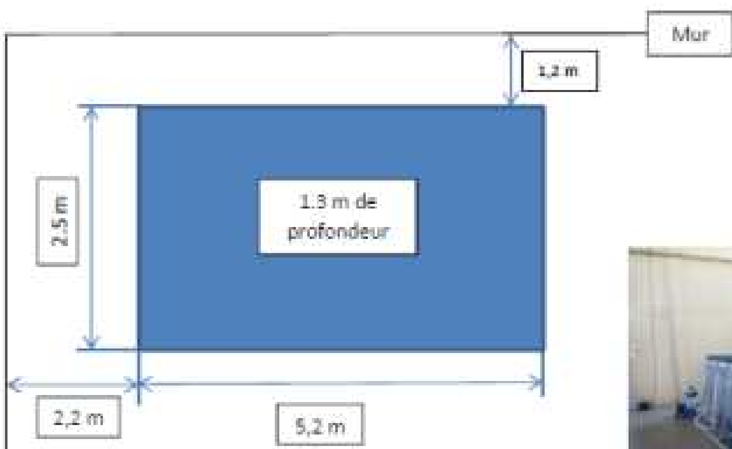

Piscine pleine d'eau salée à 4% et une température de 20°C.

Au environ de 1,1 m d'eau.

RESTRICTED CIRCULATION

Planche 21 : **Buoyancy test**

DGA TH cameras around the pool

Flaperon in the pool

Positioning the flaperon in the pool

Planche 22 : **Buoyancy test**

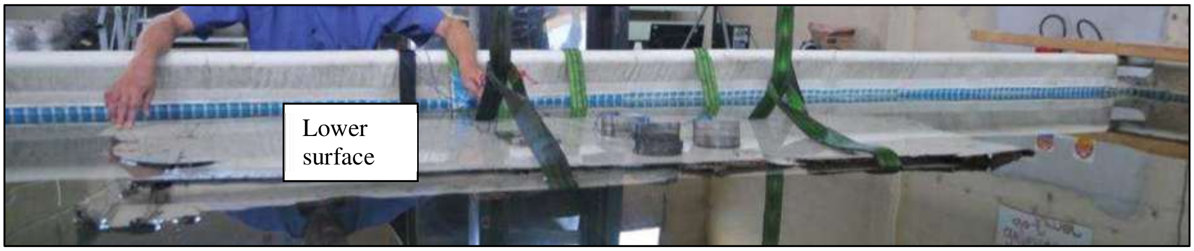

The effective weight to immerse the flaperon completely was 37 kg (41kg –Archimedes buoyancy on weights).

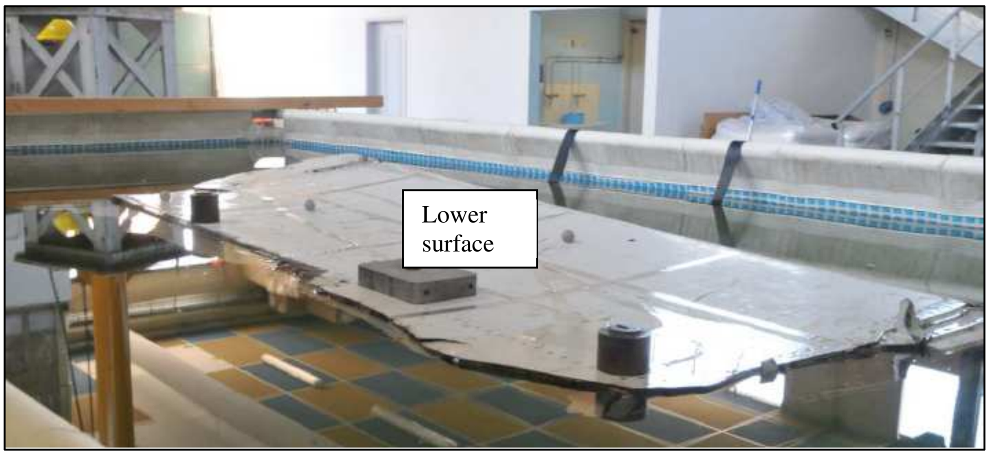

The added weight, which did not touch the water and was thus effective, to immerse the lower surface trailing edge upwards was 13.5 kg.

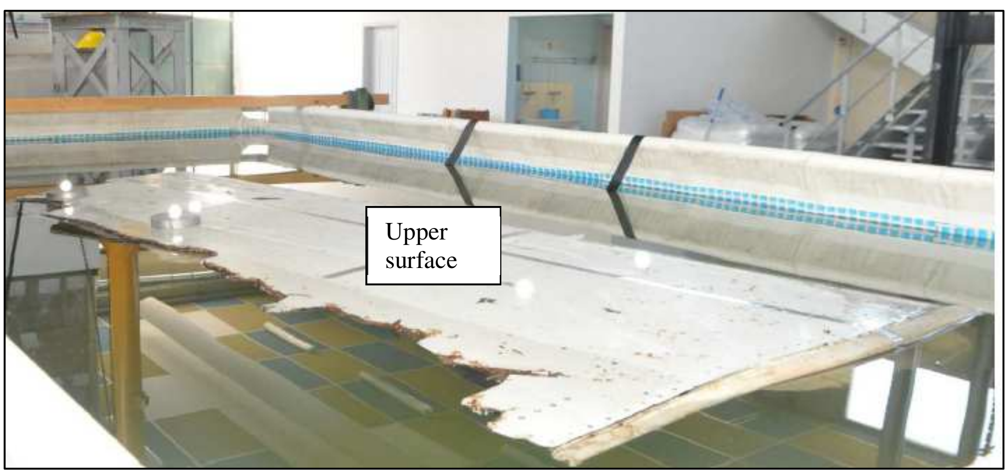

The added weight, which did not touch the water and was thus effective, to immerse the upper surface trailing edge upwards was 5 kg

EXAMINATIONS OF THE METALLIC ELEMENTS

EXAMINATIONS OF OUTBOARD HINGE FITTING AND NEARBY ELEMENTS

Planche 23 : **Hinge fitting on the outboard side**

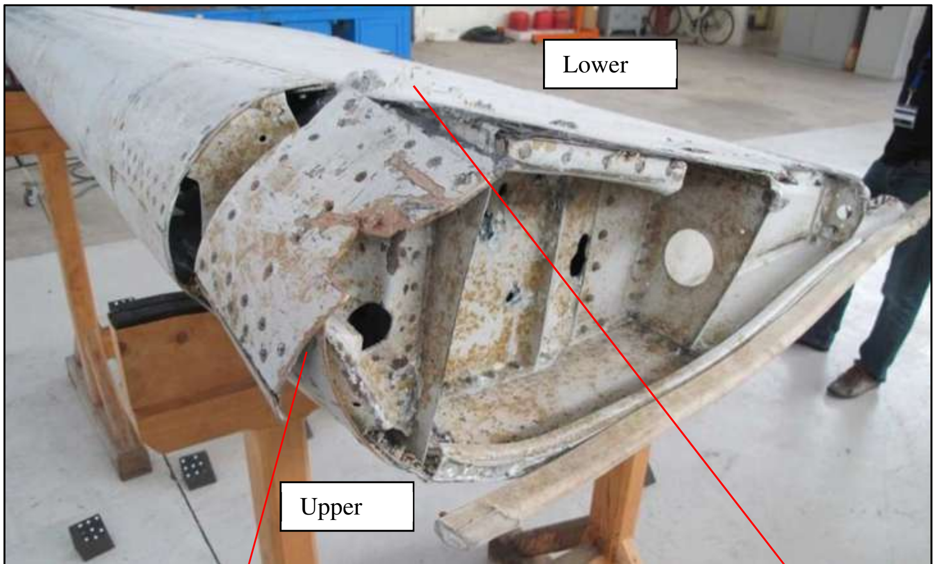

Disassembly of leading edge panel

Lower surface fracture

Leading edge fracture

Planche 24 : **Hinge fitting on the outboard side**

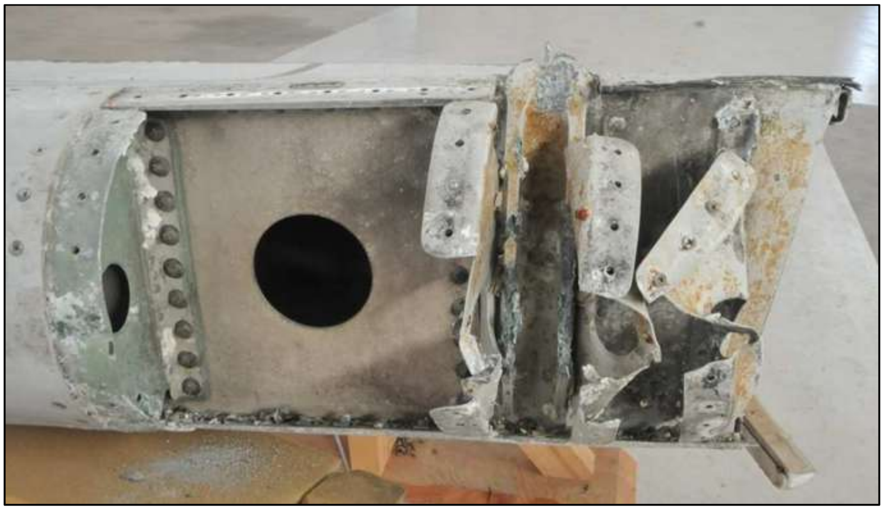

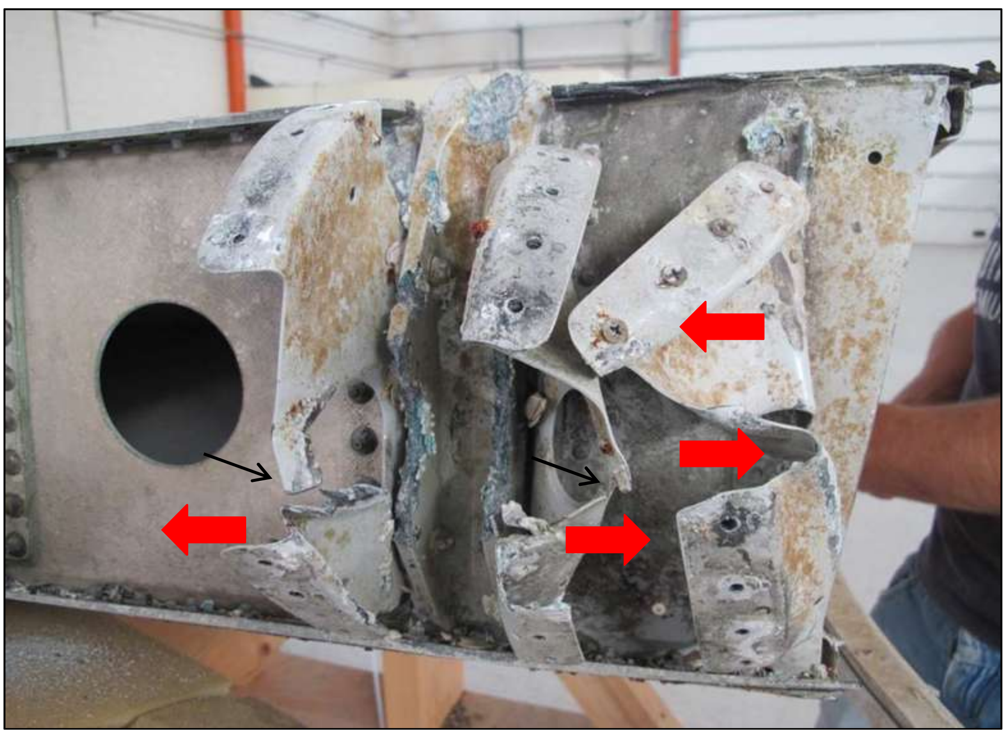

Direction of distortions on rib tears

Planche 25 : **Elements located aft of the outboard hinge fitting**

Direction of distortions

Planche 26 : **View of the flaperon after disassembly of the outboard hinge fitting**

Planche 27 : **Outboard hinge fitting disassembled**

Outboard hinge fitting dissassembled

Leading edge fracture

Lower surface fracture

Planche 28 : **Lower surface outboard side hinge fitting fracture**

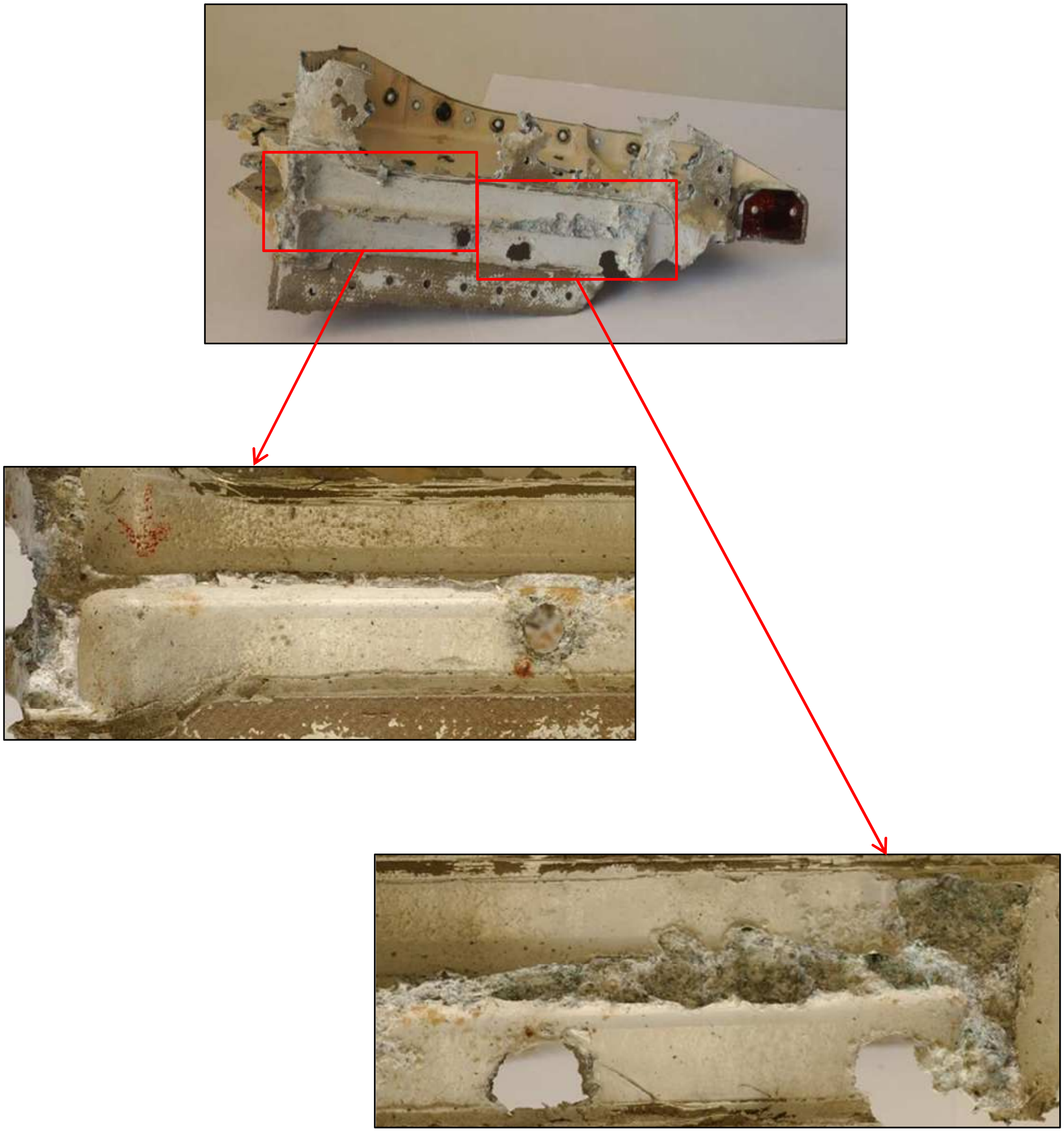

Planche 29 : **Leading edge outboard side hinge fitting fracture**

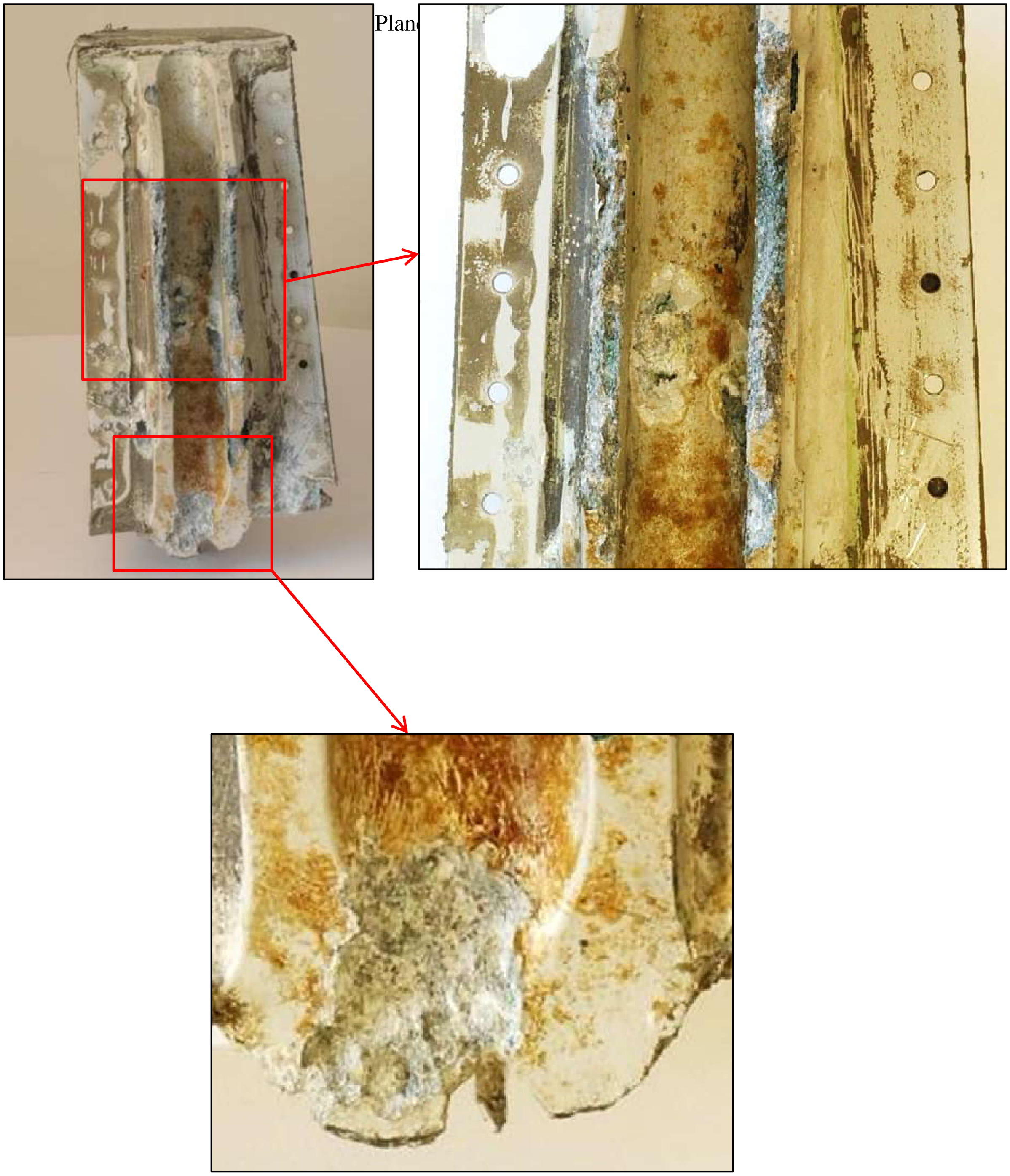

EXAMINATIONS OF INBOARD HINGE FITTING AND NEARBYELEMENTS

Planche 31 : **Inboard hinge fitting**

Disassembly of leading edge panel

Repair: disassembly of seal retainer

Planche 32 : **Inboard hinge fitting**

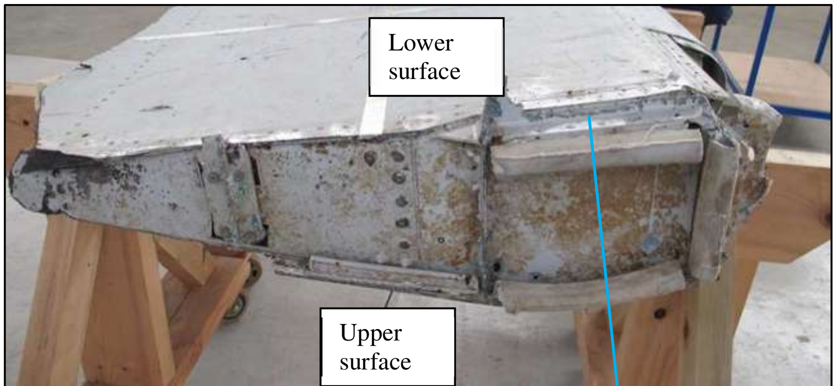

Lower surface side hinge fitting fracture

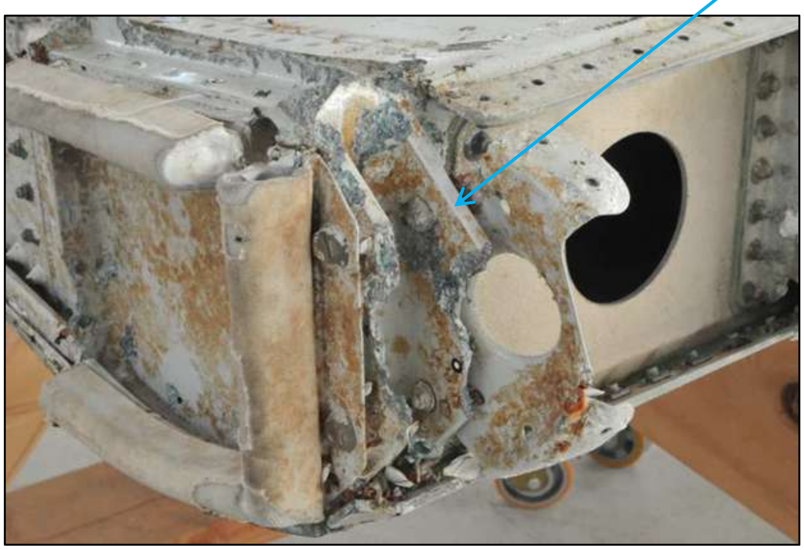

Leading edge side hinge fitting fracture

Planche 33 : **Inboard hinge fitting**

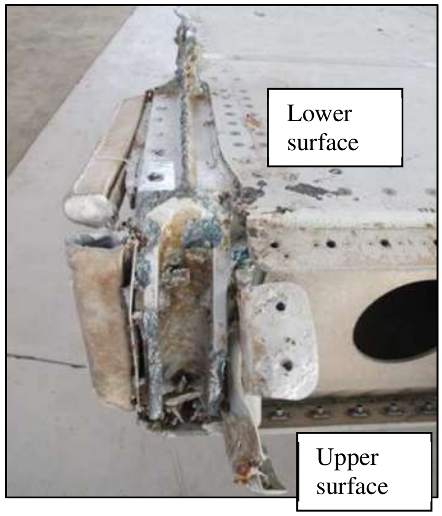

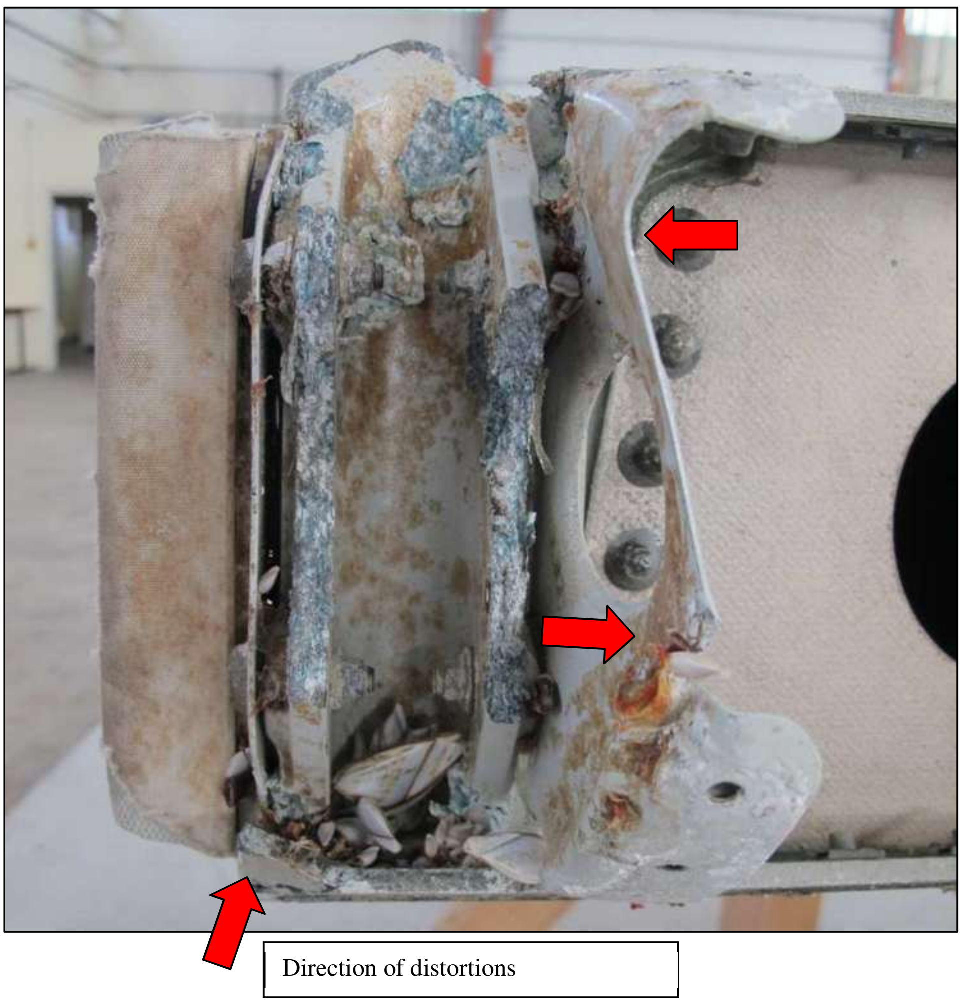

Planche 34 : **Inboard hinge fitting**

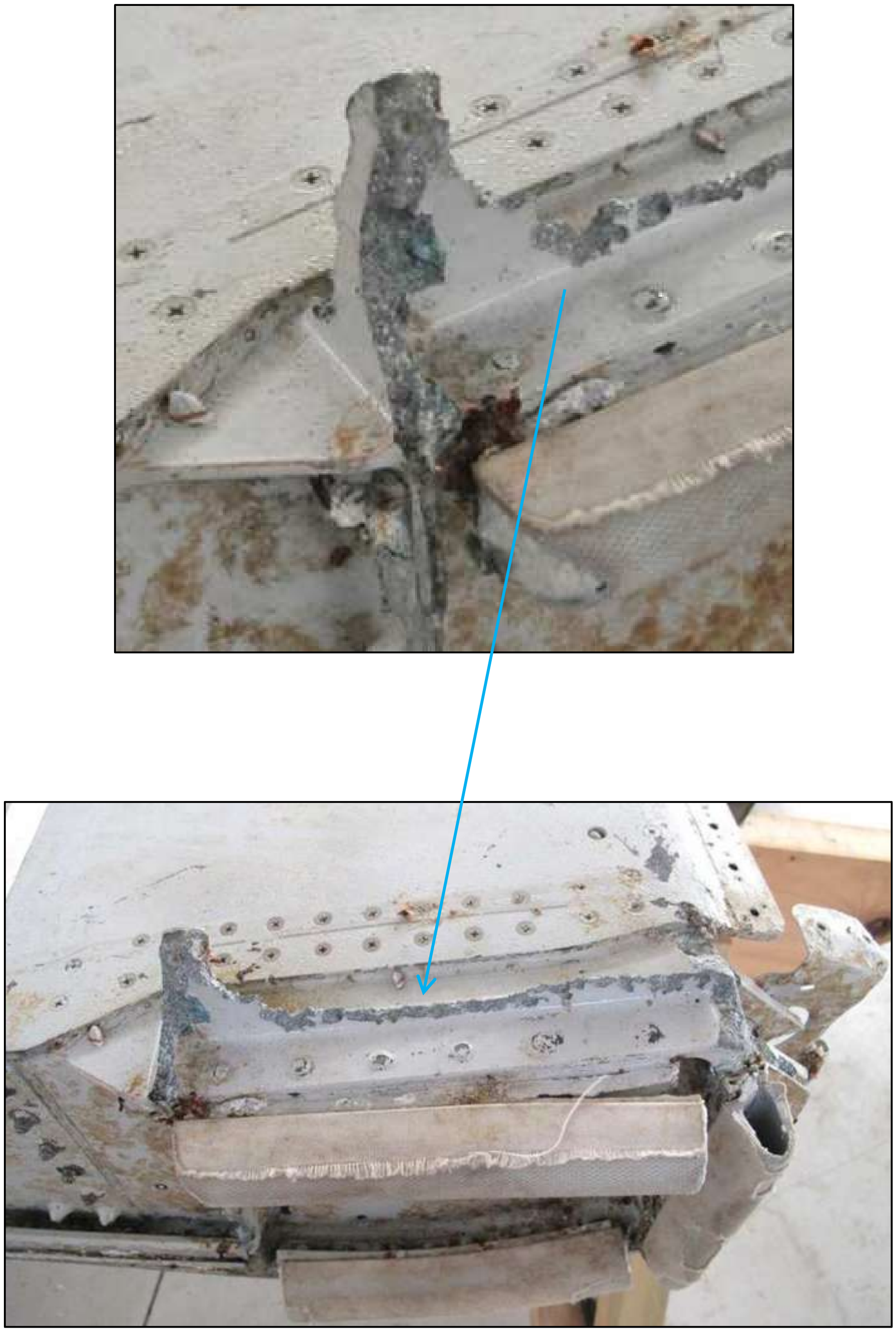

Lower surface side hinge fitting fracture

Planche 35 : **Cowling attacment on the inboard side**

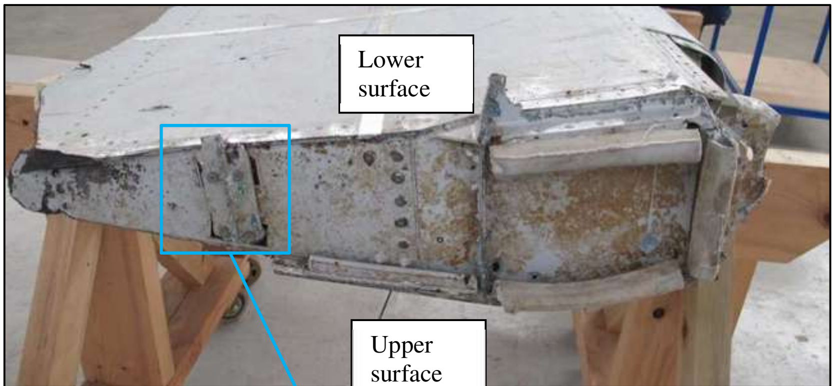

Attachment fracture

Planche 36 : **Flaperon after disassembly of the hinge fitting on the inboard side**

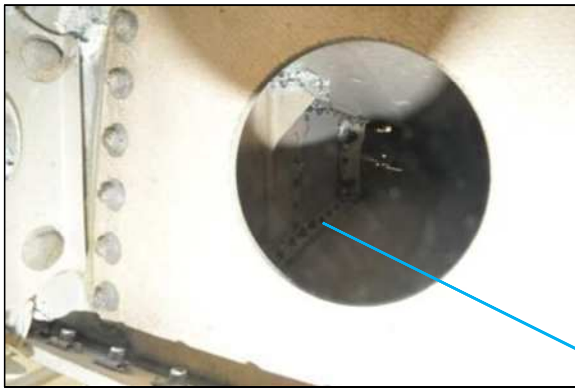

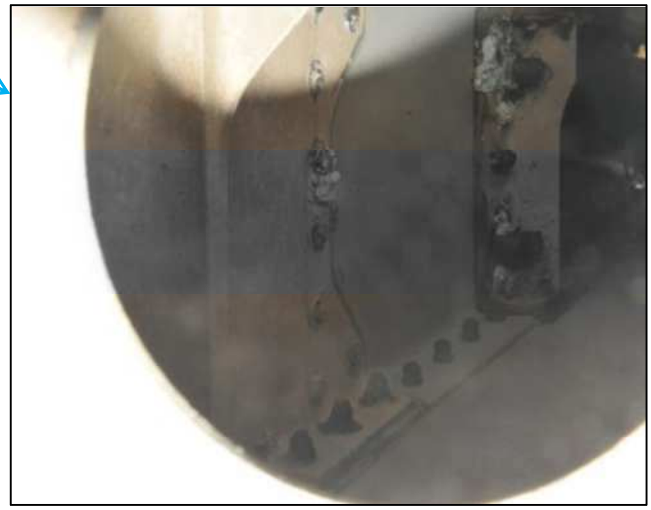

Lower surface side hinge fitting fracture

Planche 37 : **Inboard hinge fitting disassembled**

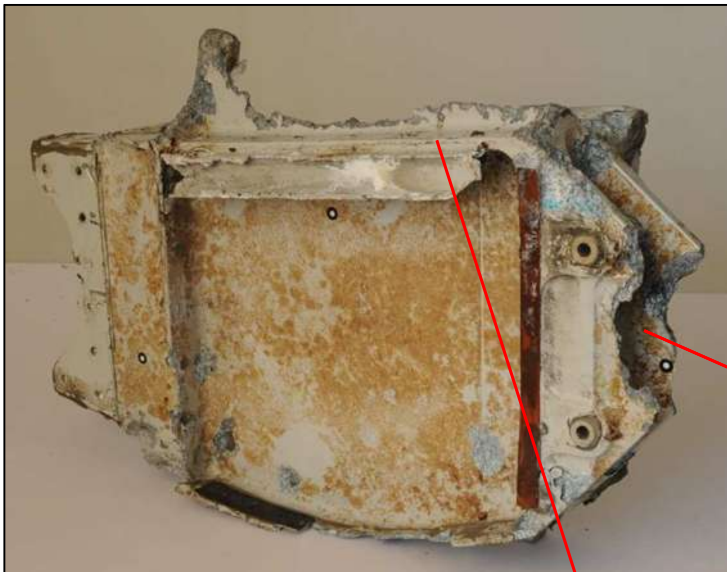

Inboard hinge fitting disassembled

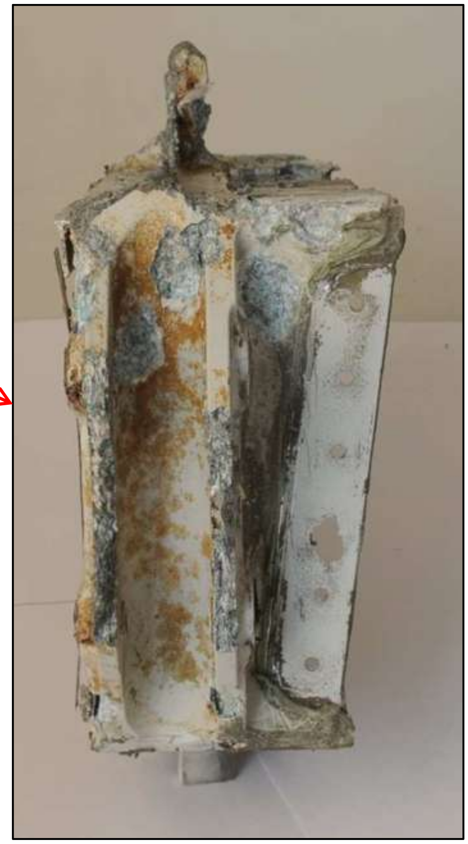

Leading edge fracture

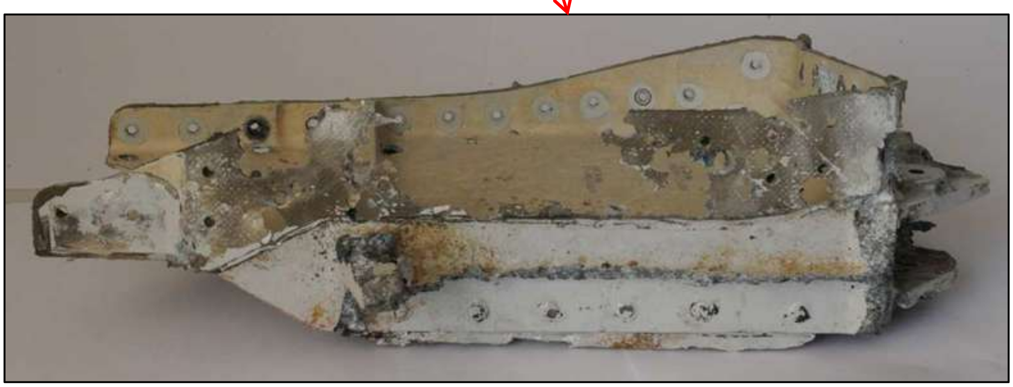

Lower surface fracture

Planche 38 : **Lower surface side inboard hinge fitting fracture**

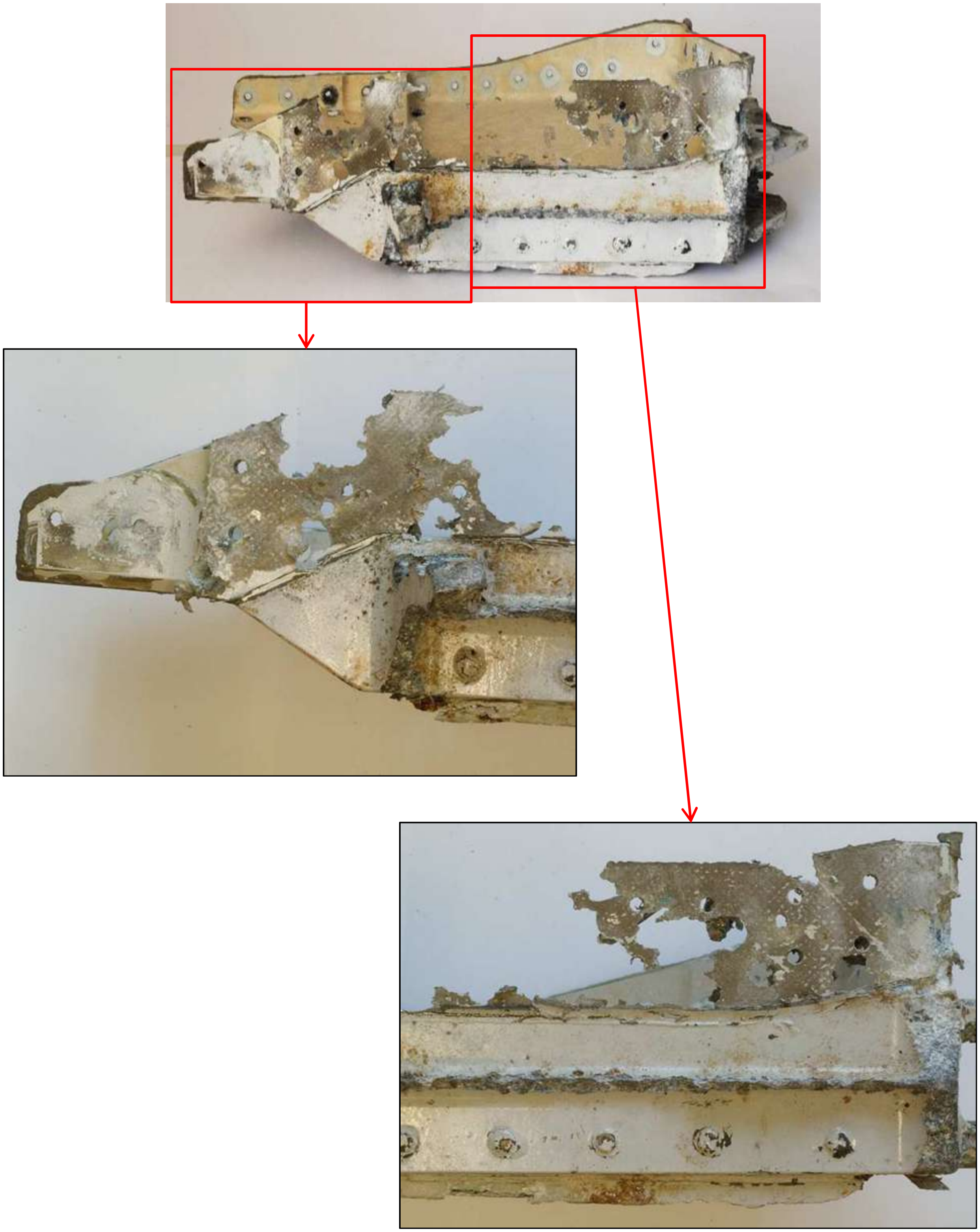

Planche 39 : **Leading edge side inboard hinge fitting fracture**

Planche 40 :

DIRECTION OF DISTORTIONS AND TEARS ON METALLIC PARTS

Planche 41 : **Metrology of the outboard hinge fitting**

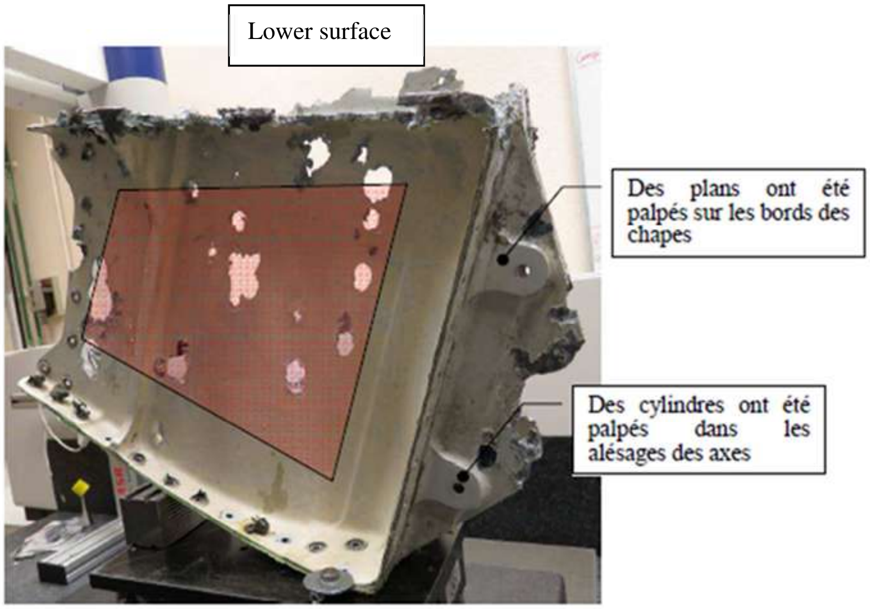

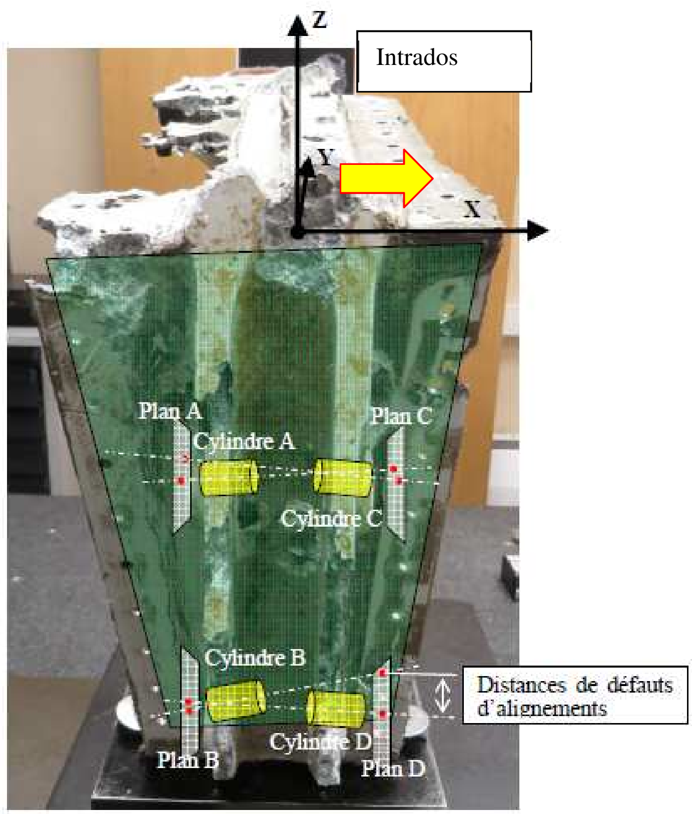

Orientation of hinge fitting in relation to reference plan

Planche 42 : **Metrology of the inboard hinge fitting**

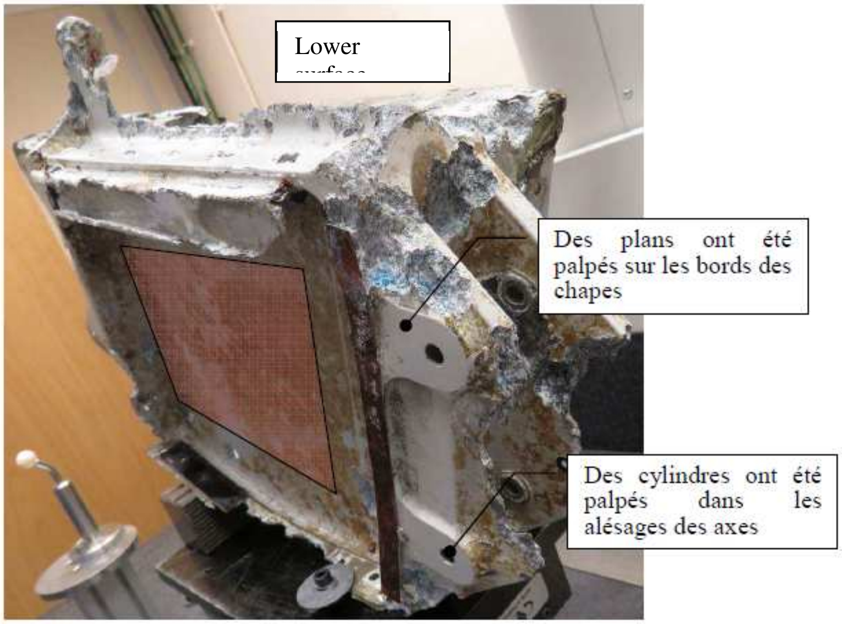

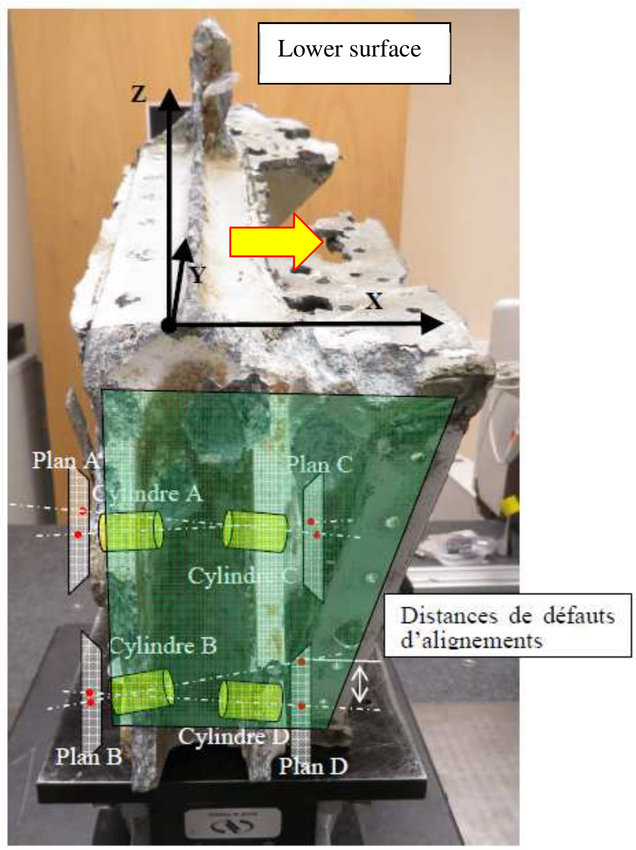

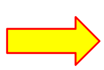
Orientation of hinge fitting in relation to reference plan

Planche 43 : **Summary of the distortions and fractures of the leading edge hinge fittings and ribs**

Lower surface

Outboard hinge fitting

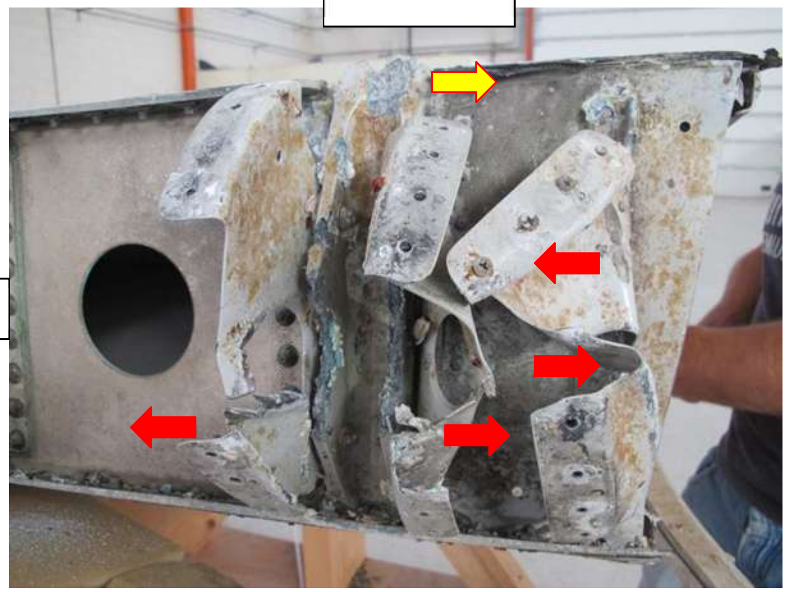

Orientation of hinge fitting in relation to reference plan

Direction of distortions

Lower surface

Inboard hinge fitting

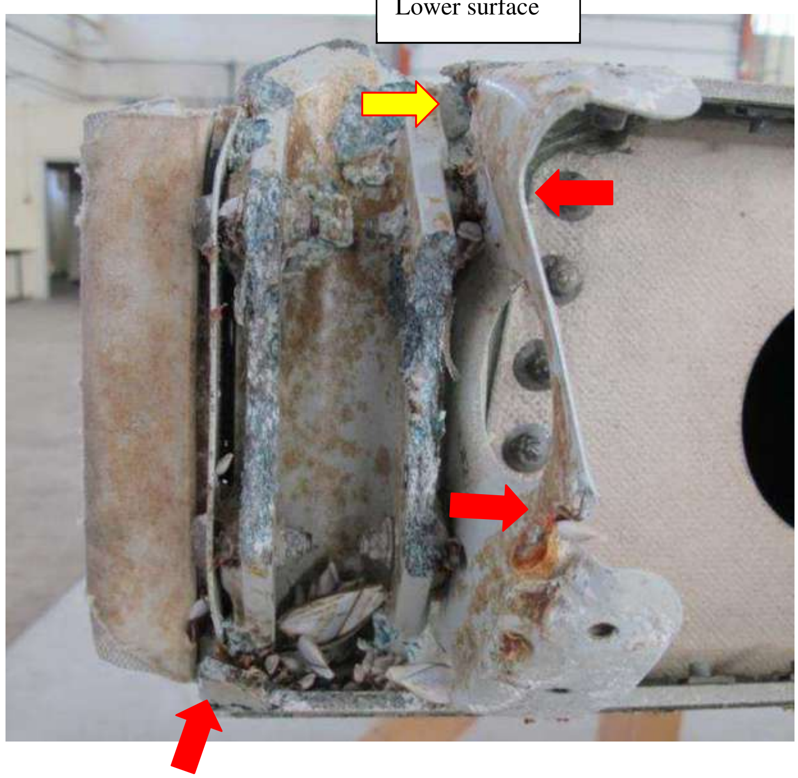

Planche 44 : **Possible explanation of the distortions and fractures of the outboard side leading edge ribs**

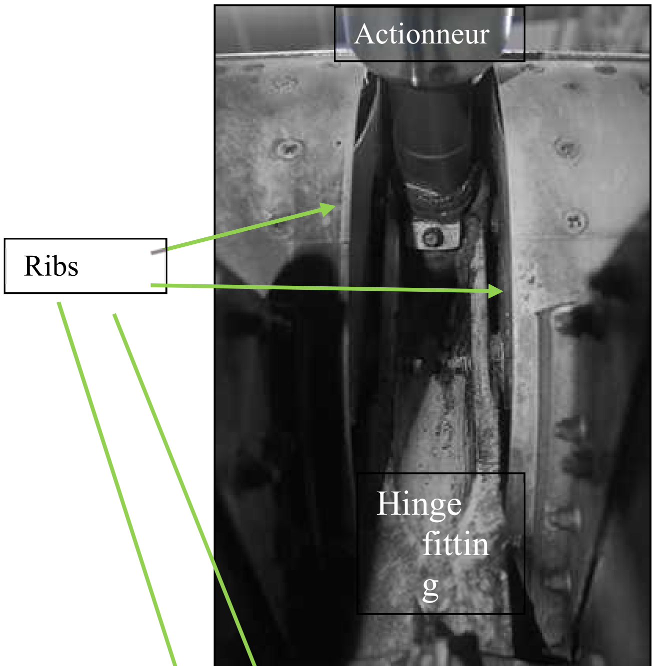

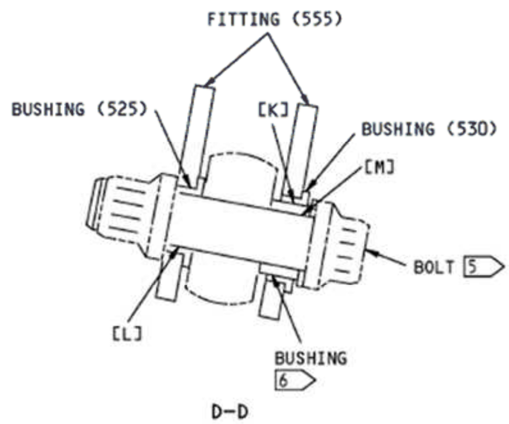

Configuration of the activator (outboard)

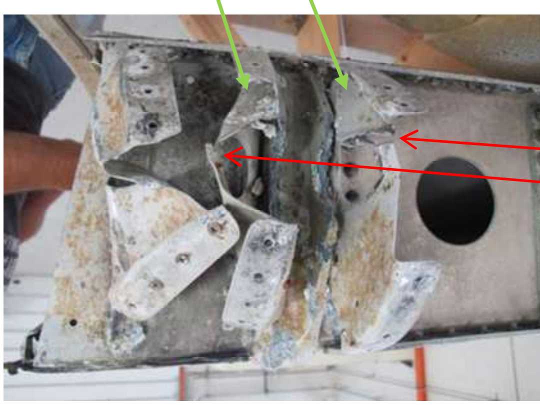

Note: photo turned around to present all the elements with the same orientation

Activator hinge point pin and other attachments

The damage to the ribs, especially the tearssemmed to be due to the activator hinge point pin tips.
The form of the folds leads one to believe that the ribs pushed onto the body of the activator during an overall rotational movement of the flaperon from the inside towards the outside.
This explanation is applicable to the inboard rib side.

EXAMINATIONS OF COMPOSITE MATERIAL PARTS

Planche 45 : **Comparison between a complete flaperon and the flaperon from MH 370**

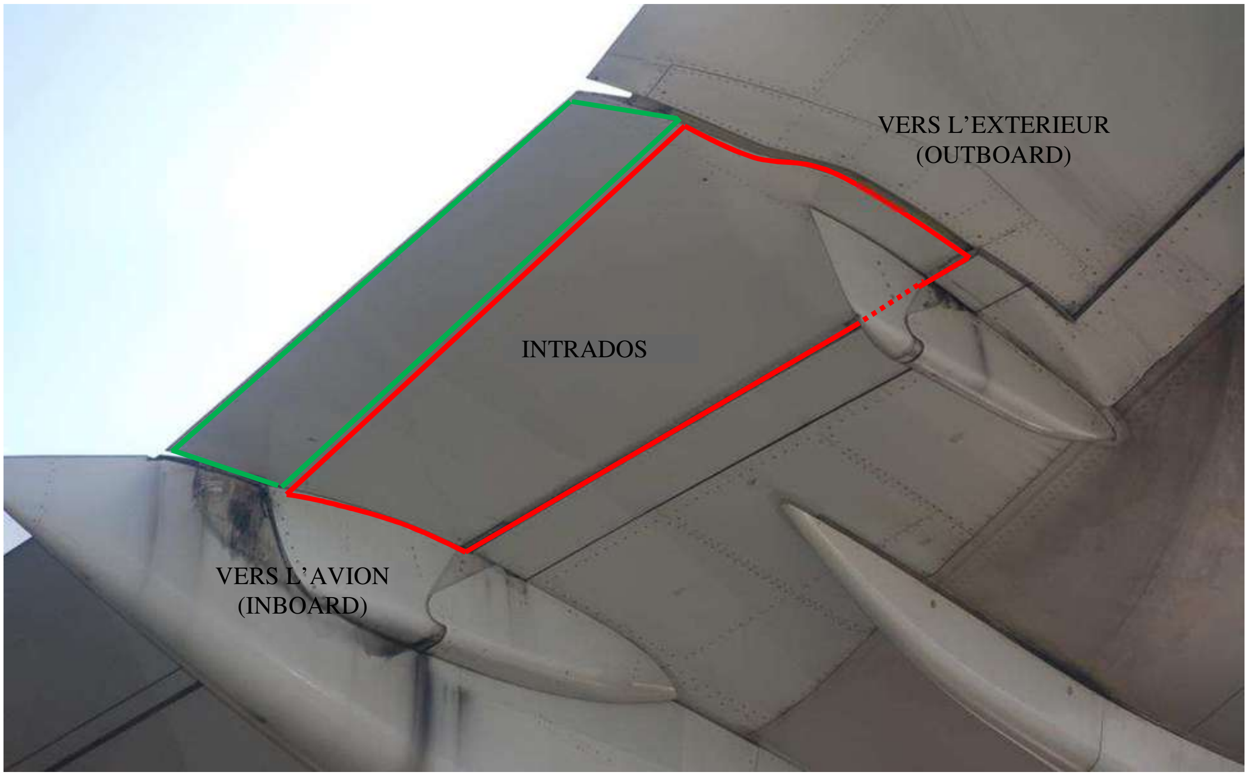

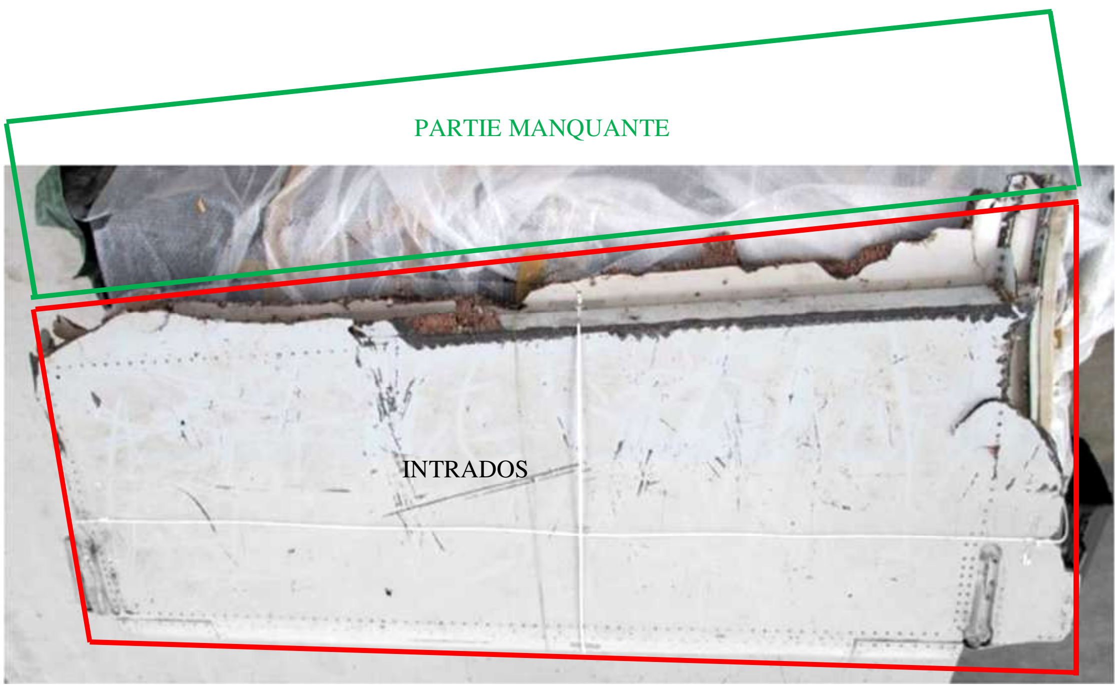

VERS L'AVION
(INBOARD)

VERS L'EXTERIEUR
(OUTBOARD)

DAMAGE ON THE LEADING EDGE

Planche 46 : **Damage at the level of the leading edge access doors**

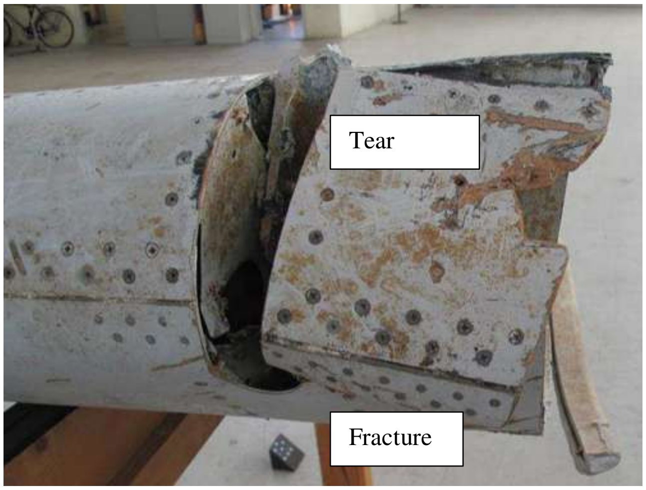

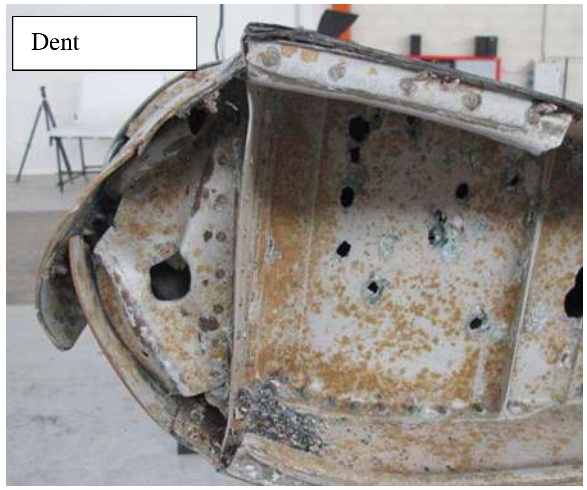

Dent and tear on the access door on the outboard side

Fracture of the access door on the inboard side

Planche 47 : **Impacts on the leading edge**

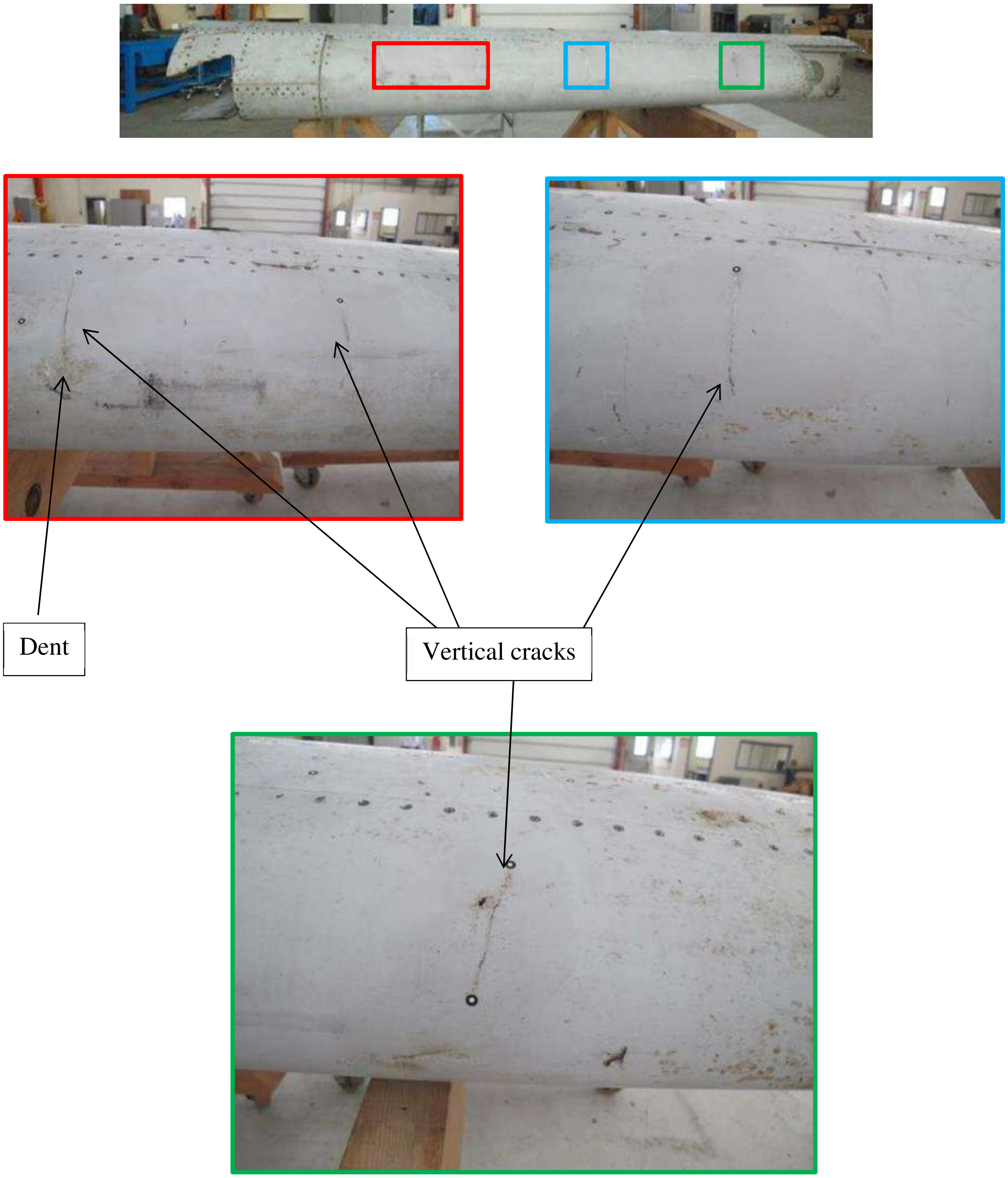

Planche 48 : **Comparison of the impacts with the facing wing panel**

OUTWARDS TOWARDS AEROPLANE

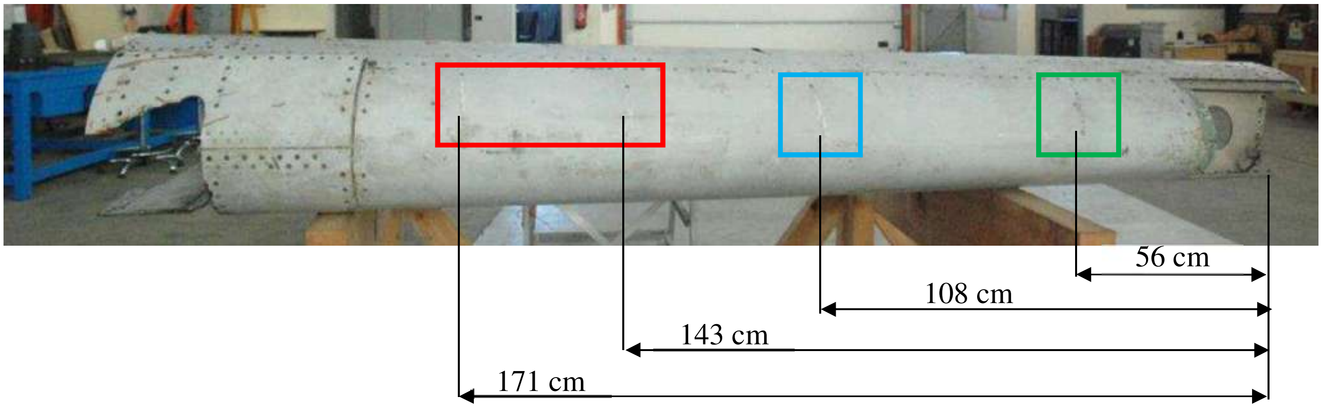

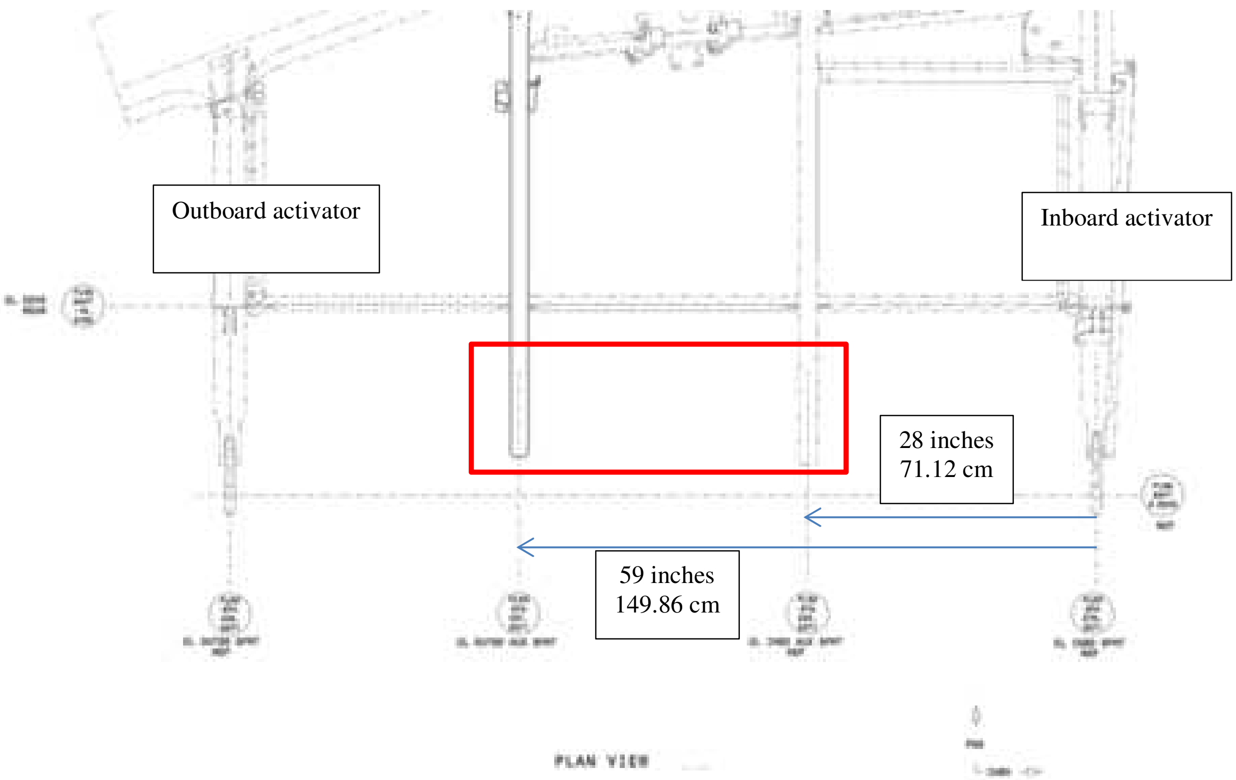

Only two parts facing according to the parts supplied by Boeing

EXAMINATIONS OF LOWER SURFACE

Planche 49 : **Lower surface: dents**

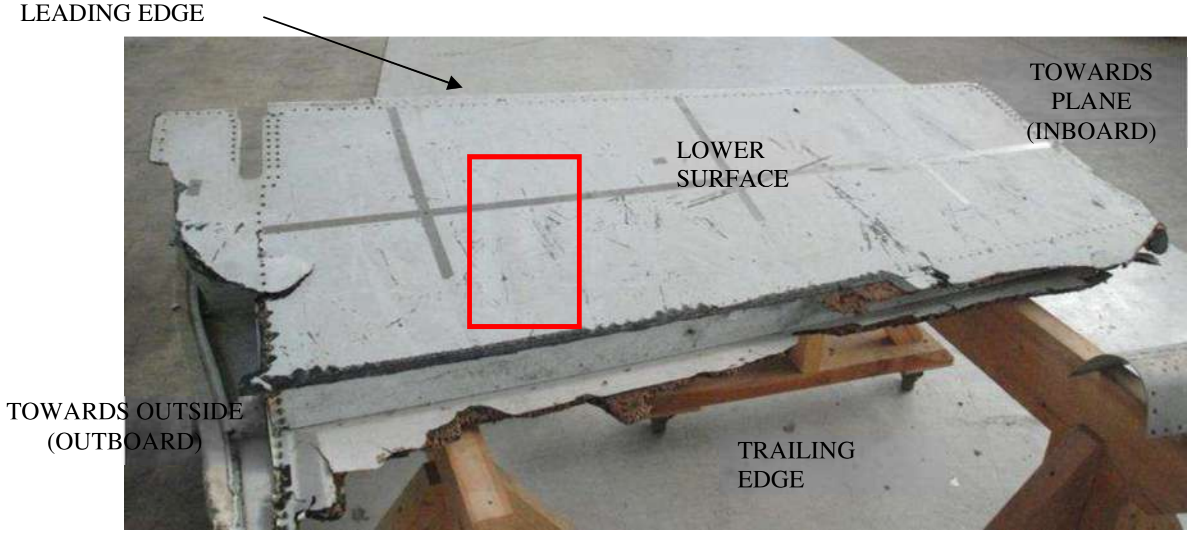

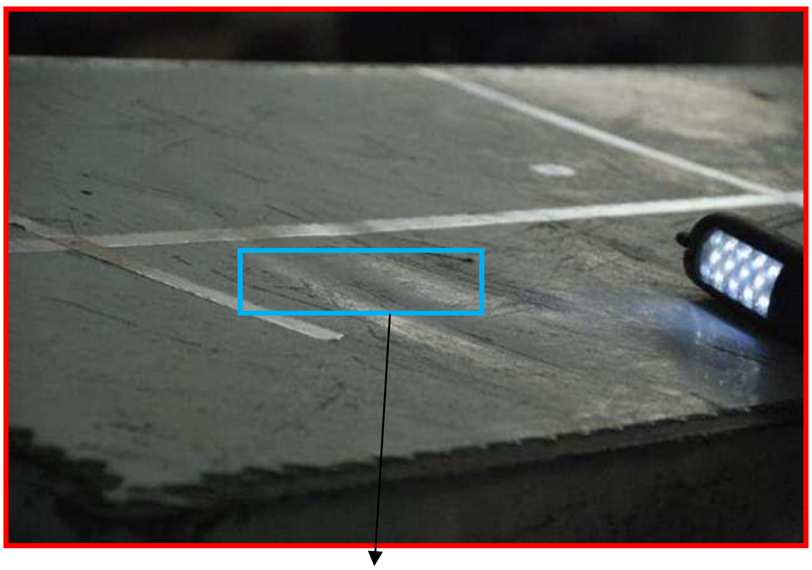

Planche 50 : **Lower surface: irregular fracture on trailing edge**

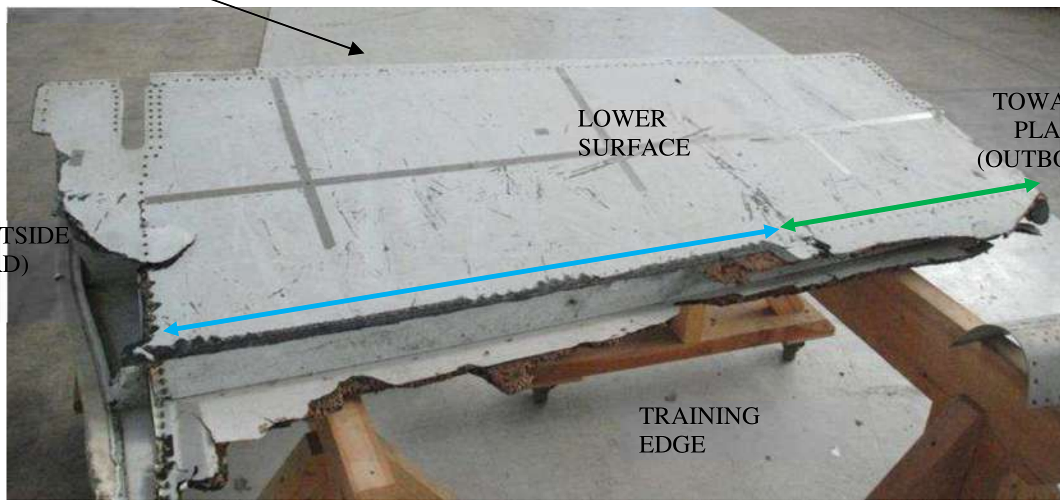

Straight fracture   Irregular fracture

Planche 51 : **Lower surface: irregular fracture on trailing edge – SEM Examination**

Outer skin

Inner skin

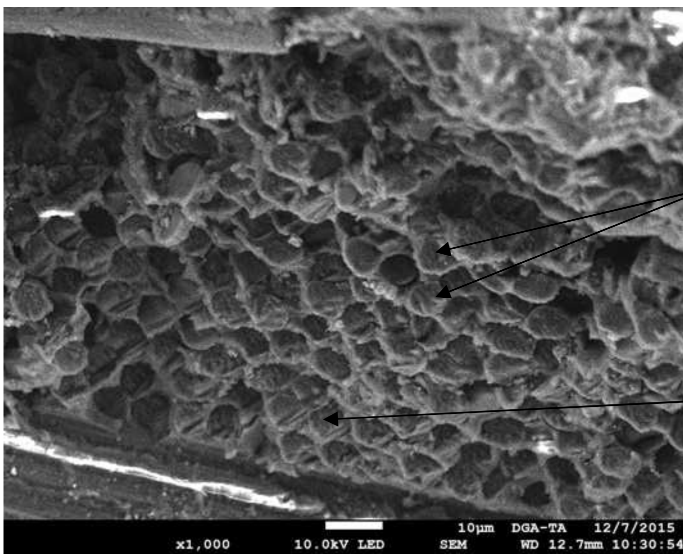

Inner skin : radiating form characteristic of a traction fracture

Inner skin: steps characteristic of a compression fracture

All of the fracture surfaces on the inner skin: majority in compression

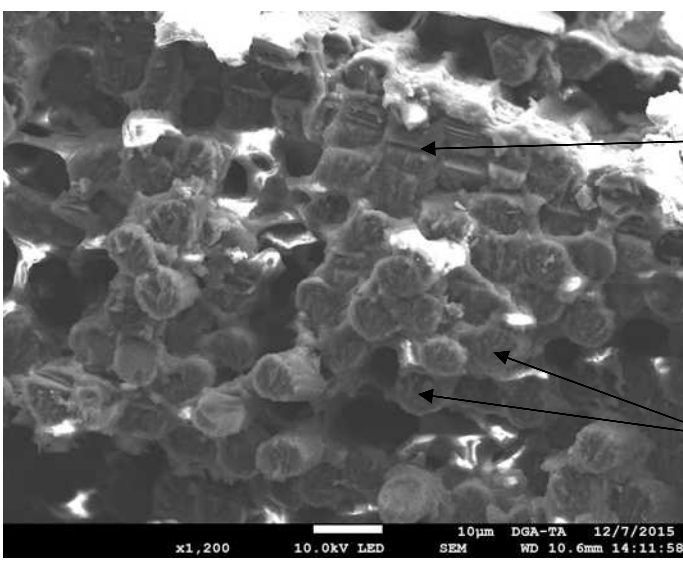

Inner skin: steps characteristic of a compression fracture

All of the fracture surfaces on the outer skin: majority in traction.

Outer skin : Inner skin : radiating form characteristic of a traction fracture

Planche 52 : **Lower surface: straight fracture on trailing edge**

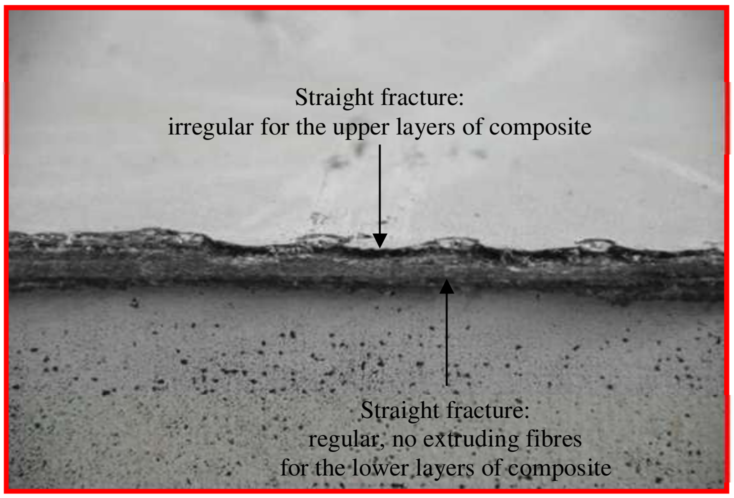

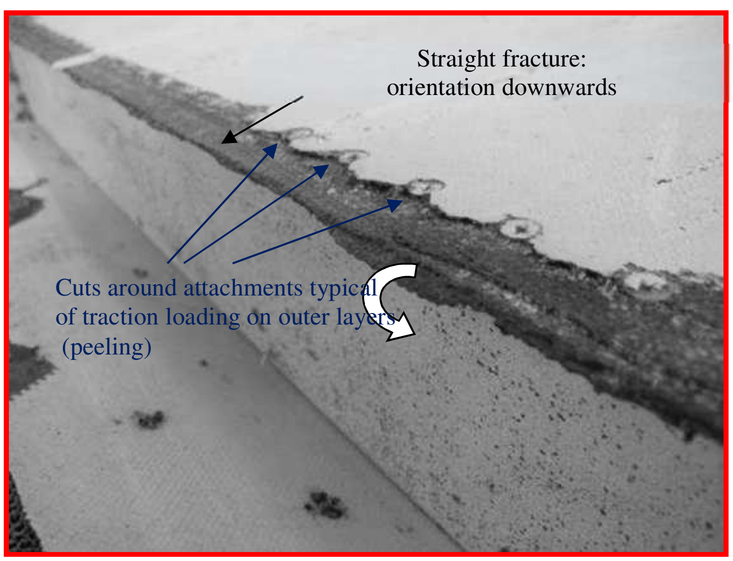

Planche 53 : **Lower surface: straight fracture on trailing edge – SEM Examination**

Upper layers

Lower layers

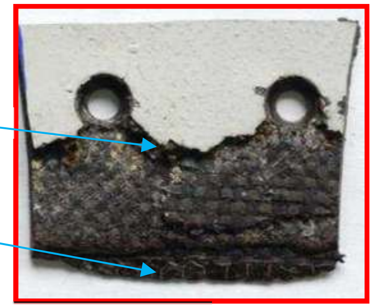

All of the fracture surfaces on the upper surfaces: majority in compression.

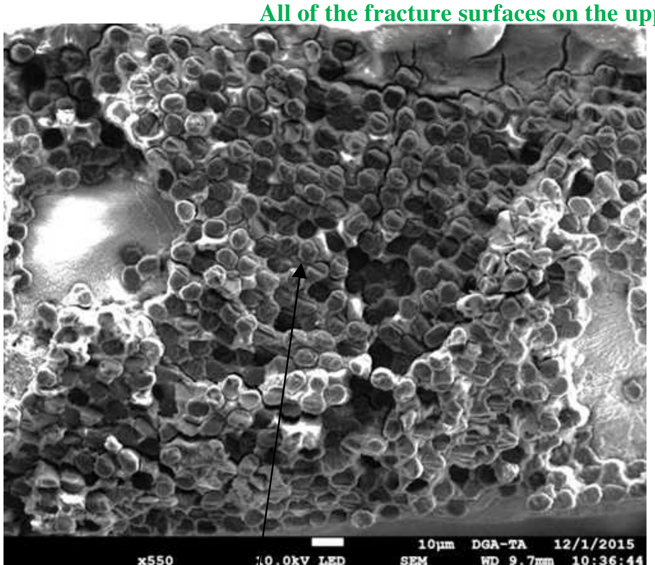

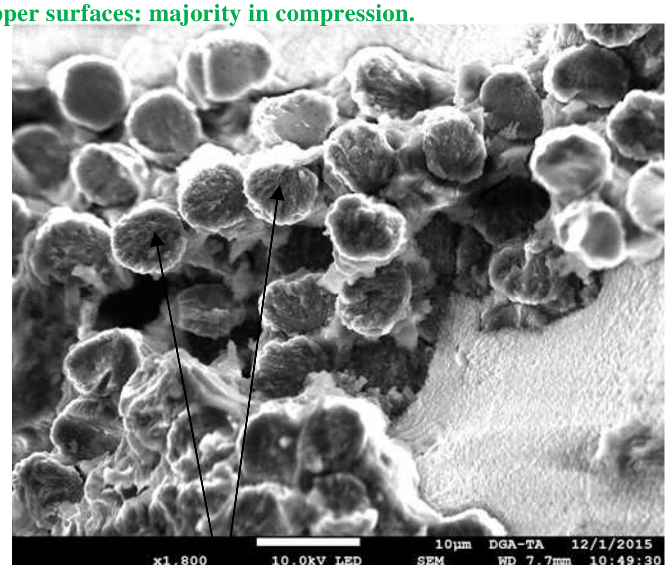

Upper layers : steps characteristic of a compression fracture

Lower layers: radiating form characteristic of a traction fracture

All of the fracture surfaces on the lower surfaces: majority in compression.

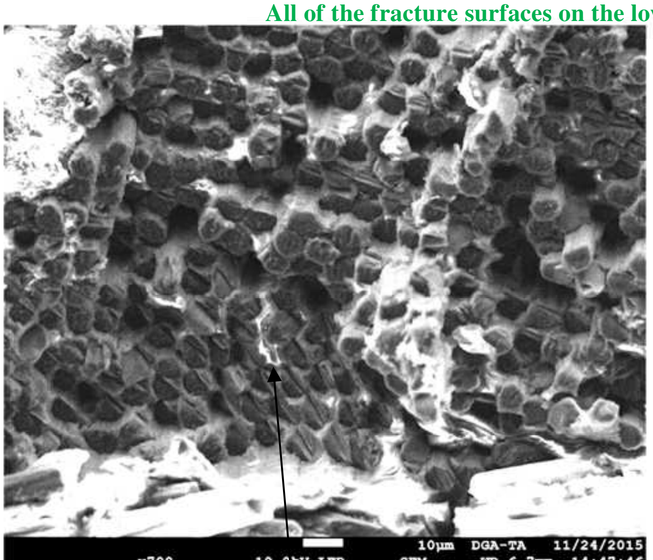

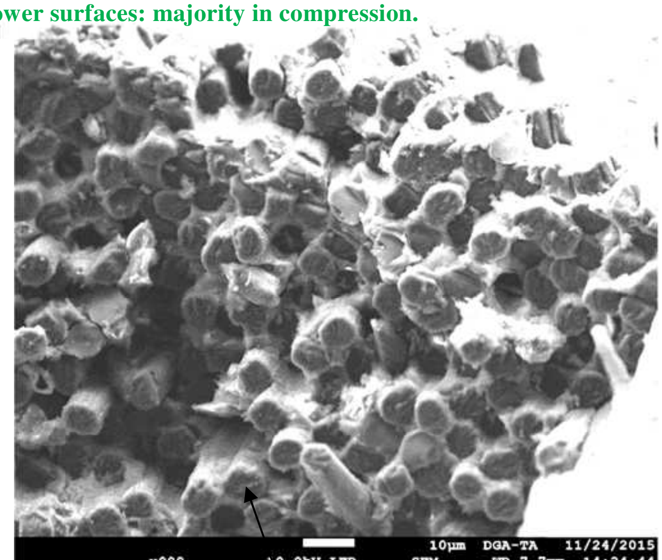

Lower layers: steps characteristic of a compression fracture

Upper layers: radiating form characteristic of a traction fracture

EXAMINATIONS OF UPPER SURFACE

Planche 54 : **Upper surface: dents, impacts, crack**

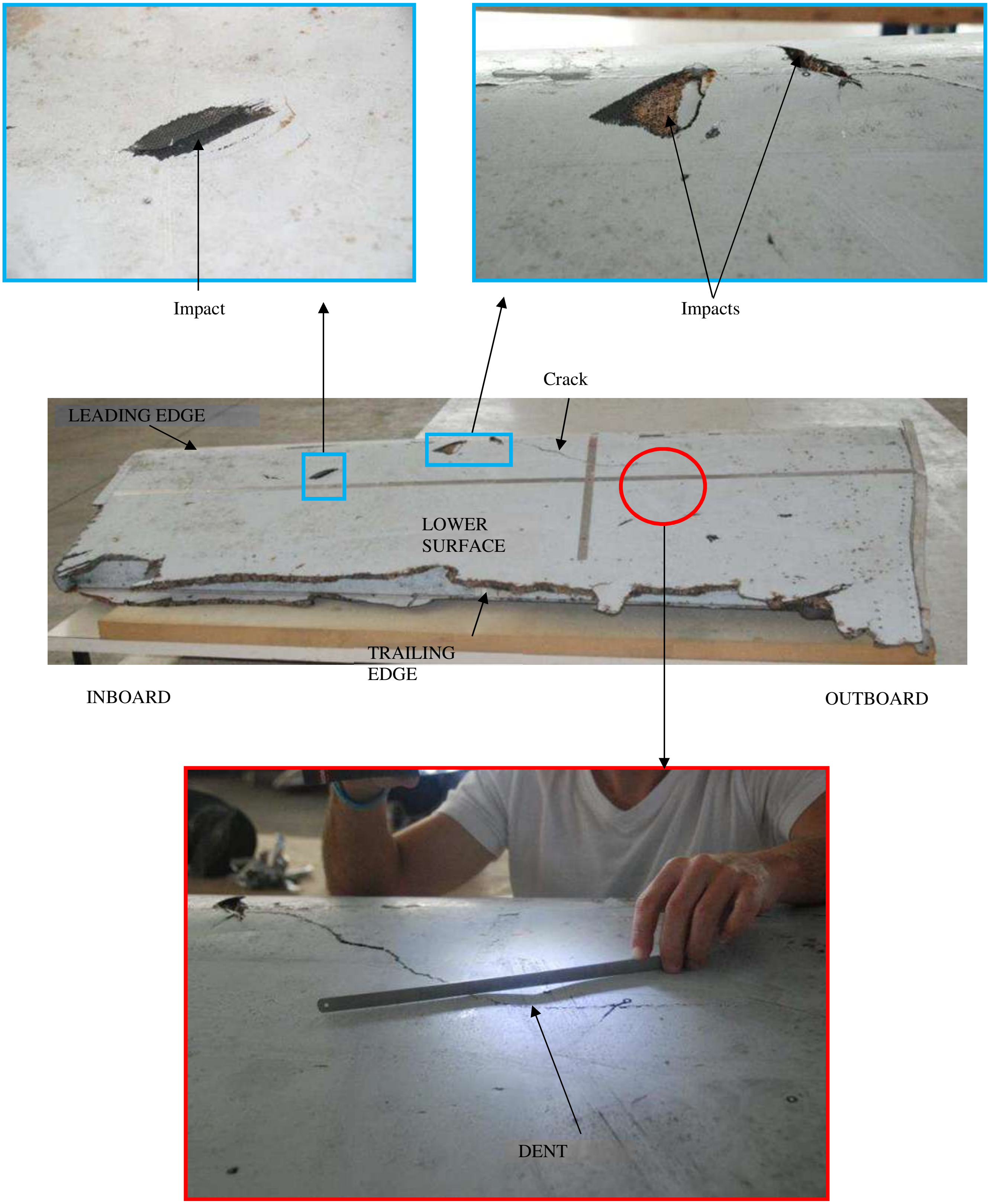

Planche 55 : **Upper surface: fracture on trailing edge**

Orientation of material upwards

Orientation of material upwards

Regular fracture, without protruding fibres

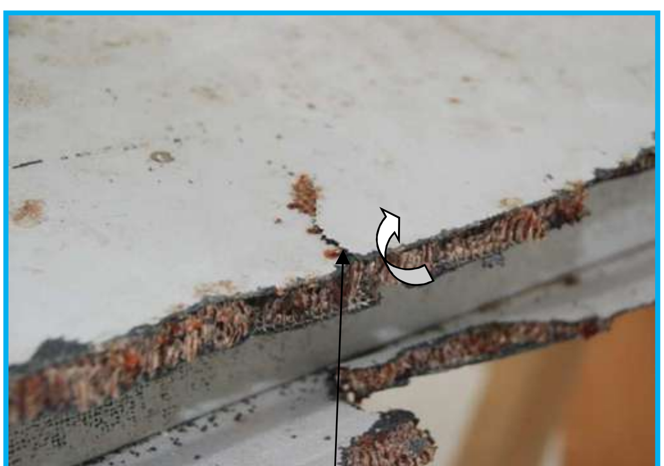

Orientation of material upwards

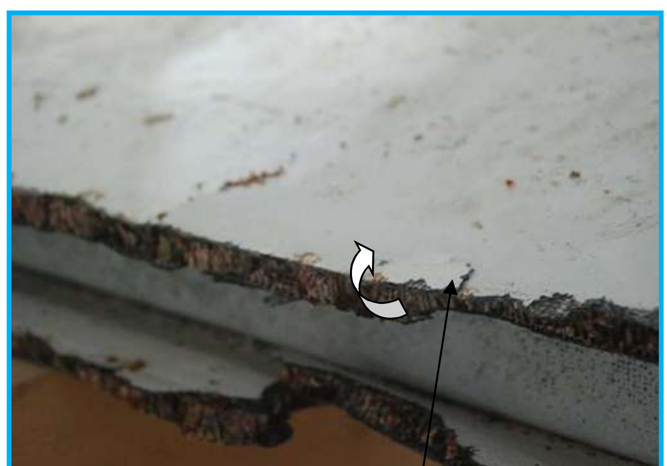

Orientation of material upwards

Planche 56 : **Upper surface: fracture on trailing edge – SEM examination**

Outer skin

Inner skin

Inner skin

Outer skin

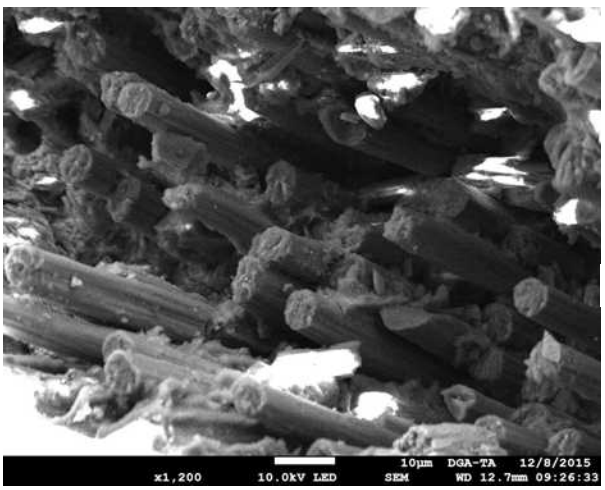

Inner skin : surfaces characteristic of a traction fracture

All inner skin surfaces : majority in traction.

All outer skin surfaces : majority in traction.

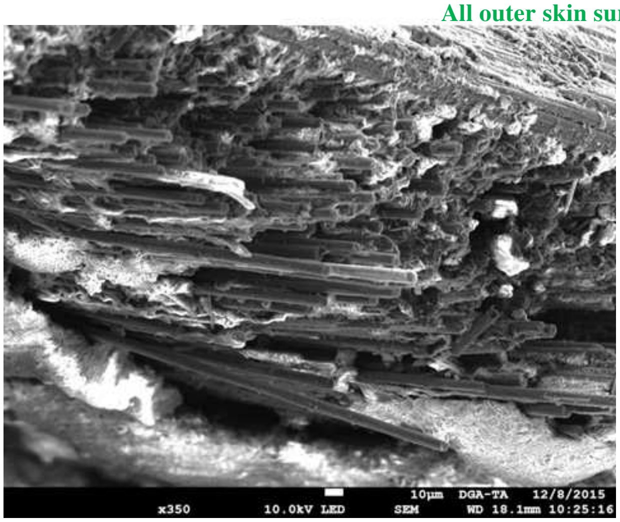

Outer skin : surfaces characteristic of a traction fracture

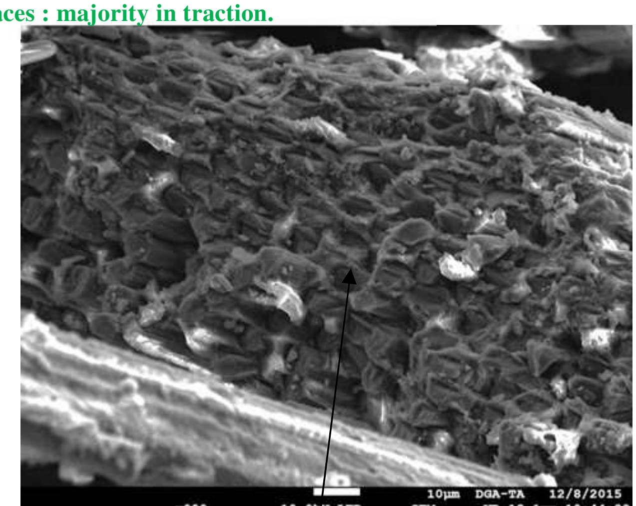

Outer skin: steps characteristic of a compression fracture

Planche 57 : **Upper surface: impact and protruding crack**

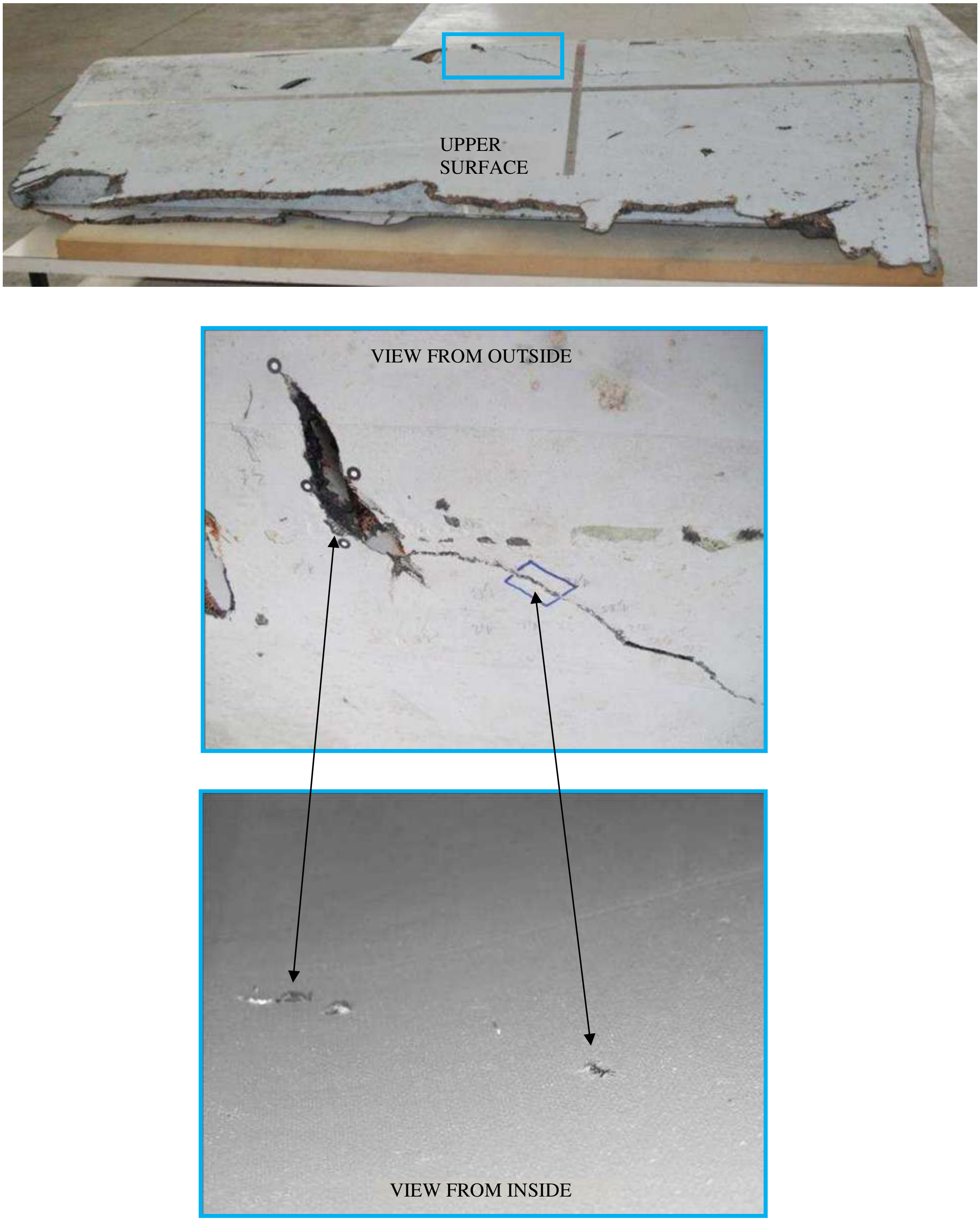

Planche 58 : **Upper surface: observation of the crack in a non-protruding part**

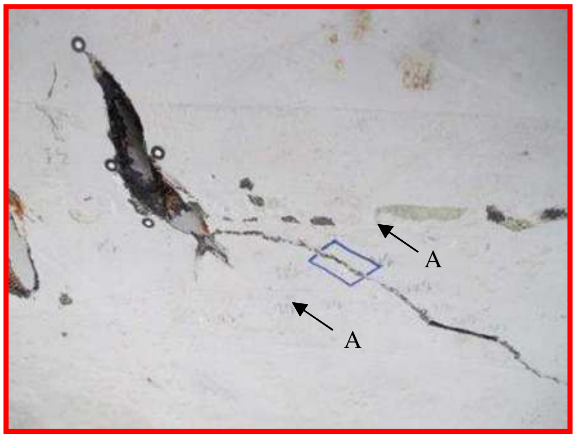

Macroscopically : bending fracture of outer skin

View along A-A

All surfaces paint side : majority in traction.

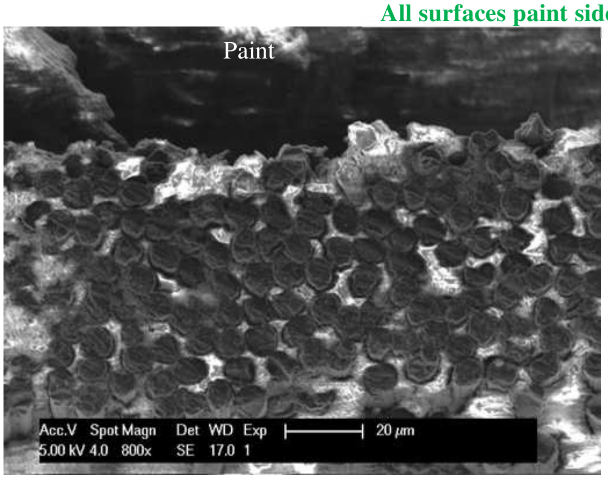

Near paint : steps characteristic of compression fracture

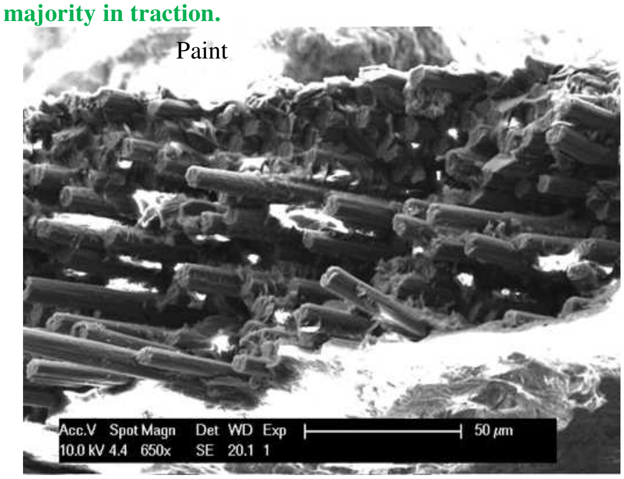

Near paint : surfaces characteristic of traction fracture

All surfaces honeycomb side: majority in compression.

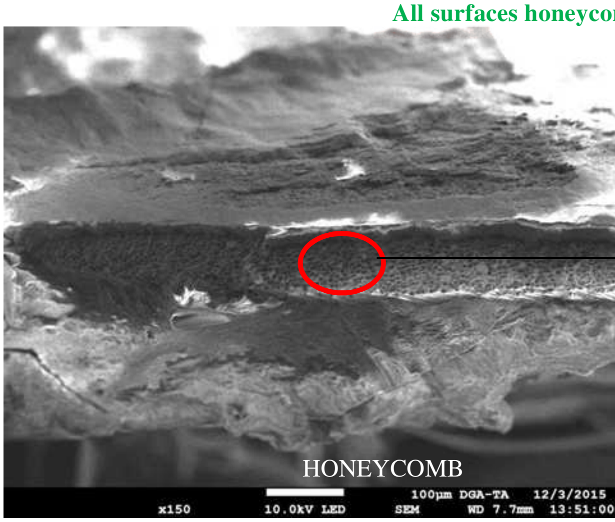

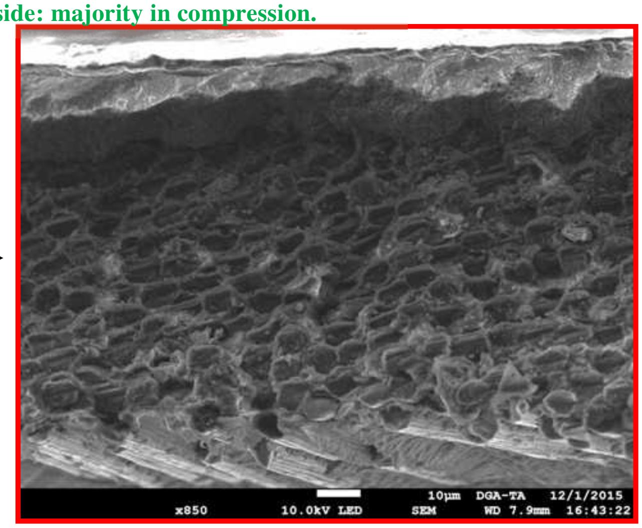

Near honeycomb : steps characteristic of compression fracture

Planche 59 : **Upper surface: orientation of outer skin folds**

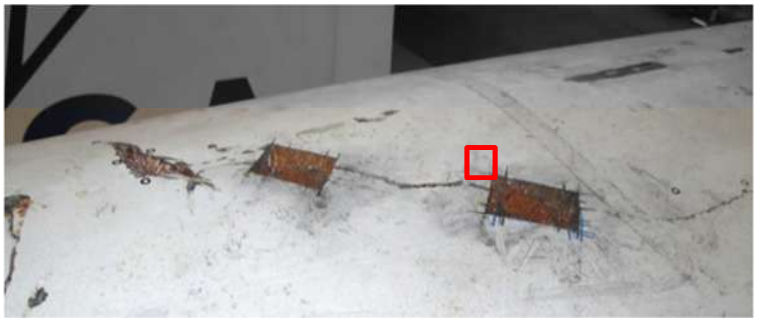

Sample zone

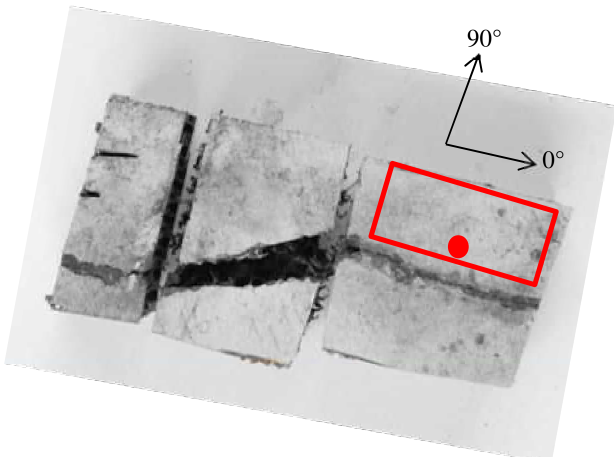

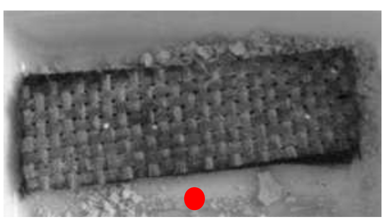

Fold n°1 : Material: 0°/90°

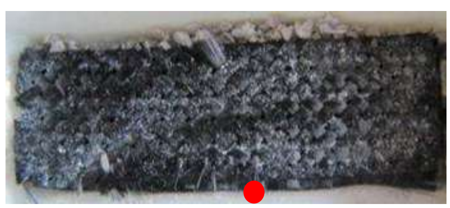

Fold n°2 : Material: 45°/-45°

Fold n°3 : Material: 0°/90°

The outer skin consists of three folds, the orientation above is in relation to the crack.

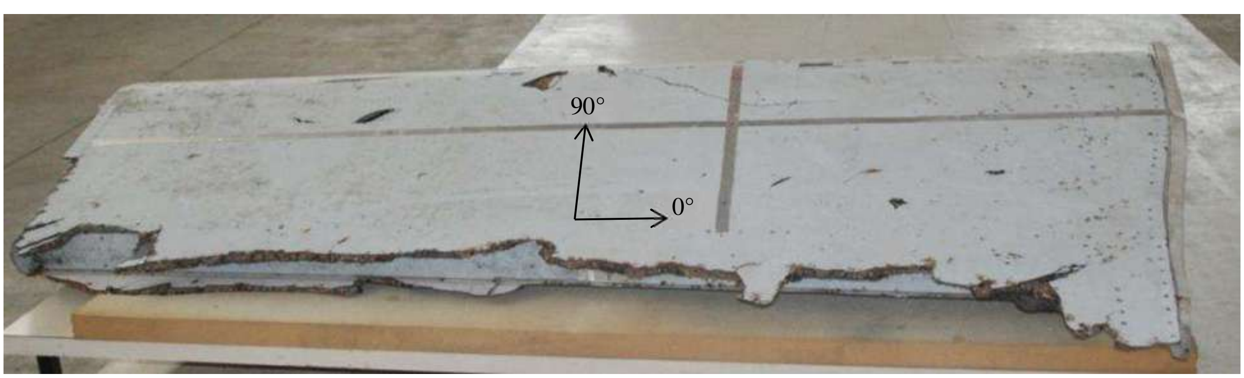

In the flaperon referential, see above, the following draping appears: +/-45°,0/90°,+/-45°.

Planche 60 : **Upper surface: observation of the crack in a protruding part (1/2)**

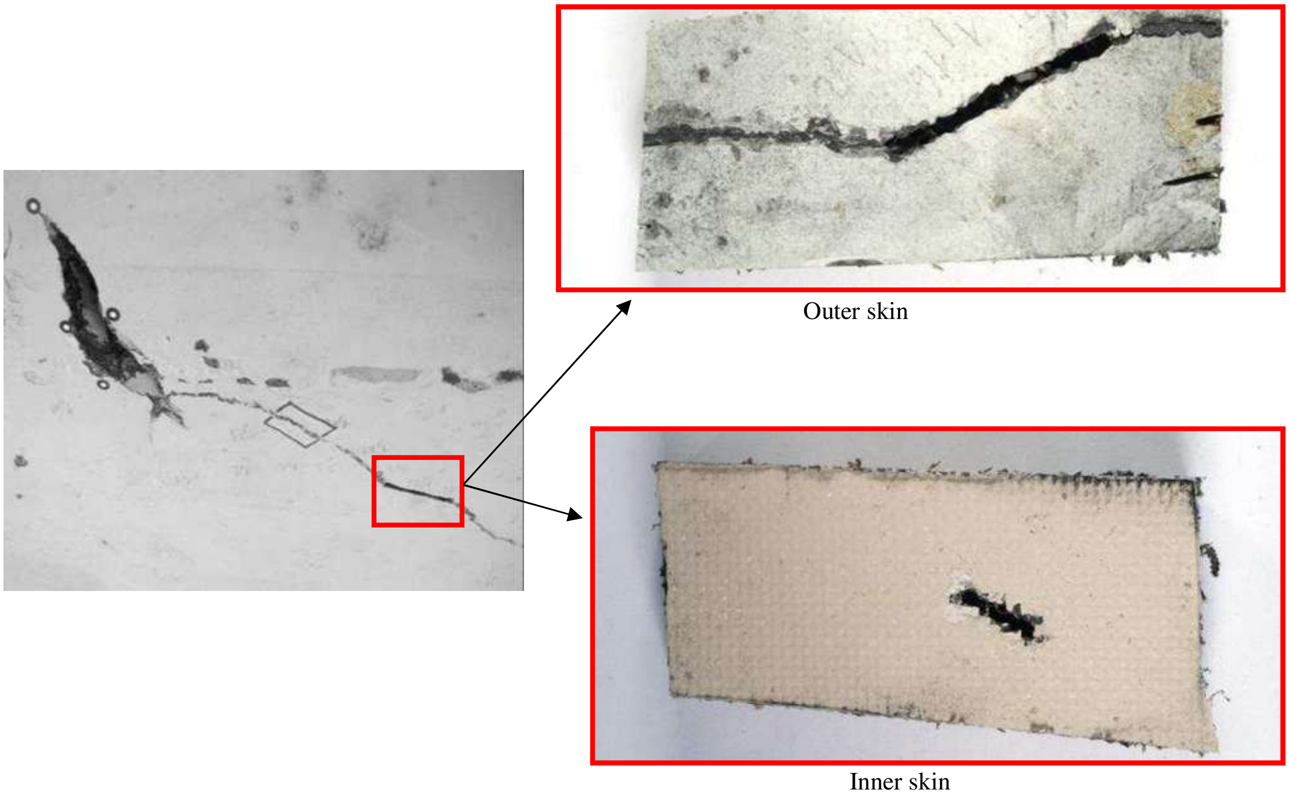

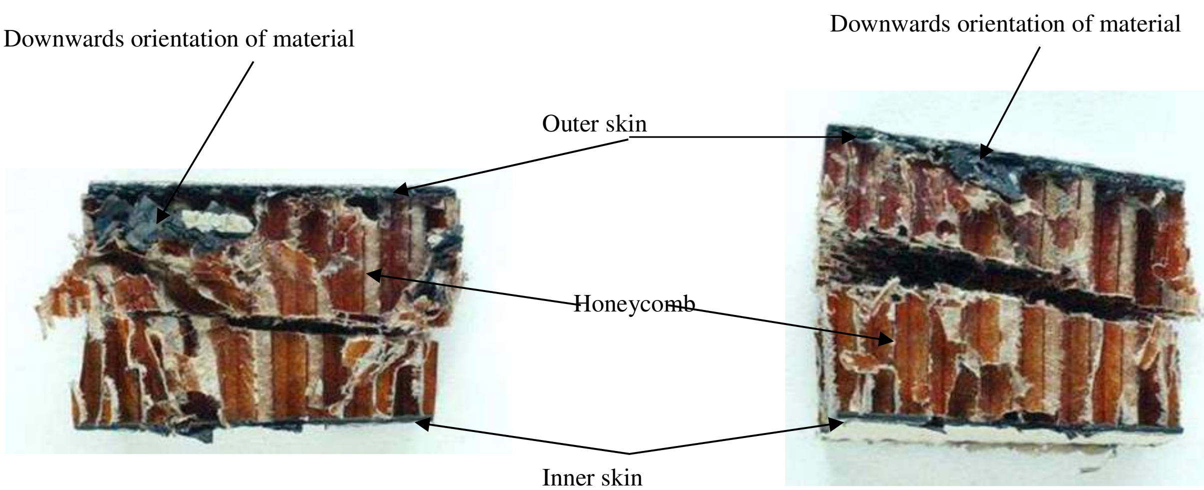

Planche 61 : **Upper surface: observation of the crack in a protruding part (2/2)**

All of inner skin fracture surfaces : majority in traction .

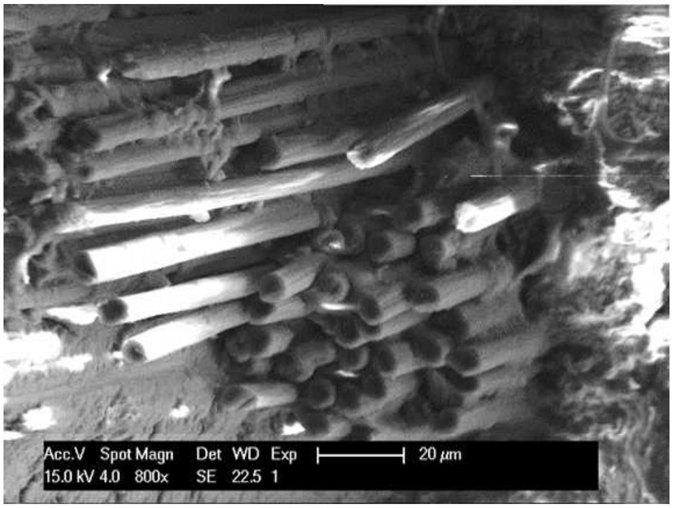

Outer skin: fracture surfaces characteristic of traction fracture

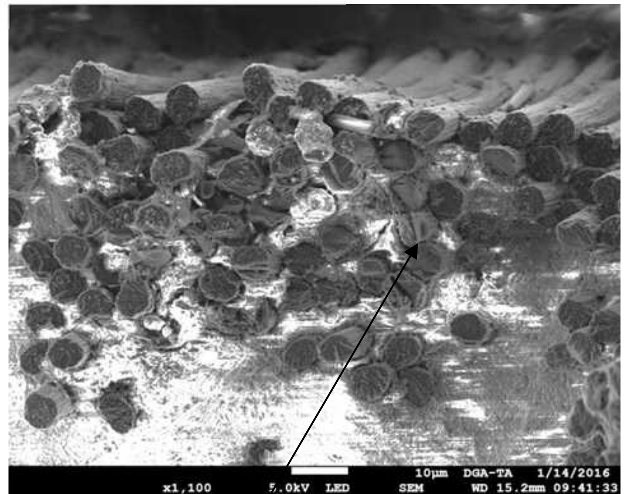

Outer skin: some fibres in compression

All of inner skin fracture surfaces : majority in traction

Peau skin: radiating form : fracture surfaces characteristic of traction:

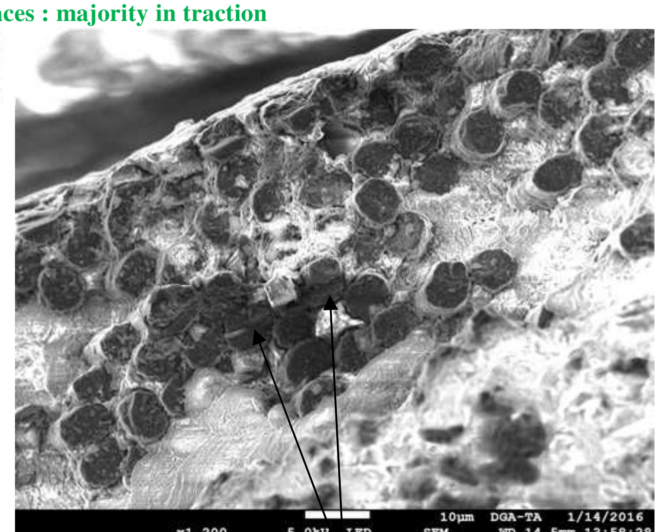

Inner skin : some fibres in compression

DGA Techniques aéronautiques

RESTRICTED CIRCULATION

RAPPORT

N° 16-DGATA-MTI-P1501516001002-DR-F-Â

Planche 62 : **Summary of the deductions made based on the observations and examinations on the composite structure of the flaperon**

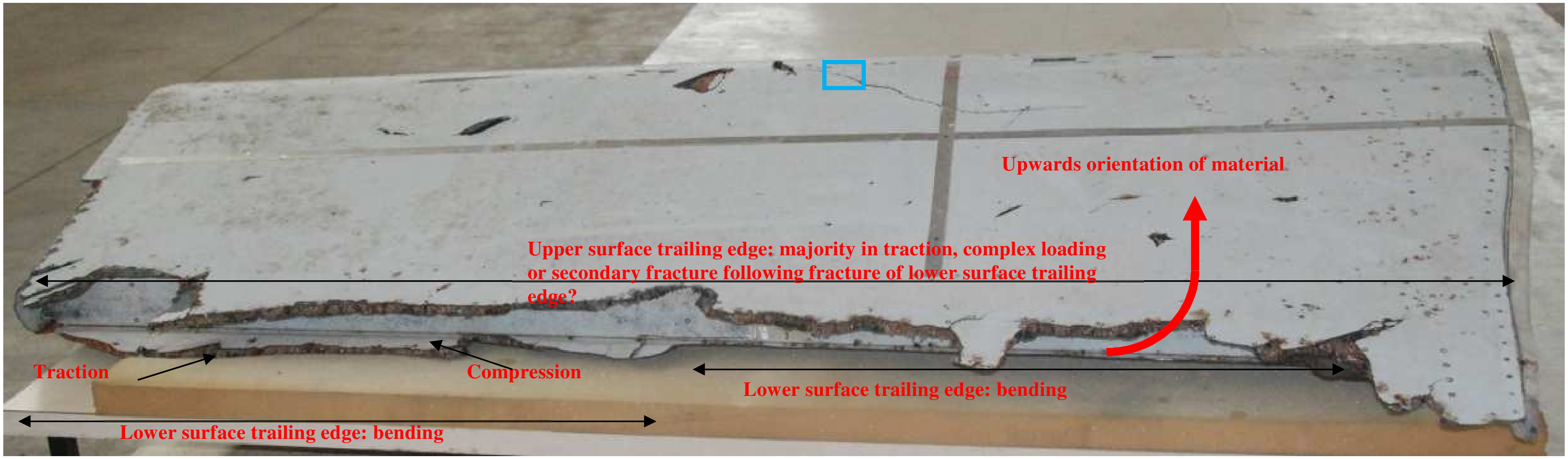

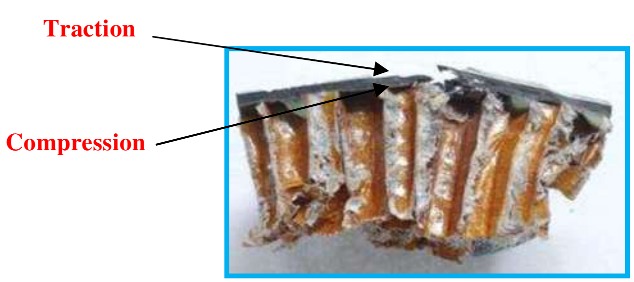

Non-protruding crack : **bending fracture : skin bowing.**